

Kerr metric bundles.

Killing horizons confinement, light-surfaces and horizons replicas

Daniela Pugliese and Hernando Quevedo*

*Institute of Physics, Faculty of Philosophy & Science, Silesian University in Opava,
Bezručovo náměstí 13, CZ-74601 Opava, Czech Republic*

Dipartimento di Fisica, Università di Roma "La Sapienza", I-00185 Roma, Italy

Instituto de Ciencias Nucleares, Universidad Nacional Autónoma de México, AP 70543, México, DF 04510, Mexico

Department of Theoretical and Nuclear Physics, Kazakh National University, Almaty 050040, Kazakhstan

(Dated: May 11, 2020)

We provide a complete characterization of the metric Killing bundles (or metric bundles) of the Kerr geometry. Metric bundles, first introduced in [21] can be generally defined for axially symmetric spacetimes with Killing horizons and, for the case of Kerr geometries, are sets of black holes (**BHs**) or black holes and naked singularities (**NSs**) geometries. Each metric of a bundle has an equal limiting photon (orbital) frequency, which defines the bundle and coincides with the frequency of a Killing horizon in the extended plane. In this plane each bundle is represented as a curve tangent to the curve that represents the horizons, which thus emerge as the envelope surfaces of the metric bundles. We show that the horizons frequency can be used to establish a connection between **BHs** and **NSs**, providing an alternative representation of such spacetimes in the extended plane and an alternative definition of the **BH** horizons. We introduce the concept of inner horizon confinement and horizons replicas and study the possibility of detecting their frequencies. We study the bundle characteristic frequencies constraining the inner horizon confinement in the outer region of the plane i.e. the possibility of detect frequency related to the inner horizon, and the horizons replicas, structures which may be detectable, for example, from the emission spectra of **BHs** spacetimes. It is shown that such observations can be performed close to the rotation axis of the Kerr geometry, depending on the **BH** spin. We argue that these results could be used to further investigate black holes and their thermodynamic properties.

I. INTRODUCTION

In this work, we present the general analysis of the metric Killing bundles (or metric bundles **MBs**) of the Kerr geometry. The definition of metric bundles was first introduced in [21] for the Kerr geometries, framed in the analysis of the Kerr black holes (**BHs**) and naked singularities (**NSs**) properties. **MBs** can be generally defined in spacetimes with Killing horizons.

The idea is to bundle geometries according to some particular characteristic common to all the geometries of the bundles, which allows us to explore the properties of the bundled metrics from a special perspective. Bundles enlighten properties attributable to different points of spacetime and connect different geometries including, for example, **BHs** and **NSs**. These properties can be measured through the observation of light-like radii and the analysis of the light surfaces implicated in many astrophysical phenomena such as **BH** shadows, accretion disks and magnetospheres. To this end, we introduce the concept of extended plane which, in brief, can be defined as a graphic representing a collection of metrics related by a common property. We specify below the details of these definitions.

A metric Killing bundle of the Kerr geometry is a collection of Kerr spacetimes characterized by a particular frequency defined as the photon (circular) orbital frequency, ω , at which the four-velocity norm of a particular stationary observer vanishes. It is straightforward to prove that ω is also the frequency (angular velocity) of a particular **BH** horizon. A metric bundle is represented by a curve in the *extended plane*, i.e., a plane $\mathcal{P} - r$, where \mathcal{P} is a parameter of the Kerr spacetime and r is the radial Boyer-Lindquist (BL) coordinate. Thus, an extended plane represents all the metrics of the Kerr family so that varying the parameter \mathcal{P} , we can extend a particular analysis to include all Kerr metrics.

Thus, the metrics of one metric Killing bundle with characteristic frequency $\bar{\omega}$ are all and the only Kerr (**BHs** or **NSs**) spacetimes, where at some point r the limiting light-like orbital frequency is $\omega = \bar{\omega}$. In the extended plane, all the curves associated to the **MBs** (bundle curves) are tangent to the horizons curve (the curve representing the Killing horizons of all Kerr **BHs**). Then, this tangency condition implies that each bundle characteristic frequency $\bar{\omega}$

*Electronic address: d.pugliese.physics@gmail.com

coincides with the frequency ω_H of a Killing horizon. Consequently, the horizons in the extended plane emerge as the envelope surface of the collection of all the metric bundles.

The metric bundles of the Kerr spacetimes contain either **BHs** or **BHs and NSs**. Therefore, it is possible to find a **BH-NS** correspondence by using the fact that all bundles are tangent to the horizon. Moreover, the metric bundles analysis provides also an alternative interpretation of **NSs** and **BHs** horizons in the extended plane.

In fact, the exploration of **MBs** as metric structures singles out some fundamental properties of the **BHs** and **NSs** solutions, which are related, in particular, to the thermodynamic properties of **BH** spacetimes and to the possibility to extract information about the **BH** horizons, i.e., to detect properties which are directly attributable to the presence of the **BH** horizons. Particularly, through the study of the Kerr metric bundles, we define the "horizons replicas" that could be detected, for example, from the spectra of electromagnetic emissions coming from **BHs** and, in particular, from locations close to the **BH** rotational axis. The horizon replicas are special orbits of a Kerr spacetime with limiting photon frequency equal to the **BH** (inner or outer) horizon frequency, which coincides with the bundle characteristic frequency in the corresponding point on the extended plane. The representation of the **BH** solutions in the extended plane, as in Figs (2), can be used to highlight some properties of the **BH** horizons that could have a significant impact on the study of **BH** physics, on the interpretation of **NS** solutions, and on the investigation of **BH** thermodynamics.

Specifically, in the case of the Kerr geometry on the equatorial plane considered in [21], it turned out that weak naked singularities (**WNSs**), for which the spin-mass ratio $a = J/M$ is close to the value of the extreme **BH**, are related to a portion of the inner horizon, whereas strong naked singularities¹ (**SNSs**) with $a > 2M$ are related to the outer horizon. In addition, **WNSs** are characterized by the presence of Killing bottlenecks, which are defined as "restrictions" of the Killing throats appearing in **WNSs**. Killing throats (tunnels) emerge through the analysis of the radii of light surfaces (related to the **MBs** definition), which are functions of the spin parameter a and the stationary observers frequency ω [20, 21]. Moreover, Killing bottlenecks, interpreted as "horizons remnants" in [21] and related to metric bundles in [21, 22], are also connected with the concept of pre-horizon regime introduced in [8, 11]. The pre-horizon regime was analyzed in [11]. It was concluded that a gyroscope would conserve a memory of the static or stationary initial state, leading to the gravitational collapse of a mass distribution [5, 10, 12, 14]. Killing throats and bottlenecks were also grouped in [32] in structures named "whale diagrams" of the Kerr and Kerr-Newman spacetimes—see also [17, 35, 36]. For an analysis of the self-force corrections to gyroscope precession in the Kerr spacetime see [2–4]. In **NS** geometries, a Killing throat is a connected and bounded region in the $r - \omega$ plane, containing all the stationary observers allowed within two limiting frequencies $[\omega_-, \omega_+]$. On the other hand, in the case of **BHs**, a Killing throat is either a disconnected region or a region bounded by singular surfaces in the extreme Kerr **BH** spacetime. The **BH** extreme Kerr spacetime, therefore, represents the limiting case of the Killing bottleneck (as defined in the BL frame), where the tunnel narrowing closes on the **BH** horizon. Metric bundles are connected with the Killing bottleneck definition and therefore with horizons remnants. In [21], we performed the **MBs** analysis corresponding to the equatorial plane of the Kerr, Reissner-Nordström and Kerr-Newman geometries. In this work we address also the off-equatorial case of the Kerr spacetime.

Metric bundles are a relatively new concept and in this article we present the general analysis for the Kerr geometries. We focus particularly on the **MBs** characteristics that can have an impact on the observational properties associated to **BH** formation and evolution. Thus, below we precise the **MBs** definitions for Kerr spacetimes and relate them explicitly to quantities of importance in **BH** thermodynamics. We then discuss the relations between **MBs** and stationary observers and light surfaces, which are used to constrain many processes associated to the physics of jet emission, accretion disks and energy extraction from **BHs**. We conclude this introduction with the article plan.

The Kerr geometry and metric bundles

The Kerr geometry in BL coordinates is described by the line element

$$ds^2 = -\frac{\Delta - a^2 \sin^2 \theta}{\rho^2} dt^2 + \frac{\rho^2}{\Delta} dr^2 + \rho^2 d\theta^2 + \frac{\sin^2 \theta \left((a^2 + r^2)^2 - a^2 \Delta \sin^2 \theta \right)}{\rho^2} d\phi^2 - 2 \frac{aM \sin^2 \theta (a^2 - \Delta + r^2)}{\rho^2} d\phi dt, \quad (1)$$

$$\Delta \equiv r^2 - 2Mr + a^2, \quad \text{and} \quad \rho^2 \equiv r^2 + a^2 \cos^2 \theta. \quad (2)$$

¹ Our definition of weak and strong naked singularities is related exclusively to the value of the spin parameter and has been explored in several works [19, 20, 26–31]. The **MBs** characteristics could provide also a different definition not exclusively dependent on the source spin. We point out also that **NSs** can be defined differently as strong curvature singularities [7].

Alternately, it is convenient to write the line element (1) as follows

$$ds^2 = -\alpha^2 dt^2 + \frac{A\sigma}{\rho^2} (d\phi - \omega_z dt)^2 + \frac{\rho^2}{\Delta} dr^2 + \rho^2 d\theta^2, \quad \sigma \equiv \sin^2 \theta, \quad A \equiv (r^2 + a^2)^2 - a^2 \Delta \sigma \quad (3)$$

where $\alpha = \sqrt{(\Delta\rho^2/A)}$ and $\omega_z = 2aMr/A$ are the lapse function and the frequency of the zero angular momentum fiducial observer (**ZAMOS**) [20], whose four velocity is $u^a = (1/\alpha, 0, 0, \omega_z/\alpha)$ orthogonal to the surface of constant t . This vacuum exact solution of the Einstein equations describes an axisymmetric, stationary, asymptotically flat spacetime, where the parameter $M \geq 0$ is interpreted as the mass of the gravitational source. The rotational parameter associated to the central singularity is the spin (the specific angular momentum) $a \equiv J/M$, while J is the total angular momentum (here related to the total ADM mass, while the product aM is the total ADM angular momentum; for a review on stationary black holes see, for example, [1]). For $a = 0$, the metric (1) describes the limiting static and spherically symmetric Schwarzschild geometry. In this work, we also consider this special case, which corresponds to the "zeros" of the Kerr **MBs** in the extended plane.

Killing horizons, metric bundles and characteristic frequencies.

The horizons and the inner and outer static limits for the Kerr geometry are, $r_{\mp} = M \mp \sqrt{M^2 - a^2}$ and $r_{\mp}^{\pm} = M \mp \sqrt{M^2 - a^2 \cos^2 \theta}$, respectively. The event horizons of a spinning **BH** are Killing horizons with respect to the Killing field $\mathcal{L}_H = \partial_t + \omega_H^{\pm} \partial_{\phi}$, where ω_H^{\pm} is the angular velocity (frequency) of the horizons representing the **BH** rigid rotation². The vectors $\xi_t = \partial_t$ and $\xi_{\phi} = \partial_{\phi}$ are the stationary and axisymmetric Killing fields, respectively. In the limiting case of spherically symmetric, static spacetimes, the event horizons are Killing horizons with respect to the Killing vector ∂_t and the event, apparent, and Killing horizons with respect to the Killing field ξ_t coincide. The results we discuss in this work follow from the investigation of the properties of the Killing vector $\mathcal{L} = \partial_t + \omega \partial_{\phi}$. The quantity $\mathcal{L}_{\mathcal{N}} \equiv \mathcal{L} \cdot \mathcal{L}$ becomes null for photon-like particles with rotational frequencies ω_{\pm} . Metric bundles correspond to the solutions of the condition $\mathcal{L}_{\mathcal{N}} = 0$. The quantity ω will be called the characteristic **MB** frequency. The vector \mathcal{L} , the frequency ω , and the limits $(\mathcal{L}_H, \omega_H^{\pm})$, enter the definition of **BHs** horizons, establishing relations between black holes, extreme black holes and their thermodynamic properties. Therefore, the Killing vector $\mathcal{L}_{\pm} \equiv \xi_t + \omega_{\pm} \xi_{\phi}$ can be interpreted as generator of null curves ($g_{\alpha\beta} \mathcal{L}_{\pm}^{\alpha} \mathcal{L}_{\pm}^{\beta} = 0$) as the Killing vectors \mathcal{L}_{\pm} are also generators of Killing event horizons. The Kerr horizons are, therefore, null (lightlike) hypersurfaces generated by the flow of a Killing vector, whose null generators coincide with the orbits of an one-parameter group of isometries, i.e., in general, there exists a Killing field \mathcal{L} , which is normal to the null surface.

Notably, many quantities considered in this analysis are conformal invariants of the metric and inherit some of the properties of the Killing vector \mathcal{L} , which identifies a Killing throat up to a conformal transformation. The simplest case is when one considers a conformal expanded (or contracted) spacetime where $\tilde{\xi}^2 \equiv \tilde{\mathbf{g}}(L, L) = \Xi^2 \mathbf{g}(L, L)$. This holds also for a "conformal expanded" Killing tensor³ $\tilde{\mathcal{L}} \equiv \Xi \mathcal{L}$

The **MBs** definition is tightly connected in the Kerr geometry to the (light-like and time-like) stationary observers definition. It also relates **MBs** with several processes in which a **BH** interacts with its environment such as the accretion disks and magnetospheres. The vector \mathcal{L} appears in the description of certain **BH** evolution processes because it enters the definitions of thermodynamic variables and stationary observers. We will see below the relation between the definition of stationary observers, **MBs** and **BH** thermodynamics.

Stationary observers

The vector \mathcal{L} , the condition $\mathcal{L}_{\mathcal{N}} = 0$ and **MBs** are closely related to the definition of stationary observers, i. e., observers with a tangent vector which is a Killing vector. Their four-velocity u^{α} is thus a linear combination of the two Killing vectors ξ_{ϕ} and ξ_t ; therefore, $u^{\alpha} = \gamma \mathcal{L}^{\alpha} = \gamma(\xi_t^{\alpha} + \omega \xi_{\phi}^{\alpha})$, where γ is a normalization factor and $d\phi/dt = u^{\phi}/u^t \equiv \omega$. The dimensionless quantity ω is the orbital frequency of the stationary observer. Because of the spacetime symmetries, the coordinates r and θ of a stationary observer are constants along its worldline, i. e., a

² The event horizon of a stationary asymptotically flat solution with matter satisfying suitable hyperbolic equations is a Killing horizon. The strong rigidity theorem connects the event horizon with a Killing horizon.

³ Concerning the conformal properties of the **MBs**, we notice that the **MBs** definition is invariant under conformal transformations of the metric and of the Killing vectors: $\tilde{\mathcal{L}} = \Xi_{\bullet}(\xi_t + \omega(r_{\bullet})\xi_{\phi}) = \Xi_{\bullet}\mathcal{L}$, where r_{\bullet} is a set of variables that do not contain t or ϕ , Ξ_{\bullet} is non-null or null in a finite number of points. Concerning the relation with the spherically symmetric (and static) case we stress here that for each **BH** spacetime the hypersurface S_+ defined by $r = r_+$ is a smooth null hypersurface. The null generator \mathcal{L}_+ of S_+ is the limit of \mathcal{L} on the horizon (r_+), the frequency is that of the horizon, with an abuse of notation here we consider $\mathcal{L} = \mathcal{L}_+$. In the Kerr spacetime, on the other hand, the Killing vector ξ_t is timelike only outside the hypersurface r_{ϵ}^+ on which it becomes null. In the region $]r_+, r_{\epsilon}^+[$, outer ergoregion, ξ_t is spacelike— these hypersurfaces are represented in Figs (1,2,12). The vector ξ_t is also spacelike on and tangent to S_+ (except on the rotation axis where ξ_t is again null). Thus, the **BH** horizon r_+ is a non-degenerate (bifurcate) Killing horizon generated by the vector field \mathcal{L} . In the case $a = 0$ (where, in this case, $\omega = 0$) ξ_t (now generator of r_+) is hypersurface-orthogonal.

stationary observer does not see the spacetime changing along its trajectory. Specifically, the causal structure defined by timelike stationary observers is characterized by a frequency bounded in the range $\omega \in]\omega_-, \omega_+[$ [16]. On the other hand, static observers are defined by the limiting condition $\omega = 0$ and cannot exist in the ergoregion⁴. The limiting frequencies ω_{\pm} , which are photon orbital frequencies, solutions of the condition $\mathcal{L}_{\mathcal{N}} = 0$, determine the frequencies ω_H^{\pm} of the Killing horizons.

Black hole thermodynamics, metric bundles and the quantity $\mathcal{L}_{\mathcal{N}}$

The thermodynamic properties of black holes are related to the definition of metric bundles in a rather immediate way. The **BH** surface gravity κ , which is also a conformal invariant of the metric, may be defined as the rate at which the norm of the Killing vector \mathcal{L} vanishes from outside (i.e. $r > r_+$). In fact, κ is in general defined through the relation $\nabla^{\alpha}\mathcal{L}_{\mathcal{N}} = -2\kappa\mathcal{L}^{\alpha}$ and for the Kerr spacetime it becomes $\kappa_{Kerr} = (r_+ - r_-)/2(r_+^2 + a^2)$. The surface gravity re-scales with the conformal Killing vector, i.e. it is not the same on all generators but, because of the symmetries, it is constant along one specific generator. The **BH** event horizon of stationary solutions has constant surface gravity—or the surface gravity is constant on the horizon of stationary black holes, which is postulated as the zeroth **BH** law-area theorem (see for example [6, 33]). More generally, the **BH** horizon area is non-decreasing, a property which is considered as the second law of **BH** thermodynamics, establishing the impossibility to achieve with any physical process a **BH** state with zero surface gravity.

Clearly, in the extreme Kerr spacetime ($a = M$), where $r_{\pm} = M$, the surface gravity is zero. This implies that the temperature is also null ($T_H = 0$), with a non-vanishing entropy⁵[6, 33, 34]. On the other hand, the condition (constance of) $\nabla^{\alpha}\mathcal{L} = 0$ when $\kappa = 0$ substantially constitutes the definition of the degenerate Killing horizon—degenerate **BH**—, in the case of Kerr geometries only the extreme **BH** case is degenerate; therefore, in the extended plane it corresponds to the point $a = M$ $r = M$. A fundamental theorem of Boyer shows that degenerate horizons are closed. This fact also establishes a topological difference between black holes and extreme black holes. More generally, the first law $\delta M = (1/8\pi)\kappa\delta A + \omega_H\delta J$ relates the variation of **BH** mass δM , **BH** horizon area δA , and angular momentum δJ with the **BH** surface gravity κ and angular velocity ω_H on the outer horizon. The term ($\omega_H\delta J$) can be interpreted as the “work”. The (Hawking) temperature term is naturally related to the surface gravity, $T_H = \hbar c\kappa/2\pi k_B$ (k_B is Boltzmann constant) and the horizon area A to the entropy, $S = k_B A/\mathcal{L}_P^2$ (\mathcal{L}_P is the Planck length, \hbar reduced Planck constant, c is the speed of light)⁶. It is convenient to re-express some of the concepts of **BH** thermodynamics in terms of the norm $\mathcal{L}_{\mathcal{N}}$, which defines the metric bundles. (1) The norm $\mathcal{L}_{\mathcal{N}} \equiv \mathcal{L} \cdot \mathcal{L}$ is constant on the horizon. (2) The surface gravity is the constant $\kappa : \nabla^{\alpha}\mathcal{L}_{\mathcal{N}} = -2\kappa\mathcal{L}^{\alpha}$, evaluated on the outer horizon r_+ (equivalently, $\mathcal{L}^{\beta}\nabla_{\alpha}\mathcal{L}_{\beta} = -\kappa\mathcal{L}_{\alpha}$ and $L_{\mathcal{L}}\kappa = 0$, where $L_{\mathcal{L}}$ is the Lie derivative, -a non affine geodesic equation, i.e., $\kappa = \text{constant}$ on the orbits of \mathcal{L}).

Article overview

This article is organized as follows. In Sec. (II), we present the main definitions and notations used in this work and introduce the concept of Kerr metric bundles. Then, in Sec. (III), we start the analysis of the **MBs** characteristic frequencies and their relation to the photon orbital frequencies and to the horizon frequencies. This will allow us to introduce the concept of horizon replicas, special orbits with the frequency equal to the horizon frequencies. Among these special orbits, there are retrograde solutions with the frequency equal in magnitude to the horizon frequency and defined in a supplement of the extended plane. A systematic analysis of this case is considered in Appendix (D1) and deepened in Appendix (B), focusing on the characterization of the horizons frequencies as **MBs** frequencies. Concluding remarks follow in Sec. (IV). In Appendix (C1), we present the explicit form of several quantities which are significant for the metric bundles: Explicit **MBs** and light surfaces are presented in Appendix (C1) and in Appendix (C2), respectively. The condition $\mathcal{L}_{\mathcal{N}} = 0$ is studied in detail in Appendix (C3). General notes on the **MBs** of the extended plane are given in Appendix (D). In Appendix (D1), we discuss the meaning of negative characteristic frequencies. In the extended plane, there are certain regions which are bounded by special curves.

⁴ Light surfaces, in fact, play a relevant role for constraining the energy extraction mechanism from **BHs**, which regulates the Blandford-Znajek process, for example. They also constrain the properties of accretion disks or the Grad-Shafranov equations for the force free magnetosphere around a **BH**. With reference to the metric in the form (3) we can define the quantities: $v = d\phi - \omega dt$, and $\varpi = \partial t + \omega\partial\phi$, which are clearly related to the Killing field \mathcal{L} and represent the co-rotation 1-form and the co-rotation vector, respectively, measuring the co-rotation in the Grad-Shafranov approach. Consequently, v and ϖ define light surfaces (where v or ϖ vanishes). The energy extraction process can take place regulated by the light surfaces which are, in general, two located outside the horizon r_+ and one within the ergoregion $]r_+, r_{\epsilon}^+[$.

⁵ This fact has consequences also regarding the stability against Hawking radiation: A non-extremal **BH** cannot reach the extremal limit in a finite number of steps—third law.

⁶ If the **BH** temperature is $T = \kappa/(2\pi)$, its entropy is $S = A/(4\hbar G)$, the pressure-term is $p = -\omega_H$, where the internal energy is $U = GM$ ($M = c^2 m/G =$ mass, where m is a mass term). The **BH** (horizon) area A is clearly related to the outer horizon definition, $A = 8\pi m r_+$, while the volume term is $V = GJ/c^2$ (where $J = amc^3/G$). The **BH** horizon area will be considered here alternatively in the extended plane in Figs 2.

TABLE I: Lookup table with the main symbols and relevant notations used throughout the article with a brief description and reference to the first place where they appear.

| | | |
|---------------------|--|--------------------------------------|
| \mathcal{L} | null Killing vector $\mathcal{L} = \partial_t + \omega \partial_\phi$ (generators of Killing event horizons) | Sec. (I) |
| \mathcal{L}_N | norm $\mathcal{L}_N \equiv \mathbf{g}(\mathcal{L}, \mathcal{L}) = \mathcal{L} \cdot \mathcal{L}$ of the Killing vector \mathcal{L} | Eq. (6)– Sec. (I)–Sec. (C 1) |
| ω_\pm | light-like (solutions of $\mathcal{L}_N = 0$) limiting frequencies for stationary observers | Eq. (6) |
| a_\pm | horizon curve in the extended plane | Eq. (4)–Figs (2) –Figs (12) |
| a_ϵ^\pm | ergosurfaces curve in the extended plane | Eq. (5)–Figs (1)–Figs (2) –Figs (12) |
| ω_b | bundle frequencies | Eq. (7)–Figs (5) |
| ω_H^\pm | horizons frequencies | Eq. (8) |
| r_g | bundle curve tangent radius to the horizon curve in the extended plane | Eq. (9) |
| $a_g(a_0)$ | bundle curve tangent spin to the horizon curve in the extended plane | Eq. (9) |
| a_0 | bundle origin spin in the extended plane | Eq. (7) |
| Γ_{a_0} | metric bundles with equal spin origin a_0 | Eq. (A1) |
| Γ_σ | metric bundles on the same plane θ ($\sigma = \sin^2 \theta$) | Eq. (A4) |
| Γ_{ω_b} | metric bundles with equal bundle frequencies ω_b | Eq. (A7) |
| Γ_{a_g} | metric bundles with equal bundle tangent spin a_g | Eq. (A8) |

The areas of these regions are calculated in Appendix (D 2). Finally, in Appendix (D 3) we present some special characteristics of the horizons replicas.

Throughout this work, we introduce a number of symbols and notations necessary to explain all the results obtained for these recently proposed concepts; however, there is in fact a relatively small set of concepts that are listed for reference in Table I and constitute the core of the MBs we analyze in this work.

II. METRIC BUNDLES OF KERR SPACETIMES

We start this Section by considering in Sec. (II A) explicitly the definitions of extended plane, metric bundles, horizons replicas, horizons confinement, and causal balls. In Sec. (II B), we deepen the discussion on the metric Killing bundles concept for the Kerr geometry. The main characteristics of the metric bundles are the subject of Sec. (II C). This Section closes in Sec. (III) with the analysis of photon orbital frequency and the horizons frequencies.

A. Extended plane, metric bundles, horizons replicas, horizons confinement and causal balls

Extended plane definition: An extended plane is a flat, two-dimensional surface, as in Figs 2. To define an extended plane $\mathcal{P} - r$, it is necessary to select a parameter \mathcal{P} of a spacetime in terms of a particular coordinate r so that varying the value of the parameter \mathcal{P} , we can extend a specific analysis to include all possible metrics of that spacetime. On an extended plane $\mathcal{P} - r$, each curve can be of particular importance. For instance, horizontal lines and vertical lines represent particular members of the spacetime family.

To analyze the details of the information contained in an extended plane, we will consider in this work the particular case of the Kerr spacetime, but this definition can be applied to any spacetime, in principle. In the Kerr spacetime, we will consider two examples of extended planes, for which we consider the BL coordinates $\{t, r, \theta, \phi\}$ and assume that $M = 1$.

Extended plane I: $\pi_a \equiv a - r$, in this case the parameter $\mathcal{P} = a$ is the dimensionless spin (r also is dimensionless). This example has been analyzed in detail previously in [21].

Extended plane II: $\pi_{\mathcal{A}} \equiv \mathcal{A} - r$, where $\mathcal{A} \equiv a\sqrt{\sigma}$ - Figs (2). In this case, the dimensionless parameter is $\mathcal{P} = \mathcal{A} = a\sqrt{\sigma}$ and r is dimensionless too. The previous case is obtained for $\sigma = 1$. A particularly important curve in this plane is the horizons curve, which represents the horizons of the entire Kerr family. The horizon curve is obviously independent from the polar angle θ ; therefore, the horizons are represented by the same curve in both planes.

Note that for a spacetimes family with a number q of parameters \mathcal{P} , the extended plane can be defined as a $(1 + q)$ dimensional surface in which the entire collection of metrics is contained. For example, in the case of Kerr-Newman (KN) spacetimes, as discussed in [21], one could identify as parameter \mathcal{P} the spin-dimensionless parameter a/M , the dimensionless electric charge Q/M or the "total charge" $Q_T \equiv \sqrt{(Q/M)^2 + (a/M)^2}$. Alternatively, one could also consider the couple $(a/M, Q/M)$, leading in each case to different extended planes.

Metric bundle definition: A metric bundle Γ_ω was defined in [21] as the set of all and only geometries with a given value of the characteristic frequency ω , which is defined from condition $\mathcal{L}_N(\omega) = 0$. Each bundle is represented as a curve in the extended plane $a/M - r/M$ or $\mathcal{A}/M - r/M$. However, it is also convenient to consider a more general

definition as follows. A metric bundle $\Gamma_{\mathbf{x}}$ is the set of all and only geometries with a given value of the characteristic quantity \mathbf{x} : $\mathcal{L}_{\mathcal{N}}(\mathbf{x}) = 0$. Metric bundles correspond to curves in the extended plane $a/M - r/M$ or $\mathcal{A}/M - r/M$.

In Table (I), we list the main **MBs** analyzed in this work. Clearly, we can consider bundles Γ_{\odot} as the set of all and only geometries having a given value of the characteristic quantities $\odot \equiv \{\mathbf{x}_i\}_i : \forall \mathbf{x}_i \in \odot : \mathcal{L}_{\mathcal{N}}(\mathbf{x}_i) = 0$. The set Γ_{\odot} corresponds to curves in the extended plane. In Sec. (A 0 a), we consider two quantities $\{\mathbf{x}_i\}_i \equiv \{x, y\}$ so that $\Gamma_{\mathbf{x};\mathbf{y}}$ is the set of all and only geometries having a give value of the characteristic quantities \mathbf{x} : $\mathcal{L}_{\mathcal{N}}(\mathbf{x}) = 0$ and \mathbf{y} : $\mathcal{L}_{\mathcal{N}}(\mathbf{y}) = 0$. In general, $\Gamma_{\mathbf{x};\mathbf{y}}$ cannot be represented as $\Gamma_{\mathbf{x};\mathbf{y}} = \Gamma_{\mathbf{x}} \cap \Gamma_{\mathbf{y}}$, i.e., the condition $\{\mathbf{C}_{\mathbf{x};\mathbf{y}} \in \Gamma_{\mathbf{x};\mathbf{y}} : \mathbf{C}_{\mathbf{x};\mathbf{y}} \in \Gamma_{\mathbf{x}}\}$ is satisfied only in special cases.

Horizons replicas

Let $\varphi(\bar{r})$ be the curve representing the horizon in the extended plane. We say that there is a replica of the horizon (on an horizontal line $\mathcal{P} = \text{constant}$), if there exists a radius (orbit) $r_{\bullet} < \bar{r}$ such that $\varphi(r_{\bullet}) \equiv \varphi_{\bullet} = \varphi(\bar{r})$, where r_{\bullet} is a point of the horizon curve in the extended plane, for example, the horizon frequency ω , evaluated on \bar{r} . We are, in fact, interested mostly in the case $\varphi = \omega$, which is the bundle characteristic frequency and horizon frequency. According to the definitions of metric bundles, there are clearly replicas in different geometries, i.e. there is a pair of metric parameters values, $p \neq \bar{p}$, and a couple of points, $\bar{r} > r_{\bullet}$, such that there is $\omega(r_{\bullet}(p), p) \equiv \omega_{\bullet}^p = \omega(\bar{r}(\bar{p}), \bar{p})$, where p and \bar{p} are values of the extended plane parameter, corresponding therefore to two different geometries, i.e. two horizontal lines in the extended plane. To the two points (p, r_{\bullet}) and (\bar{p}, \bar{r}) of the extended plane, there corresponds an equal light-like particle orbital frequency. (It is clear that in the Kerr extended plane, the particular case $\omega_+ = \omega_-$ holds only on the horizon point $a = M$ and $r_{\pm} = M$.) We prove in this analysis that these structures reveal their significance in the region proximal to $(\theta \approx 0, \sigma \approx 0)$. Examples of these orbits are in Figs (9).

Horizons confinement and causal balls

Opposite with respect to the horizon replicas, the **(MBs) horizon confinement** is a concept interpreted as due to the presence of a "local causal ball" in the extended plane, which is a region of the extended plane $\mathcal{P} - r$ where the **MBs** $\Gamma_{\mathbf{x}}$ are entirely confined, i.e., there are no horizons replicas in any other region of the extended plane outside the causal ball. Particularly, we can restrict this definition to the case $\mathcal{P} = \text{constant}$. For example, in the Kerr extended plane a causal ball is the region upper bounded by a portion of the inner horizon, which means that the horizons frequencies defined for these points of the inner horizons cannot be measured (locally) outside this region.

B. Developing the concept of metric Killing bundles of the Kerr geometry

Metric bundles were first introduced in [21] as sets of Kerr geometries that can include **BHs** or **BHs and NSs**, where each spacetime of the bundle has, at a certain radius r usually different for different geometries of the bundle, an equal limiting photon frequency $\omega_b \in \{\omega_+, \omega_-\}$, or simply ω , called the *characteristic bundle frequency*.

Metric bundles are defined in the Kerr extended plane. In general, in an extended plane, we can consider the entire collection of metrics of a parameterized family of solutions. Examples of extended planes are given in Figs (13,12,14,16). The characterization of the extended plane of Kerr geometry gives rise to the representation of **BH** solutions as in Figs (2). A metric bundle, as a set of spacetimes defined by one characteristic photon orbital frequency ω , is therefore a curve on the extended plane, characterized by a particular relation between the metrics parameters. These objects turn out to establish a relation between **BHs** and **NSs** the extended plane and allow us to reinterpret the Killing horizons and to find connections between black holes and naked singularities throughout the horizon curve. All the metric bundles are tangent to the horizon curve in the extended plane. Then, the horizon curve emerges as the envelope surface of the set of metric bundles. As a consequence, in [21] we defined weak naked singularity (**WNS**), related to a part of the inner horizon, whereas strong naked singularities (**SNSs**) were related to the outer horizon.

The definition of metric bundles is based upon the analysis of the condition $\mathcal{L}_{\mathcal{N}} = 0$, which depends on the even powers of $\sin \theta$ or $\cos \theta$. Therefore, it is convenient to introduce the quantity $\sigma \equiv \sin^2 \theta \in [0, 1]$. Moreover, the condition $\mathcal{L}_{\mathcal{N}} = 0$ is invariant under the transformation (a, ω) in $(-a, -\omega)$; therefore, we focus on the case $a \in \text{Re}$ and $\omega \geq 0$. However, in this work we also consider, particularly in Sec. D 1, the case of negative characteristic frequencies ω_b , which corresponds to an extended plane with $a_0 < 0$, see Figs (2), where a_0 is the bundle origin- Figs (12).

In the section $a_0 > 0$ of the extended plane, each metric bundle is tangent to the horizon curve; viceversa, each point of the horizon is tangent to a metric bundle. The points $(r = 0, a = 0)$, $(r = 2M, a = 0)$ and $(r = 2M, a = +\infty)$ of the extended plane are special limiting cases corresponding to the static Schwarzschild geometry. This property implies that the bundle frequency coincides with a frequency ω_H^{\pm} of the horizon at the tangent point, i.e. $\omega_b \in \{\omega_+, \omega_-\} = \omega_H^{\pm}$. As at a point r , in general, there are two different limiting photon frequencies ω_{\pm} , then it follows that at each point of the extended plane (with the exception of the horizon curve) there have to be a maximum of two different crossing metric bundles (with the same value of θ). The bundle frequency is in particular the frequency of the horizon at the point of tangency with the bundle -see for example Figs (14) for the representation of metric bundles tangent to the horizon curve in the extended plane. The metric bundle is defined by the tangent point on the horizon r_g , and the

horizon defines all metric bundles (including **BHs** or **BHs and NSs**) depending only on the plane θ . On the other hand, as we shall see below, there are classes Γ_ω of metric bundles with equal frequencies ω_b (equal tangent radius r_g), but different bundle origins i.e. the point $(r = 0, a = a_0)$ – Figs (14). The bundle tangency point (a_g, r_g) , and therefore the bundle frequency ω_b , is independent of the polar angle θ . It follows that the horizons frequencies ω_H^\pm in the extended plane are sufficient to define the limiting frequencies ω_\pm at any point (r, θ, φ) in any geometry a . The tangency property is independent of θ and φ ; this reflects the fact that the horizon curve in the extended plane, which is a sphere of radius $r = M$ centered in the point $(r = M, a = 0)$ with area $A_\pm = \pi M^2$, is independent of the plane θ and azimuthal angle φ (a property related to the rigidity of the **BH** Killing horizons).

More precisely, in the extended plane, the horizon a_\pm (solution of $\Delta \equiv a^2 + (r - 2M)r = 0$) and the ergosurface curve a_ϵ^\pm , are

$$a_\pm \equiv \sharp \sqrt{r(2-r)}, \quad \sharp = \pm \quad (4)$$

and

$$a_\epsilon^\pm \equiv \pm \sqrt{\frac{(r-2)r}{\sigma-1}} = \pm \frac{a_\pm}{\sqrt{1-\sigma}}, \quad \text{for } \sigma \neq 1, \quad \text{thus } \lim_{\sigma \rightarrow 1} a_\epsilon^\pm = \pm \infty, \quad (5)$$

respectively (see Figs 1). For the sake of simplicity here and in the following sections we mainly adopt dimensionless quantities where $r \rightarrow r/M$ and $a \rightarrow a/M$. Note that curve a_ϵ^\pm is defined for $\sigma \in [0, 1[$ in $r \in [0, M]$ (corresponding to the inner ergosurface r_ϵ^- , with $r_\epsilon^- = 0$ for $\sigma = 1$), where for $\sigma = 1$ there is $r = 0$ with $a \geq 0$ and for $\sigma \in [0, 1[$ with $r \in [M, 2M]$ (corresponding to the outer ergosurface r_ϵ^+), with $r_\epsilon^+ = 2M$ for $\sigma = 1$. In most cases, we will consider the sector of the extended plane $a > 0$ with $a_\pm > 0$, and therefore $\sharp = +1$.

Explicitly, we can define the photon orbital limiting frequencies ω_\pm as

$$\begin{aligned} \mathcal{L}_N = \mathcal{L} \cdot \mathcal{L} = 0 \quad \text{for} \quad \omega = \omega_\pm &\equiv \frac{\pm \sqrt{\sigma \Delta \Sigma^2 - 2a r \sigma}}{\sigma [a^2 \sigma \Delta - (a^2 + r^2)^2]}, \\ \text{where } \Delta &\equiv a^2 + (r-2)r, \quad \text{and} \quad \Sigma \equiv r^2 - a^2(\sigma-1), \quad \sigma \equiv \sin^2 \theta \\ \text{with } \lim_{r \rightarrow \infty} \omega_\pm &= 0, \quad \lim_{a \rightarrow \infty} \omega_\pm = 0, \quad \lim_{a \rightarrow 0} \omega_\pm = \mp \frac{(r-2)r}{\sqrt{(r-2)r^5 \sigma}}. \end{aligned} \quad (6)$$

On the origin $r = 0$ of the extended plane, there is

$$\omega_b = \omega_0^\pm \equiv \pm \frac{1}{a\sqrt{\sigma}}. \quad \text{The bundle origin spin is} \quad a_0(\omega, \sigma) \equiv \pm \frac{\csc(\theta)}{\omega} = \pm \frac{1}{\omega\sqrt{\sigma}}, \quad (7)$$

Similarly to the case of equatorial bundles (for $\sigma = 1$) investigated in [21], the bundle frequency ω_b is constant along the curve that represents the bundle (for any constant σ). Thus, in particular, the frequency of the origin ω_0 coincides with the bundle frequency ω_b ; on the other hand, we note that the origin spin a_0 depends on the plane σ at fixed ω .

For a fixed radius r , there are two limiting photon frequencies ω_\pm . Then, it follows that at each point of the extended plane (with the exception of the horizon curve) there have to be a maximum (for a fixed value of θ) of two different crossing metric bundles. The bundle frequency coincides with the frequency of the horizon at the point where the bundle is tangent to the horizon curve, as illustrated in Figs (14). The fact that metric bundles are tangent to the horizon sphere in the extended plane has some significant properties. Explicitly, we can write

$$\forall \theta \neq 0, \quad \omega_b \equiv \omega_\pm(a_\pm) = \frac{\sqrt{(2-r)r}}{2r} = \frac{a_\pm}{2r} \equiv \omega_H^\pm(r), \quad (8)$$

$$\text{with bundle tangent radius:} \quad r_g(\omega) = \frac{2}{4\omega^2 + 1}, \quad \omega_H^\mp(a) \equiv \frac{r_\pm}{2a},$$

$$\text{and bundle tangent spin:} \quad a_g(a_0) \equiv \frac{4a_0\sqrt{\sigma}}{a_0^2\sigma + 4}, \quad \text{bundle origin spin:} \quad a_0 = \frac{1}{\sqrt{\sigma}\omega_b}. \quad (9)$$

Then, for $\sigma = 1$ and $r = M$, we have that $\omega_b = 1/2$, which corresponds to the origin $a_0 = 2M$. Moreover, for $a_0 = +\infty$, it holds that $r = 2M$ and $\omega_b = 0$, where ω_H^\mp are the frequencies of the horizons r_\mp respectively in the extended plane, r_g is the radius at the tangent point of the metric bundle with the horizon in the extended plane—see Fig (1)–(4). The tangent spin a_g and the tangent radius r_g are respectively the spin and the radius defined from the tangency of the metric bundle with the horizon curve in the extended plane. We note that the bundle frequency in

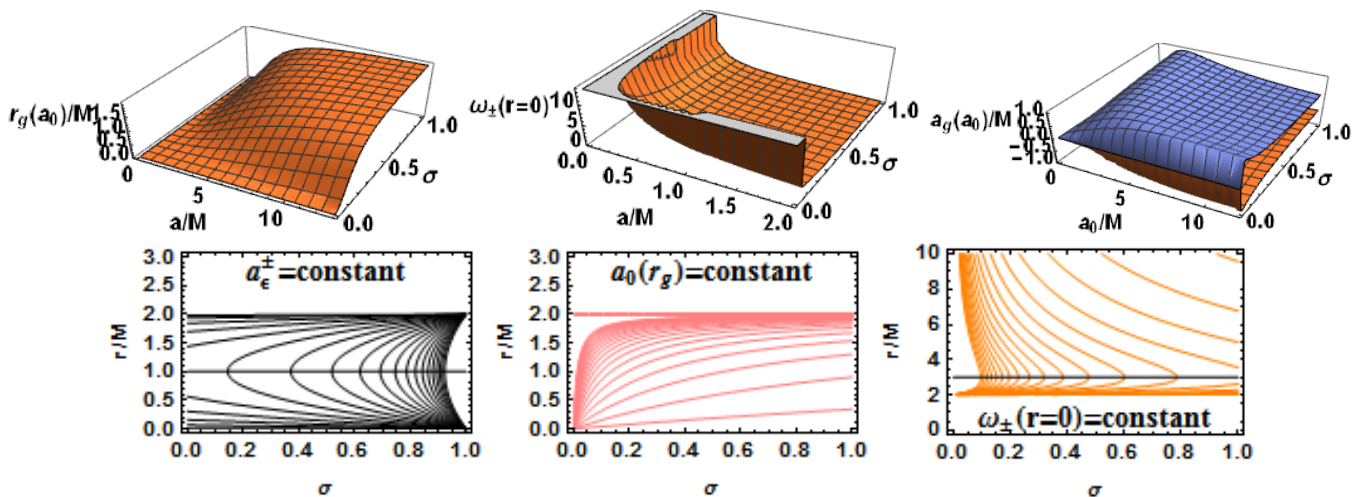


FIG. 1: Upper panels: 3D plots of the bundle tangent radius $r_g(a_0)/M$ as function of a/M and $\sigma \in [0, 1]$ (left), the origin frequencies (singularity frequencies) $\omega_{\pm}=\text{constant}$ for $r = 0$ as function of $(a/M, \sigma)$ (center), the tangent spin $a_g(a_0)/M \in [0, 1]$ as function of $(a/M, \sigma)$ (right). Below panels. Left panel: ergosurface $a_{\epsilon}^{\pm}=\text{constant}$ of Eq. (C7) in the extended plane as function of r/M and $\sigma = \sin\theta^2$. Center panel: the bundle origin spin $a_0(r_g)$ of Eq. (A6) as function of the tangent spin $r_g \in [0, 2M]$ in the plane $(\sigma, r/M)$. Right panel: the origin frequencies (singularity frequencies) $\omega_{\pm}=\text{constant}$ for $r = 0$ in the plane $(\sigma, r/M)$ see Eq. (C7).

terms of the origins spin a_0 , for fixed plane σ , is maximum for the limiting case $a = 0$ and null for $a \rightarrow \infty$, moreover there is $\omega_0^{\pm} = 1/\sqrt{\sigma}$ for the extreme **BH**, and it is minimum on the equatorial plane where it is $\omega_0^{\pm} = M/a$, in agreement with [21]. (As per definition the metric bundle has constant frequency at any point of the bundle in the extended plane, then particularly the bundle characteristic frequency ω_b is the frequency of the bundle origin a_0 .)

Metric bundles constitute the basis for the representation of the Kerr extended plane in Figs (2) where the **BH** is represented by the isosceles triangle with height $h_{\pm} = M$, base $b_{\pm} = 2M$, sides length $l_{\pm} = \sqrt{2}M$ and area $A_{\pm} = M^2$ or, in the case of negative frequencies (corresponding to the extension $a_0 < 0$), by a rhombus.

In this work, we discuss the transformations that are needed to draw these diagrams based on the metric bundles explicitly discussed in Eq. (B3) and represented in Figs (2), where we also define the inner and outer regions of the extended plane and the Killing bottleneck relevant for the problem of the horizon confinement discussed in [21]. The bottleneck region identifies the spin interval connected to the emergence of the Killing bottleneck in the Killing throat of weak naked singularities, structures emerging from the light surfaces as functions of the orbital frequency ω introduced in [20, 21]. The bottleneck region is related to the concept of the horizon remnants, which were also highlighted as pre-horizons of [8, 11] and whale diagrams in [17, 32, 35, 36]. It is important to note that the quantities of Figs (2) are essentially defined according to the variable $\mathcal{A} \equiv a\sqrt{\sigma}$, we will discuss the importance of this element in details below ⁷.

Although we consider the inside region bounded by the inner horizon, we are also interested in the information contained in outer region in the whole extended plane.

Horizontal lines in the **BH** sector, $a_0 \in [0, M]$, correspond to a particular **BH** source so that a translation along the triangle (horizon curve) describes the evolution in the vicinity of the source (rigid in the sense of the metric bundles [21]). The metric bundles of the set Γ_{a_g} considered in Eq. (A8), have equal tangent spin (but, in general, different tangent radius r_g) and relate points on the horizontal lines on the triangle. In Figs (2), we illustrate the concept of "replicas" of the **BH** triangle.

In Figs (9), a horizontal line in the **BH** region shows particular intersections with the metric bundles. The black

⁷ It has also been noted in [18] that quantity \mathcal{A} , and specifically $\bar{\ell} \equiv \ell/\mathcal{A}$ poses constraints on the relativistic (geometrically) thick accretion toroidal configurations in the Kerr spacetimes, where ℓ is the specific fluid angular momentum $\ell \equiv L/E$, (L, E) being the const of motions associated to the Killing fields (ξ_{ϕ}, ξ_t) respectively. This quantity is also related to the rotational version of the Killing vectors ξ_t and ξ_{ϕ} i.e. the canonical vector fields $\tilde{V} \equiv (r^2 + a^2)\partial_t + a\partial_{\phi}$ and $\tilde{W} \equiv \partial_{\phi} + \mathcal{A}\partial_t$ then the contraction the geodesic four-velocity with \tilde{W} leads to the (non-conserved) quantity $L - E\mathcal{A}$, function of the conserved quantities (E, L) , the spacetime parameter a and the polar coordinate θ . When we consider the principal null congruence $\gamma_{\pm} \equiv \pm\partial_r + \Delta^{-1}\tilde{V}$ the angular momentum $L = \mathcal{A}$ that is $\bar{\ell} = 1$ (and $E = +1$, in proper unit), every principal null geodesic is then characterized by $\bar{\ell} = 1$, on the horizon it is $L = E = 0$.

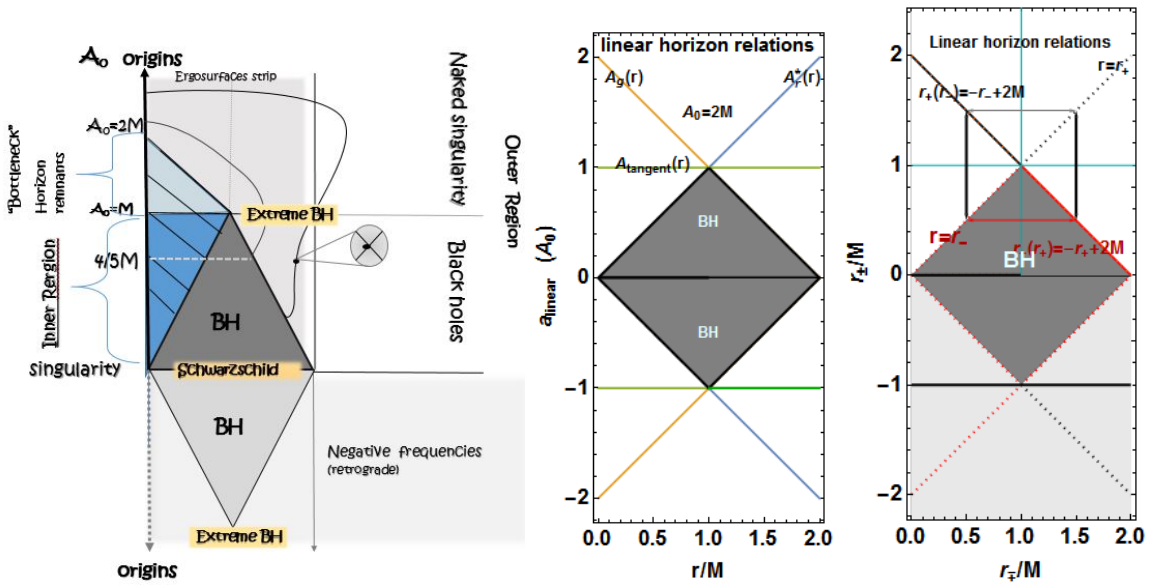


FIG. 2: **Kerr extended plane.** Horizons properties are independent of the plane $\sigma \equiv \sin^2 \theta$. Here $\mathcal{A} \equiv a\sqrt{\sigma}$. The plane is split in the negative frequencies region ($a < 0$) (below part) and the upper part for positive bundle characteristic frequencies. Central gray triangle is the **BH** in the positive $a_0 > 0$ region of the extended plane. This contains all the Kerr **BH** geometries. Each point of a bundle is represented on the plane. In the left panel, each point of a bundle is a crossing point of two bundles. The *interior region*, *exterior region* and the *bottleneck* region are defined, for example, in Fig. (19). The transformations are given in Eq. (B3). The linear relations for the horizons in the extended plane are obtained explicitly in [21], for example, in the $(r - r)$ plane. The center panel represents the extended plane (a, r) with the transformations given in Eq. (B3)–Fig. (19). The right panel shows the linear relations within the transformations $r_{\mp}(r_{\pm})$ of [21].

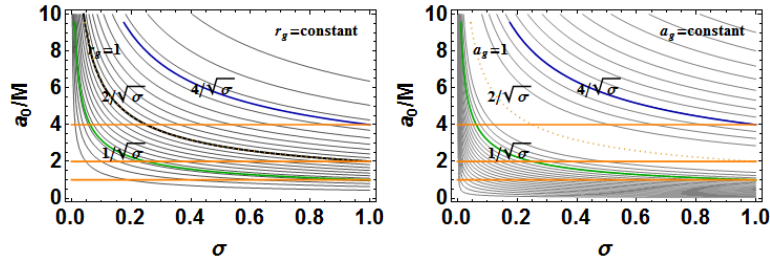


FIG. 3: Plot of the constant bundle tangent radius r_g/M and tangent spin a_g/M on the plane $\sigma \in [0, M]$ and for $a_0 > 0$. Special values and curves are also show. These special values play an essential role for the characteristic frequencies of the bundles (see also Sec. B). It refers to the analysis of Eq. (A15).

hole is “inaccessible” to the metric bundles since they are tangent to the horizon (do not penetrate the sphere of **BH** region in the extended plane). Replicas of the **BH** triangle and the set Γ_{a_g} allow us to establish a connection between the inner regions, bounded by the inner horizon, and the region outside the outer horizon.

The explicit expression a_{ω} , which determines metric bundles, can be found in Sec. (C1). The condition $\mathcal{L} \cdot \mathcal{L} = 0$ can also be solved for the radius r (light surfaces r_s^i as functions of the frequencies ω and the polar plane σ for fixed values of a), as explained in Sec. (C2). Otherwise, the condition $\mathcal{L} \cdot \mathcal{L} = 0$ can be solved for the polar plane $\sigma \in]0, 1]$ in terms of a, ω and r , as presented in Sec. (C3).

C. Characteristics of the metric bundles

We explore the **MBs** considering the more general definition $\Gamma_{\mathbf{x}}$ and $\Gamma_{\mathbf{x},\mathbf{y}}$ introduced in Sec. (II A), for various quantities \mathbf{x} and \mathbf{y} listed in Table (I). This analysis is focused on the characteristics and properties of bundles as curves in the extended plane $\mathcal{P} - r$, where $\mathcal{P} = \{\mathcal{A}, a\}$. We start in Sec. (II C 1) with the analysis of the limiting case of static geometry (the Schwarzschild background) corresponding to the zeros of the **MBs** curves, i.e. the

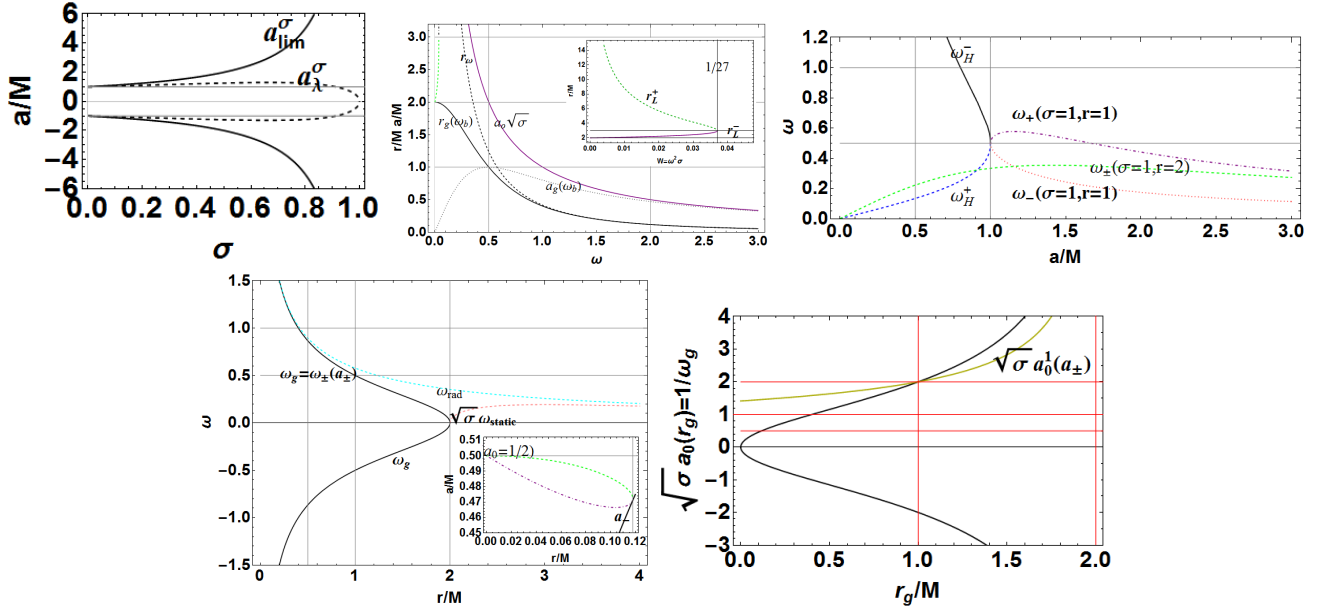


FIG. 4: Panels refer to the analysis of the metric bundles zeros, determined by Eq. (10), and to the results presented in Sec. (C3) regarding spins, frequencies and planes limiting values, which are relevant for the existence of bundles. Upper panels. Left: spins a_{lim}^σ and a_λ^σ of Eq. (C5) as functions of $\sigma = \sin^2 \theta$. Center: Inner panel: r_L^\pm as function of $W \equiv \omega^2 \sigma$ of Eq. (10), the limiting value $W = 1/27$ is also shown. Plot of r_ω of Eq. (C8). The tangent radius $r_g(\omega_b)$ of Eq. (A4) as function of the bundle frequency. The bundle origin is $a_0 \sqrt{\sigma}$ and the tangent spin is $a_g(\omega_b)$ as given in Eq. (A4). Right panel: frequencies of Eq. (C7) and the horizon frequencies ω_H^\pm . Bottom panels. Left: Horizon frequencies, as bundle tangent frequencies $\omega_b = \omega_\pm(a_\pm)$ of Eqs. (8), as functions of the radius r/M , ω_{static} of Eq. (10) and ω_{rad} of Eq. (C5). The inner panel is the bundle with origin $a_0 = 1/2$. Right panel: origin spins a_0/M .

metric bundles curves \mathbf{C} intersections with the axis $a = 0$. The main features of metric bundles are discussed in Sec. (II C 2). The crossing of \mathbf{MBs} with notable curves of the extended plane is discussed in Sec. (II C 2); we also study the intersections of the curves \mathbf{C} with the horizontal lines $\mathcal{P} = \text{constant}$, which represent a single geometry, exploring, therefore, the metric bundles characteristics in one specific spacetime. The analysis of the intersections of the \mathbf{MBs} curves with the vertical lines of the plane singles out a fixed orbit $r = \text{constant}$. Finally, we explore the tangency conditions of the bundles with the horizon curve. In Sec. (A 0 a), we study in details the \mathbf{MBs} Γ_x for different quantities \mathbf{x} as listed in Table (I) This subsection closes in Sec. (II C 3) with the investigation of crossing metric bundles, i.e., the intersections of \mathbf{MBs} curves in the extended plane, determining the couple of light-like orbital limiting frequencies for time-like stationary observers.

1. The zeros of the metric bundles: the static geometry

The zeros of the metric bundles, i.e. solutions $a_\omega(\sigma) = 0$ explicitly given in Sec. (C 1), correspond to the static case described by the Schwarzschild metric. The frequencies are (see Figs 4)

$$\omega_{\text{static}} = \pm \frac{\sqrt{r-2}}{r^{3/2} \sqrt{\sigma}}. \quad \text{Equivalently, in terms of radii (light surfaces)} \quad (10)$$

$$r_L^+(W) \equiv \frac{2\sqrt{\frac{1}{W}} \cos \left[\frac{1}{3} \cos^{-1} \left(-\frac{3\sqrt{3}}{\sqrt{W}} \right) \right]}{\sqrt{3}}, \quad r_L^-(W) \equiv -\frac{2\sqrt{\frac{1}{W}} \cos \left[\frac{1}{3} \left[\cos^{-1} \left(-\frac{3\sqrt{3}}{\sqrt{W}} \right) + \pi \right] \right]}{\sqrt{3}},$$

$$\text{where } W \equiv \sigma \omega^2 \geq 0, \quad W_{\sigma=1} \equiv \frac{r-2}{r^3}, \quad r_L^+(W) = r_L^-(W) = 3M \quad \text{for } W = W_{\text{max}} \equiv \sigma \omega^2 = 1/27$$

which also depend on the polar angle and on the metric bundle origin. The radii $r_L^\pm(W)$ are solutions of the condition $\mathcal{L} \cdot \mathcal{L} = 0$. The general form of these solutions (light surfaces) for the stationary case can be found in Sec. (C 2). It is clear, in fact, that the problem for the static case can be written in terms of the variable $W \equiv \sigma \omega^2 \geq 0$. This quantity,

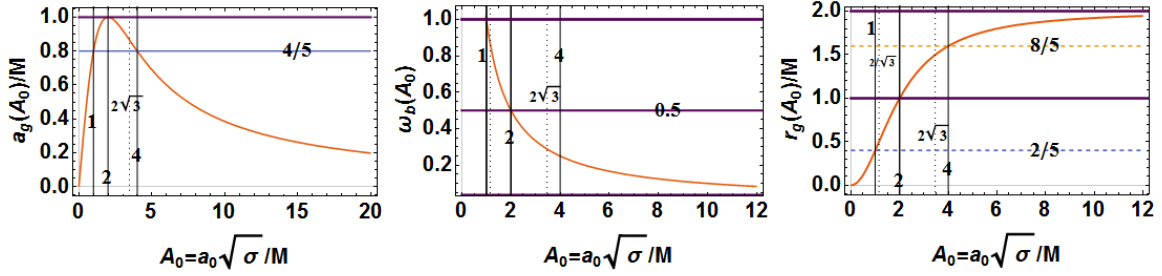


FIG. 5: Tangent spin $a_g(\mathcal{A}_0)$ (left panel), bundle frequency $\omega_b(\mathcal{A}_0)$ (center panel) and tangent radius $r_g(\mathcal{A}_0)$ (right panel) of the bundle as functions of $\mathcal{A}_0 \equiv a_0\sqrt{\sigma}$, where a_0 is the bundle origin $\sigma = \sin^2\theta$ —see Eqs (A4).

in fact, defines the bundle origin a_0 in terms of its frequency according to Eqs. (7). The limiting values $W_{\max} = 1/27$, which occurs for $r = 3M$, corresponds to a photon (last) circular orbit and is also an extremum for ω_{static} , where $\omega_{static} = 1/3\sqrt{3}\sqrt{\sigma}$. Finally the condition $\mathcal{L} \cdot \mathcal{L} = 0$ can be solved for the bundle frequency $\omega(a) = \omega_0^\pm(a_s)$, leading to relations between the spins (a, a_s) as follows

$$\text{from } \omega(a) = \omega_0^b(a_s) \quad a_s^{b,\mp} \equiv b \frac{2ar\sqrt{\sigma} \mp \sqrt{\Delta\Sigma^2}}{a^2(\sigma - 1) - (r - 2)r}, \quad \text{where } b \equiv \pm \quad (11)$$

2. Main features of metric bundles

The main quantities describing metric bundles, as used in Figs (2), are related in a simple way as follows

$$(1) \quad \frac{r_g}{a_g} = \frac{a_0\sqrt{\sigma}}{2}, \quad (2) \quad \frac{r_g}{a_g} = \frac{1}{2\omega_b} \quad \text{from} \quad (3) \quad a_0 = \frac{1}{\sqrt{\sigma}\omega_b}, \quad (4) \quad a_0(a_g) = \frac{2r_\mp(a_g)}{a_g\sqrt{\sigma}} = \frac{4\omega_H^\pm(a_g)}{\sqrt{\sigma}}. \quad (12)$$

Relation (1) relates the bundle tangent spin a_g and bundle origin a_0 with the tangent radius r_g and depends on σ . On the contrary, relation (2) does not depend on the plane σ as it relates r_g and a_g which are defined at the horizon, with the bundle frequency ω_b . We recall that the bundle frequency is uniquely determined by the radius r_g (but not by the tangent spin a_g). Furthermore, relation (2) is more general than relation (1) since it defines the class Γ_{ω_b} of bundles with equal frequencies ω_b as studied in Eqs. (A7) and Figs (14). However, according to Eq. (A7) for fixed ω_b , a_g , and r_g , there is a class of bundles related by means of σ planes (for a fixed r_g , there is one and only one characteristic frequency ω_b independently of the plane σ). Finally, regarding relation (4), which defines the bundle origin $a_0(a_g)$ as function of the bundle tangent point a_g , it is worth noting that this is the inverse relation of $a_g(a_0, \sigma)$ given in Eq. (9) and shown in Figs (5).

We now study some important properties of metric bundles and introduce the concept of pairs of corresponding bundles.

Note that each metric bundle corresponds to one and only one bundle frequency ω_b and to one and only one tangent point r_g . To each frequency ω_b corresponds one and only one tangent spin and tangent radius and, viceversa, to a tangent radius r_g corresponds only one ω_b . There is, therefore, the class Γ_{ω_b} composed by metric bundles with equal characteristic frequency (and equal tangent spin a_g and radius r_g) having, in general, different planes σ and, consequently, different origins a_0 . We study the class Γ_{ω_b} in Eqs. (A7). The class Γ_{a_g} is composed of metric bundles with equal tangent spin a_g , but different planes σ and, therefore, different origins a_0 , with the tangent radius $(r_g, r_g^1) \in r_\pm(a_g)$ and frequencies $(\omega_b, \omega_b^1) \in \omega_H^\pm$. This case is studied in Eqs. (A7). Bundles of this class form the **BH** spacetime horizon with spin a_g . The class Γ_σ is composed by metric bundles on the same plane σ ; we study this case in Eq. (A4). We note that the condition $\mathcal{L}_\mathcal{N} = 0$ depends on the angle θ ; therefore, as we will also see in detail, many essential bundle properties can be described in terms of the variable $\mathcal{A} \equiv a\sqrt{\sigma}$, except for the fact that bundles are tangent to the horizon which is independent of θ . For instance, Γ_{a_0} is the class of metric bundles with the same origin a_0 ; this case is studied in Eq. (A1).

Notable curves in the extended plane

In the extended plane, there are certain curves representing geometries with similar properties. We consider the following notable curves:

(1) Vertical lines, $\bar{r} = \text{constant}$ can be used to analyze properties of Kerr geometries, for all $a \in [0, M]$, at the point \bar{r} on different planes σ . At \bar{r} , for fixed $a = \bar{a}$, there is an even number of bundles that intersect at \bar{r} , apart from the horizon curve a_\pm .

(2) Horizontal lines $\bar{a} = \text{constant}$ characterize properties of a fixed Kerr geometry. The spin \bar{a} can be considered as origin a_0 , if $a_0 > 0$, or also as tangent spin a_g , if $a \in [0, M]$.

3. Crossing of metric bundles: determination of the orbital limiting frequencies

Metric bundles cross on the extended plane at a point (a, r) . The two frequencies (ω_1, ω_2) of a **MB** with fixed (a, σ, r) are related as

$$\omega_2 = -\frac{4ar}{a^2\sigma\Delta - (a^2 + r^2)^2} - \omega_1, \quad (13)$$

where ω_1 and ω_2 are given as ω_{\pm} in Eq. (6). The two origins of the **MBs**, as functions of any point in the bundle (r, a, σ) , are

$$\begin{aligned} a_0^1 &\equiv \frac{\sqrt{\sigma\Delta\Sigma^2 + 2ar\sigma}}{\sqrt{\sigma}[a^2(\sigma - 1) - (r - 2)r]} & a_0^2 &\equiv \frac{\sqrt{\sigma}[a^4(1 - \sigma) + a^2r[2\sigma + r(2 - \sigma)] + r^4]}{\sqrt{\sigma\Delta\Sigma^2 + 2ar\sigma}}, \quad \text{where} \\ a_0^1 a_0^2 &= \frac{(a^2 + r^2)^2 - a^2\sigma\Delta}{a^2(\sigma - 1) - (r - 2)r}, \quad \text{for } (a, r, \sigma) \text{ at the bundle crossing.} \\ \text{Then } a_0^1 &= a_0^2 \text{ for } a = a_{\pm}(r) \text{ (} r = r_{\pm}(a)\text{),} & (14) \\ \text{or } a = \tilde{a}_{\pm} &= \pm \frac{r}{\sqrt{\sigma - 1}}, \quad (r = \tilde{r}_{\pm} = \pm a\sqrt{\sigma - 1}) \text{ or } \sigma = \tilde{\sigma} \equiv \frac{a^2 + r^2}{a^2}. \end{aligned}$$

Conditions (14) show **MBs** solutions with the same origin a_0 and tangent point in (a, r, σ) , that is, the same spin a , equal plane σ and crossing radius r . This analysis is related to the horizon curve, where

$$a_0^1(r_{\pm}(a)) = \frac{2r_{\pm}}{a\sqrt{\sigma}}, \quad a_0^1(a_{\pm}) = \pm \frac{2r}{a_{\pm}\sqrt{\sigma}}, \quad a_0^1(\tilde{a}_{\pm}) = \pm \frac{r\sqrt{\sigma}}{\sqrt{\sigma - 1}}, \quad a_0^1(\tilde{r}_{\pm}) = a\sqrt{\sigma}, \quad a_0^1(\tilde{\sigma}) = a\sqrt{\frac{r^2}{a^2} + 1}. \quad (15)$$

Obviously, the second frequency at a point of the bundle geometry is also a horizon frequency, that is, if ω_b is a bundle frequency, then at the point r a photon will have orbital frequency ω_b , while the second frequency of the couple ω_{\pm} is associated with the horizon frequency of the bundle crossing at the point (a, r) .

If (a_{\times}, r_{\times}) represent the crossing points of two **MBs** with frequencies $\omega_b(a_g) < \omega_b^p(a_g^p)$, it is clear that $\omega_b(a_g) = \omega_H^+(a_g)$ and $\omega_b^p(a_g^p) = \omega_H^-(a_g^p)$. It follows that the two crossing **MBs** are necessarily one tangent to an outer horizon and another one tangent to an inner horizon. On the other hand, the relation between **MBs** frequencies is independent of the angle θ (equivalently σ) as the bundle characteristic frequencies are horizon frequencies (they will, of course, depend on the plane σ when related to their bundle origin spins). Now, it is possible to find **MBs** crossing at a point (r_{\times}, a_{\times}) of the extended plane, which have different planes σ . However, such **MBs** relate, in the geometry with crossing spin a_{\times} , frequencies associated with the crossing orbit r_{\times} , but on different planes (σ, σ_p) of the same Kerr geometry. It is possible to constraint this case considering ω_{\pm} in Eq. (6) as functions of σ only or, viceversa, using the solutions σ_{ω}^{\pm} of Eqs (C6) as functions of ω .

However, we note that for fixed σ at the point (a_{\times}, r_{\times}) there are frequencies $(\omega_H^+(a_g), \omega_H^-(a_g^p))$ for two tangent bundle spins (a_g, a_g^p) , respectively. Because of the existence of the two frequencies ω_{\pm} per point per spin and per plane, we infer that at each point of the extended plane there is an even number of crossing **MBs** (a part of the limiting case of the horizon curve). In particular, for the same plane σ , we have that $(\omega_H^+(a_{g,1}, \sigma^1), \omega_H^-(a_{g,1}^p, \sigma^1))$ and the relations (A4) hold as special cases of Γ_{σ} . In general, the following relations hold:

$$a_g = \frac{4\omega_+(a_{\times})}{4\omega_+(a_{\times})^2 + 1} \quad a_g^p = \frac{4\omega_-(a_{\times})}{4\omega_-(a_{\times})^2 + 1} \quad a_0 = \frac{1}{\sqrt{\sigma}\omega_+(a_{\times})} = \frac{2r_+(a_g)}{\sqrt{\sigma}a_g} \quad a_0^p = \frac{1}{\sqrt{\sigma_p}\omega_-(a_{\times})} = \frac{2r_-(a_g^p)}{\sqrt{\sigma_p}a_g^p}. \quad (16)$$

In Fig. (6), we show the frequencies at a fixed point (a, r) of the extended plane for different σ . Notice the frequency signs (negative for retrograde photon motion) and the decreasing behavior of the frequencies in terms of the plane σ at fixed r . Notice also the role of the ergoregion. In the next Section, we will focus particularly on **MBs** with fixed a and characteristic frequency equal to $\omega_H^{\pm}(a)$. This is clearly the problem of the **MBs** confinement with a frequency equal to the horizon frequency.

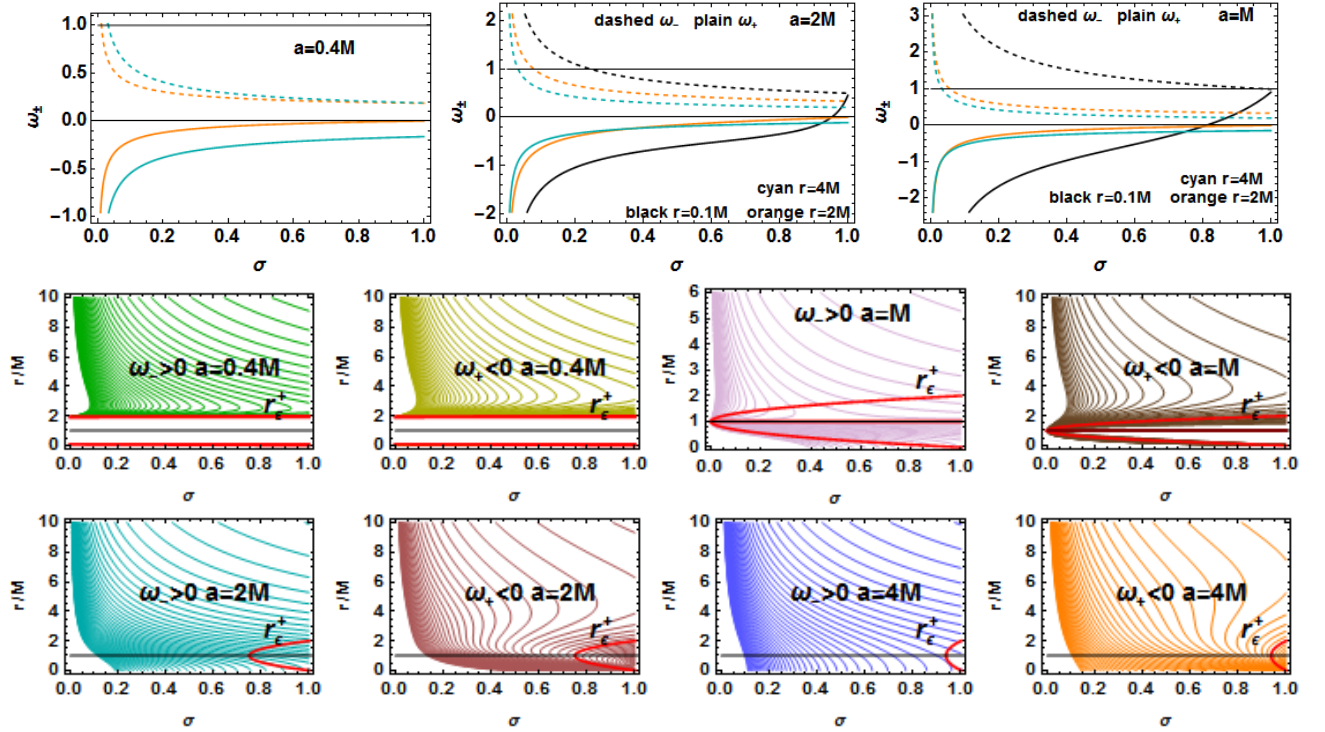


FIG. 6: Upper lines: bundle frequencies ω_{\pm} as functions of the plane $\sigma \in [0, 1]$ for fixed spin a/M and radius r/M of the extended plane. Note the frequencies signs (negative for retrograde photon motion) and the decreasing magnitude with the plane σ at fixed r . The limiting roles of the horizons and ergosurfaces can also be noted. Below lines: solutions $\omega_{\pm} = \text{constant}$ on the $(r/M, \sigma)$ plane. Note the frequencies sign, always positive in the ergoregion (red curves are the ergosurfaces r_{ϵ}^{\pm}), horizons are also show. The curves are studied for different spins $a/M > 0$. See the analysis of Sec. (II) on the crossing of metric bundles and determination of orbital limiting frequencies

III. EXTRACTING INFORMATION FROM KERR METRIC BUNDLES: PHOTON FREQUENCY AND HORIZON FREQUENCIES

We now consider the condition $\omega_x = \omega_y$, where $\omega_x \in \{\omega_+, \omega_-\}$ and $\omega_y \in \{\omega_H^-, \omega_H^+\}$. We look for all those solutions of $\mathcal{L}_{\mathcal{N}} \equiv \mathcal{L} \cdot \mathcal{L} = 0$ associated to orbits r different from the horizon, but characterized by a photon with orbital frequency equal to that of the horizon per equal a . We are looking for solutions of the normalization condition $\mathcal{L}_{\mathcal{N}} = 0$ when $\omega = \omega_H(a)$ for a geometry with spin a with a $\bar{r} \neq r_{\pm}$. We are particularly interested in cases where $\bar{r} > r_+$, from which the most relevant case is for $\bar{r} > r_+$ with $\omega_*(\bar{r}) = \omega_H^-$ for $\omega_* \in \{\omega_+, \omega_-\}$.

Combining the considerations of the bundle crossing and inner horizon confinement problem, we note that the existence of an “external” orbit (at $r > r_+$), with one frequency equal to the inner horizon frequency on the extended plane, implies that in the region $r > r_+$ bundles tangent to the inner and outer horizons intersect. We are then confronted with a two-sided problem: **1.** The problem of finding a point $r > r_+(\bar{a})$ in $\bar{a} \in [0, M]$ with frequency $\omega_H^-(a_*)$ for a general spin $a_* \neq \bar{a}$ such that $\omega_{\pm}(\bar{a}) = \omega_H^-(a_*)$. **2.** The problem of finding a solution $\omega_{\pm}(\bar{a}) = \omega_H^-(\bar{a})$ (i.e. $a_* = \bar{a}$). We have met this kind of problems in several parts of our investigation. We will show that the second problem exists on planes very close to the rotation axis. Consider the spin $\bar{a} = \text{constant}$ of a bundle with frequency $\omega_H^-(\bar{a})$ on a plane σ and analyze the problem for σ with $r > r_+(\bar{a})$ and $\omega_{\pm}(\bar{a}) = \omega_H^-(\bar{a})$. It can be proved that solutions of this problem are $r_{\mathcal{L}}$ (or, equivalently, in terms of the spin $a_{\mathcal{L}}$ and in terms of the plane $\sigma_{\mathcal{L}}$), if the following conditions are satisfied

$$\sigma \in [0, \sigma_{descr}], \quad \text{or} \quad \sigma \in [0, \sigma_{\delta}], \quad r \in [M, r_{descr}], \quad a \in [a_{\delta}, M] \quad (17)$$

$$\text{where} \quad \sigma_{\delta} \equiv \frac{1}{2} \left[r(r+2) - \sqrt{(r+1)^2[r(r+2)+9]} + 5 \right]; \quad r_{descr} \equiv \sqrt{\sigma + \frac{4}{\sigma} - 4} - 1;$$

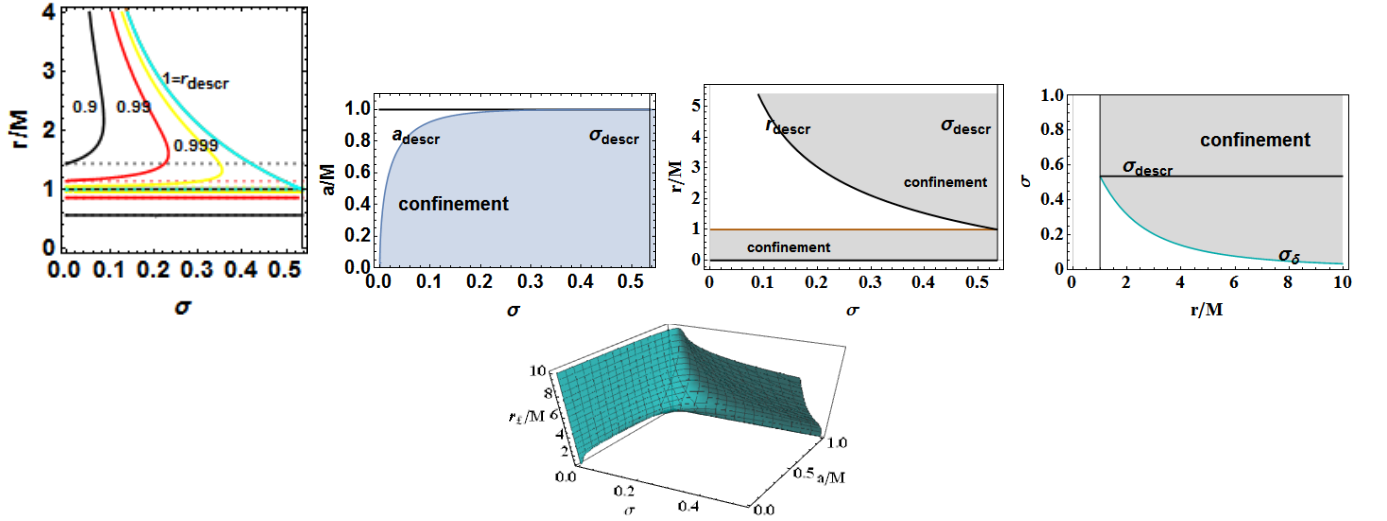


FIG. 7: Inner horizon confinement on the extended plane. Constraints on the existence of orbits of the exterior region on the extended plane $r > r_+$ with frequencies $\omega_- = \omega_H^-$. See the analysis of Sec. (III) and Eq. (17). Left panel: orbits $r_{\mathcal{L}}$ solutions of $\omega_- = \omega_H^-$ (photons defined by the condition $\mathcal{L}_{\mathcal{N}} = 0$) as function of the plane $\sigma \in [0, 1]$ for different spins a/M . The limiting value $a = M$, black curve coincident also with $r_{desc}(\sigma)$. The solutions of $\omega_- = \omega_H^-$ clearly include also the inner horizon $r_-(a)$. The horizons $r_{\pm}(a)$ are also showed (horizontal lines). The limiting value $\sigma_{desc} \approx 0.53M$. A solution is clearly the inner horizon r_- . The larger is the **BH** spin, the larger can be the plane value function $\sigma \leq \sigma_{desc}$. Shaded regions are confinement regions. Below: 3D plot is $r_{\mathcal{L}}$, containing a solution of $\omega_- = \omega_H^-$ as function of a/M and σ . Quantities are defined in Eq. (21,18,19,20).

and $\sigma_{\mathcal{L}}$, $a_{\mathcal{L}}$ and $r_{\mathcal{L}}$ are solutions of the equations

$$\sigma_{\mathcal{L}}: \quad \sigma^4 [a^8 + a^6(r-2)r] - 2a^4\sigma^3 [a^4 + 2a^2(r^2-2) + r^4 - 8r + 8] + 16[a^4 + a^2(r-2)r] + 8\sigma(a^6 + 2a^4(r^2-3) + a^2r(r^3-4r+8) - 2r^4) + \sigma^2[a^8 + a^6(r-2)(3r+8) + a^4[(r-2)r(r+2)(3r+4) + 48] + a^2r[r(r(r(r+2)+4) - 8) + 16] - 32] = 0, \quad (18)$$

$$\mathbf{a}_{\mathcal{L}}: \quad a^8(\sigma^4 - 2\sigma^3 + \sigma^2) + a^6(\sigma-1)\sigma[\sigma[r^2(\sigma-3) - 2r(\sigma+1) + 8] - 8] + a^4(-2(r^4-8r+8)\sigma^3 + 16(r^2-3)\sigma + [(r-2)r(r+2)(3r+4) + 48]\sigma^2 + 16) + a^2r(8(r^3-4r+8)\sigma + (r(r(r(r+2)+4) - 8) + 16) - 32)\sigma^2 + 16(r-2) - 16r^4\sigma = 0, \quad (19)$$

$$\mathbf{r}_{\mathcal{L}}: \quad a^2r^6\sigma^2 + 2a^2r^5\sigma^2 + 4a^2(a^2-2)r^3\sigma^2 - 2a^2r(\sigma-1)(a^2\sigma-4)[\sigma(a^2(\sigma+1)-4) + 4] + r^4\sigma[a^4\sigma(3-2\sigma) + 4a^2(\sigma+2) - 16] + a^2r^2(\sigma(a^4(\sigma-3)(\sigma-1)\sigma + 4a^2(4-3\sigma) + 16(\sigma-2)) + 16) + a^4(\sigma-1)^2(a^4\sigma^2 + 8(a^2-2)\sigma + 16) = 0, \quad (20)$$

respectively, whereas the limiting spin a_{δ} is a solution of the following equation

$$\mathbf{a}_{\delta}: \quad a^{10}(\sigma-1)^2\sigma^6 - 2a^8(\sigma-1)\sigma^4(3\sigma(5\sigma-28) + 68) + a^6\sigma^2[\sigma(\sigma(201\sigma+1160) - 2784) + 1408] + 16, \quad (21)$$

$$+ 8a^4\sigma[(\sigma((1045-411\sigma)\sigma - 1228) + 588) + 16] + 16a^2(\sigma-1)(\sigma(97\sigma+447) - 312) - 16 - 6912(\sigma-1)^2\sigma = 0.$$

We show the behavior of these quantities and the constraints for the existence of orbits with frequency of the inner horizon in the outer region of the extended plane $a > a_+$ in Fig. (7). A more detailed study of the frequency ratio of **MBs** as horizon frequencies is given in Sec. (B).

As we shall see in detail also in Sec. (B), bundles with origin spin in the weak black holes (**WBH**) region of the extended plane, i.e., with $\mathcal{A}_0 = a_0\sqrt{\sigma} \leq 4/5 \leq 0.8M$, for sufficiently large values $\sigma \gtrsim 1$ and particularly on the equatorial plane, are *entirely confined* in the **BH** region (the inner region of the extended plane as in Fig. 2). It follows that their characteristic frequencies (with tangent spin $r_g \in]0, 2M/5[$ and characteristic frequencies $\omega_b \geq 1$) can never be "replicated" in those planes in the outer region of the extended plane. However, constraints can be found in terms of the variable \mathcal{A}_0 . Frequencies $\omega_b \geq 0.5$ (range of ω_H^-) for orbits in the outer region are shown in Figs (8,13,12,14, 16,9).

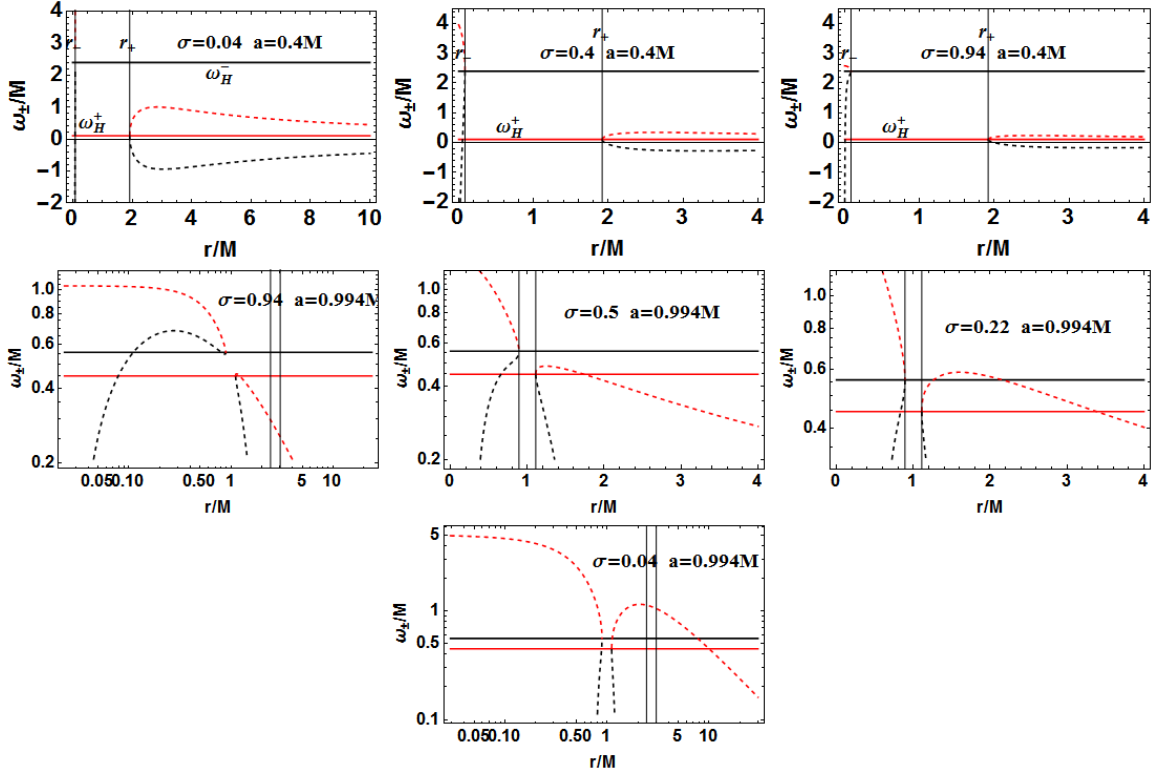


FIG. 8: Frequencies ω_{\pm} for different spins a/M and planes σ , as functions of r/M . The horizontal lines are horizon frequencies ω_{H}^{\pm} , vertical lines are the inner and outer horizons r_{\pm} . There are solutions $\omega = \omega_{H}^{\pm}$ particularly for $r > r_{+}$, according to Eqs. (25,26).

This is a consequence of the fact that if the (a_g, r_g) relations can be expressed as functions of $\mathcal{A} = a\sqrt{\sigma}$, this does not hold for the quantity $\mathcal{L}_{\mathcal{N}}$; consequently, it follows that the bundles can extract “information” on the inner horizons frequencies near the rotation axis and, therefore, in this sense, the inner region is not entirely confined. Equally, **MBs** with weak naked singularities (**WNS**) origins, i. e., with $\mathcal{A}_0 = a_0\sqrt{\sigma} \in]M, 2M]$, which complete the inner horizon with tangency radius $r_g \in]2M/5, M[$, spin $a_g \in]0.8M, M]$ and characteristic frequency $\omega_b \in [0.5, 1[$, for small σ can be found in the outer region of the extended plane. We shall see this in details in Sec. (B).

For the equatorial plane, $\sigma = 1$, this condition was considered in detail in [21], where the concept of inner horizon confinement was introduced. We resume this issue as follows (see Fig. 8). It was shown that there are two radii r_{\pm}^{\pm} such that $r_{-}^{-} < r_{-} < r_{+} < r_{+}^{+}$ almost everywhere (exceptions are at $a_g = 0$ and $a_g = M$) and $\omega_{*}(r_{\pm}^{\pm}) = \omega_{H}^{\pm}$, respectively.

The problem of finding solutions of $\mathcal{L}_{\mathcal{N}} = 0$ for ω_{H}^{\pm} is clearly related to the characterization of the **MBs** Γ_{a_g, ω_b} , constituted by the **MBs** Γ_{a_g} with equal tangent spin a_g and already analyzed in Eqs. (A8), and equal frequency Γ_{ω_b} (and equal tangent radius r_g) also analyzed in Eqs. (A7). Therefore, the particular relations given in Eqs (A9) are valid.

There are then two classes of **MBs** to be considered. Firstly, we focus on equal σ solutions, discussed in Eq. (A9). Solutions $r : \omega_{\pm}(r) = \omega_{H}^{\pm}(a_g)$ belong to the same bundle and, therefore, depend on the bundle curves bending (curvature) on the extended plane. In fact, as follows from Figs 13,12,14 and 16, the situation is simple in the case $\sigma = 1$, where there are two bundle branches (closed on the horizons) corresponding to the two solutions r_{\pm}^{\pm} , respectively. Alternatively, the analysis can be performed by considering the frequency solutions (6) directly (see Fig. (8)), where the horizon-frequency solutions are given by horizontal lines (corresponding to $\omega = \omega_{H}^{\pm}$) on the extended plane.

Solutions for equal planes and equal tangent frequencies belong to the same metric bundle; therefore, they must share the same origin a_0 . (The relevance of the equatorial case $\sigma = 1$ for the Kerr **MBs** analysis lies also in the fact that for the spherically symmetric, static and electrically charged Reissner Nordström solution, the **MBs** curvature properties in the extended plane are similar to the off-equatorial case of the Kerr geometry, showing the interplay between symmetries and geometry in defining the **MBs** properties– [21].) Then, for a general σ , we consider the two-faced problem for the orbits of frequencies ω_{H}^{\pm} , considering the **MBs** $\Gamma_{a_g}^{-} \equiv \{g_{\omega}(a_g, r_g^{-})\}_{\sigma}$ and $\Gamma_{a_g}^{+} \equiv \{g_{\omega}(a_g, r_g^{+})\}_{\sigma}$,

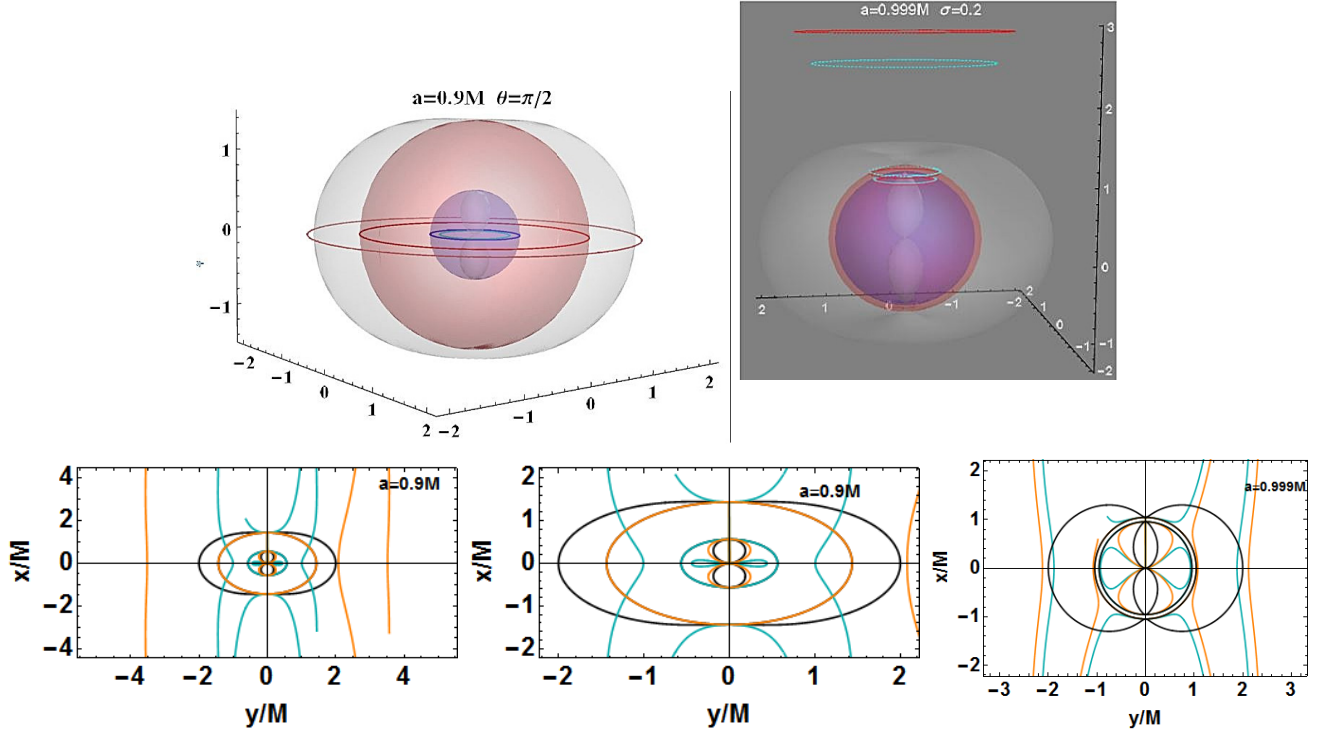


FIG. 9: Horizon frequency solutions of the **MBs** in the exterior region are horizontal lines of the extended plane in Figs (2). The plots show, for fixed plane $\sigma \equiv (\sin \theta)^2$, the inner and outer horizons, the inner and outer ergosurfaces, the circle in the outer horizon, (red) on the inner horizon (blue) and orbital solutions with frequency of the inner (blue) and outer (red) horizon. In the frame we use, the **BH** Kerr ring singularity is at $r = 0$. In the lower panels, the light surface solutions $\{r_s^1, r_s^2, r_s^4\}$ of Eq. (C2) are plotted for $\omega = \omega_H^+$ (orange) in $\omega = \omega_H^-$ (darker cyan). Black curves are the inner and outer ergosurfaces and the inner and outer Killing horizons. These orbits contain replicas of the horizons as defined in Eq. (D7).

where r_g^\pm are, respectively, the tangent points of the two bundle families on the outer and inner horizons of the **BH** with spin a_g . To these **MBs** correspond, respectively, the horizon frequencies $\omega_b^- > \omega_b^+$ of the **BH** spacetime with spin $a = a_g$. In the second case, we consider in the classes $\Gamma_{a_g}^\pm$ the pairs $(g_\omega(a_g, r_g^-, \sigma), g_\omega(a_g, r_g^+, \sigma)) \in \Gamma_{a_g, \sigma}^- \times \Gamma_{a_g, \sigma}^+$ i.e. with the same a_g on the same σ (recall that the horizon frequencies ω_b^\pm are independent of σ , a property linked to the **BHs** horizon rigidity).

We now focus on the range $a \in [-M, M]$ of **BH** spacetimes. In fact, for different a , solutions are provided as **MBs** intersections which, for each plane σ at each point r (except for the origin), involve only two bundles. This case is considered in Fig. (10), where we see solutions for $r \neq r_\pm$ for small values of σ and for $r_-^o > r_+$ with frequencies ω_H^- , that is, equal to the frequency of the inner horizon which, therefore, is not confined to $r < r_-$.

1. Results

We study the problem of finding solutions with a frequency that coincides with that of the inner horizon ω_H^- . There are two possibilities:

- (1) There are no solutions of $\omega_+ = \omega_+(r_-)$ for $r > r_-$ in $a \in [0, M]$.

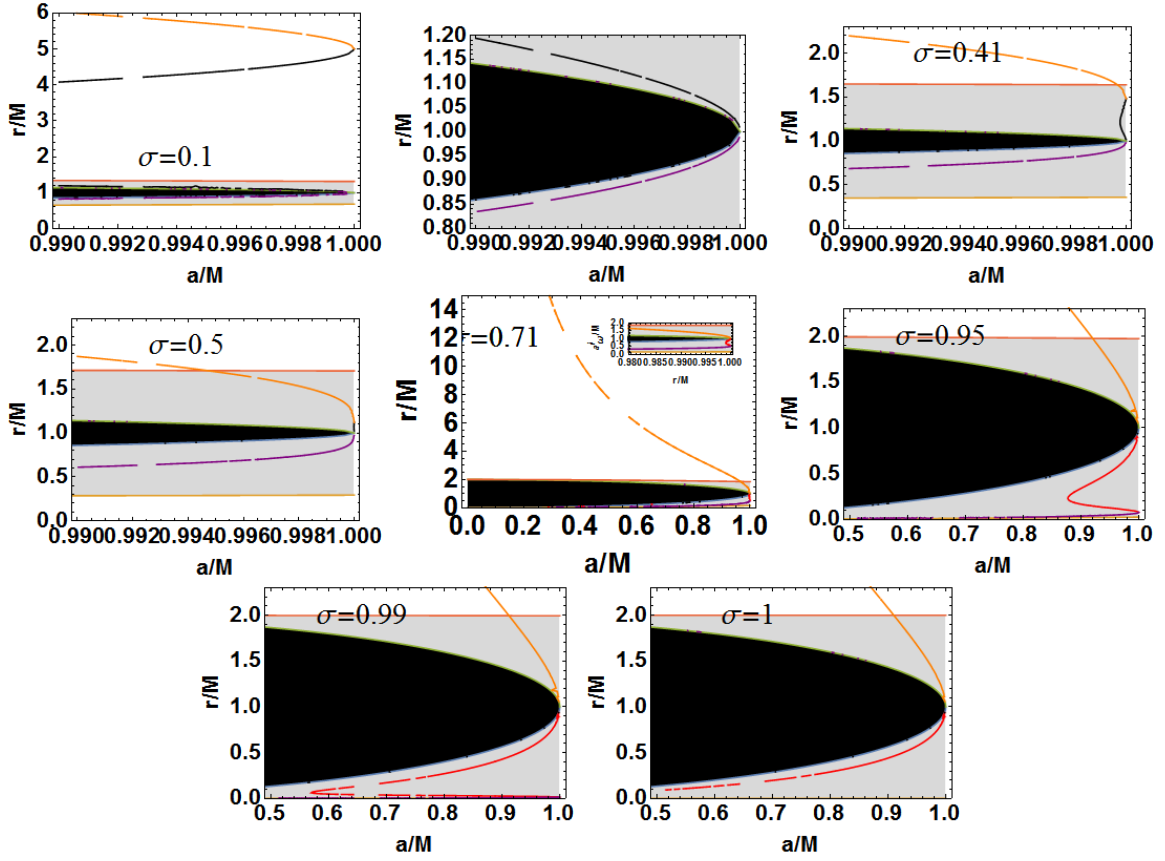


FIG. 10: Photon orbital frequencies and horizon frequencies. In the plane $(a/M, r/M)$, for different planes σ , the solutions $\omega_+ = \omega_+(r_-)$ red curve, $\omega_- = \omega_-(r_-)$ black curve, $\omega_- = \omega_-(r_+)$ orange curve, $\omega_+ = \omega_+(r_+)$ purple curve. The black region is a **BH** on the extended plane $r \in [r_-, r_+]$, the gray region is the ergoregion.

(2) There are instead solutions of $\omega_- = \omega_-(r_-)$. In this case, we express the solutions in terms of the plane σ :

$$\sigma_\gamma^\pm \equiv \frac{\mathcal{B}}{2} \pm \mathcal{L}\mathcal{L} - \frac{\sqrt{\mathcal{B}^2 + \mathcal{F} - \mathcal{Y}}}{2}, \quad \text{where } \mathcal{B} \equiv \frac{a^4 + 2a^2r^2 - 4a^2 + r^4 - 8r + 8}{a^2(a^2 + r^2 - 2r)}, \quad \text{and } \mathcal{F} \equiv -\frac{8(a^2 - 2)}{a^4}, \quad (22)$$

$$\mathcal{L}\mathcal{L} \equiv \frac{1}{2} \sqrt{2\mathcal{B}^2 - \frac{8\mathcal{B}^3 - \mathcal{M} - \mathcal{R}}{4\sqrt{\mathcal{B}^2 + \mathcal{F} - \mathcal{Y}}} - \mathcal{F} - \mathcal{Y}}; \quad \mathcal{M} \equiv \frac{64(a^6 + 2a^4r^2 - 6a^4 + a^2r^4 - 4a^2r^2 + 8a^2r - 2r^4)}{a^6(a^2 + r^2 - 2r)};$$

$$\mathcal{R} \equiv 8(a^4 + 2a^2r^2 - 4a^2 + r^4 - 8r + 8) \cdot$$

$$\frac{(a^6 + 3a^4r^2 + 2a^4r - 16a^4 + 3a^2r^4 + 4a^2r^3 - 12a^2r^2 - 16a^2r + 48a^2 + r^6 + 2r^5 + 4r^4 - 8r^3 + 16r^2 - 32r)}{a^6(a^2 + r^2 - 2r)^2};$$

$$\mathcal{Y} \equiv \frac{a^6 + a^4(r - 2)(3r + 8) + a^2[(r - 2)r(r + 2)(3r + 4) + 48] + r[r(r[r(r(r + 2) + 4) - 8] + 16) - 32]}{a^6 + a^4(r - 2)r}.$$

The behavior of these quantities is illustrated in Figs 11 and 10.

2. The discriminant spin $a_{descr}(\sigma)$

For the problem under consideration an important quantity is the discriminant spin $a_{descr}(\sigma) \in [0, M]$, which is a solution of the following equation

$$a^{10}(\sigma - 1)^2\sigma^6 - 2a^8(\sigma - 1)\sigma^4[3\sigma(5\sigma - 28) + 68] + a^6\sigma^2[\sigma(\sigma(201\sigma + 1160) - 2784) + 1408] + 16 + 8a^4\sigma[\sigma((1045 - 411\sigma)\sigma - 1228) + 588] + 16a^2(\sigma - 1)[\sigma(\sigma[97\sigma + 447] - 312) - 16] - 6912(\sigma - 1)^2\sigma = 0. \quad (23)$$

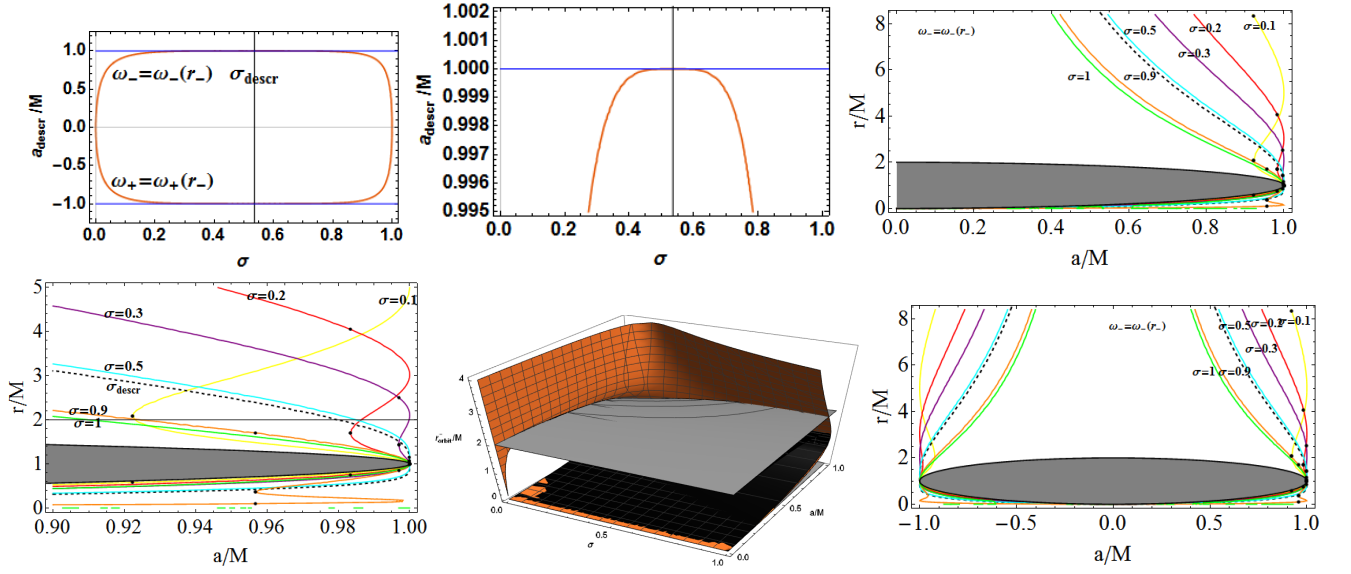


FIG. 11: Photon orbital frequencies as horizons frequencies. Solutions of $\omega_- = \omega_-(r_-)$ for $a \in [0, M]$, and of $\omega_+ = \omega_+(r_-)$ for $a \in [-M, 0]$ for $r > r_-$ —Eqs (25) and (22). Left panel: a_{desc}/M as function of $\sigma \equiv \sin^2 \theta$. Center panel: solutions $\omega_- = \omega_-(r_-)$ on the plane $(r/M, a/M)$ for different planes $\sigma \in [0, 1]$; a zoom for $a \approx M$ is in the right panel. The black region is a **BH** on the extended plane ($r \in [r_-, r_+]$). Below panel: solutions $\omega_- = \omega_-(r_-)$ as functions of r/M for $\sigma \in [0, 1]$ and $a \in [0, M]$. The gray region represents the ergosphere on the extended plane.

The radii r corresponding to frequencies equal to that of the horizon are solutions of the equation

$$\begin{aligned}
 & a^2 r^6 \sigma^2 + 2a^2 r^5 \sigma^2 + 4a^2 (a^2 - 2) r^3 \sigma^2 - 2a^2 r (\sigma - 1) (a^2 \sigma - 4) [\sigma (a^2 (\sigma + 1) - 4) + 4] + \\
 & + r^4 \sigma [a^4 \sigma (3 - 2\sigma) + 4a^2 (\sigma + 2) - 16] + a^2 r^2 (\sigma (a^4 (\sigma - 3) (\sigma - 1) \sigma + 4a^2 (4 - 3\sigma) + \\
 & + 16(\sigma - 2)) + 16) + a^4 (\sigma - 1)^2 (a^4 \sigma^2 + 8(a^2 - 2)\sigma + 16) = 0.
 \end{aligned} \tag{24}$$

More precisely, there are solutions of the problem $\omega_- = \omega_-(r_-)$ as follows:

Solutions $\omega_-(r) = \omega_-(r_-)$ for $r > r_-$: (25)

For $\sigma \in]0, \sigma_{desc}[$ where $\sigma_{desc} \approx 0.535898$:

and (a) $a = M$ with $r = \hat{r}_-$ or (b) for $a \in [a_{desc}, M[$ $r = \check{r}_-$ and (c) $a \in]a_{desc}, M[$ for $r = \hat{r}_-$

Solutions $\omega_-(r) = \omega_-(r_-)$ for $r < r_-$: (26)

For $\sigma \in [\sigma_{desc}, M[$ and $a = a_{desc}$ with $r = r_*$ or $a \in]a_{desc}, M[$ with $r \in (r_*, r_\diamond)$ or $(a = M, r = r_\diamond)$

For $\sigma = 1$ and $a \in]0, M[$ with $r = r_-$.

This implies that the occurrence of orbits $r > r_-$ with photon orbital frequency equal to that of the *inner* horizon is expected for small σ ($\sigma \in [0, \sigma_{desc}]$) and larger spins ($a \in [a_{desc}, M]$)—Figs 11, 10 and 8. It should be noted, as evident also from Fig. 8, that $a_{desc} \approx M$ for $\sigma \lesssim M$ and $\sigma \gtrsim 0$. Finally, the radii $(r_-, r_\diamond, r_*, r_\diamond, \hat{r}_-, \check{r}_-)$ of Eqs. (25 and (26), are solutions of Eq. (24), where r_- is provided in [21].

We now consider negative spins for retrograde orbits, i.e., $a \in [-M, 0]$. There are solutions of $\omega_+ = \omega_+(r_-)$ for $r > r_-$ similarly to the conditions (25) and (26) in $a \in [-M, 0]$ —Fig. (8). We also address this analysis in more details in Sec. (D 1).

There are no solutions of $\omega_- = \omega_H^+$ for $r > r_-$. Moreover, for $\omega_+ = \omega_H^+$, we obtain

Solutions $\omega_+(r) = \omega_+(r_+)$ **for** $r \geq r_-$: (27)

For $\sigma \in]0, \sigma_{descr}[$ and **(a)** $a \in]0, a_{descr}[$ $r \in (r_+, \hat{r})$ or **(b)** $a \in [a_{descr}, M[$ $r \in (r_+, r, \tilde{r})$ or **(c)** $(a = M, r = \check{r})$

For $\sigma = \sigma_{descr}$ and $a \in]0, M[$ $r \in (r_+, r_+^+)$.

For $\sigma \in [\sigma_{descr}, M[$ and **(a)** $a \in]0, a_{descr}[$ $r \in (r_+, \hat{r})$ or **(b)** $a \in [a_{descr}, M[$ $r \in (r_+, \tilde{r})$.

For $\sigma = 1$ and $a \in]0, M[$ $r \in (r_+, \tilde{r})$.

Solutions $\omega_+(r) = \omega_+(r_+)$ **for** $r < r_-$: (28)

For $\sigma \in]0, \sigma_{descr}[$ and $a \in]0, M[$ $r = \tilde{r}$.

For $\sigma \in [\sigma_{descr}, M[$ and $a \in]0, M[$ $r = \tilde{r}$.

Note that the radii $(\hat{r}, \tilde{r}, \check{r}, \tilde{\tilde{r}})$ are solutions of Eq. (24), where r_+^+ is given in [21]. For $a \in [-M, 0]$, there exist solutions for $\omega_- = \omega_H^+$, similarly to the former case (in fact, the equations have some remarkable symmetries). The second frequency at point r is

$$\omega_+(r) = \omega_H^\pm(r) + \Delta\omega(r), \quad \omega_-(r) = \omega_H^\pm(r) - \Delta\omega(r), \quad \Delta\omega(r) \equiv \frac{4\sqrt{\sigma\Delta\Sigma^2}}{\sigma \left[a^2\sigma\Delta - (a^2 + r^2)^2 \right]}. \quad (29)$$

In Sec. (D3), we complete this analysis by introducing the definition of *horizon replicas*. We investigate the vertical lines of the extended plane crossing the horizon curve, in other words, the metric bundles with characteristic frequencies $\omega_b(a) \in \{\omega_H^+(a_p), \omega_H^-(a_p)\}$ with orbits located exactly in $r_\pm(a_p) > r_+(a)$, that is, on the horizon with frequency $\omega_b(a) = \omega_H^\pm(a_p)$.

3. On retrograde solutions with frequencies equal to the horizon frequencies.

We also investigate photon orbits, solutions of $\mathcal{L} \cdot \mathcal{L} = 0$, with frequencies equal and opposite to the horizon frequencies. Because of the symmetries we can restrict ourselves to the case $\omega > 0$ and $a \in]-M, 0[$. We recall that the condition $\mathcal{L}_{\mathcal{N}} = 0$ is symmetric under the inversion $a \rightarrow -a$ and $\omega \rightarrow -\omega$, i.e. $\mathcal{L}_{\mathcal{N}}(a, -\omega) = \mathcal{L}_{\mathcal{N}}(-a, \omega)$ and thus $\mathcal{L}_{\mathcal{N}}(-a, -\omega) = \mathcal{L}_{\mathcal{N}}(a, \omega)$. Our analysis is not focused on the retrograde case (negative frequencies); however, this case is relevant because the corresponding frequencies are equal in magnitude to the horizon frequencies. A systematic analysis of this case is considered in Sec. (D1).

IV. CONCLUDING REMARKS

In this work, we presented a complete characterization of the **MBs** of the Kerr geometries. Metric bundles are curves of the extended plane, which represent collections of **BH** geometries or **BH** and **NS** geometries. All the geometries of a bundle have the same limiting photon (orbital) frequency $\omega = \omega_b$, the characteristic frequency of the metric bundle, which coincides with the horizon frequency ω_H^\pm corresponding to the tangent point a_g of the metric bundle with the horizon curve a_\pm on the extended plane. All the **MBs** are tangent to the horizon curve on the extended plane and, viceversa, the horizon curve emerges as the envelope surface of all the **MBs**. In this sense, the horizons are constructed by all the **MBs** on the extended plane throughout the tangency property. In the sense of the frequencies coincidence, the horizon curve on the extended plane contains the information of all the Kerr geometries. The **MBs** frequencies (and the limiting frequencies at any point of any spacetime of the bundle) are all and only the horizon frequencies defined on the extended plane.

We summarize below the main steps of this analysis, briefly commenting on the main results regarding the bundle structures. We conclude this final section of our work with comments on some aspects relating **MBs** to various astrophysical contexts involving **BHs** in interaction with its environments of matter and fields and, more generally, in processes of formation and evolution of singularities. This work is also part of the more general study of the significance and interpretation of naked singularity geometries.

Analysis and results

MBs in the extended plane In Sec. (II), we analyzed special sets of metric bundles Γ_x , which are characterized by the constant parameter x , such as the bundle origin a_0 or the bundle frequency ω_b , and provide a division of the extended plane into parts. We used this particular split to construct the Kerr extended plane in the representation of Fig. (2), through transformations presented and discussed in Eq. (B3) and Fig. (19), where we pointed out the particular role of the parameter $\mathcal{A} \equiv a\sqrt{\sigma}$ —Fig. (5).

Horizons confinement We analyzed in detail the conditions for the inner horizon confinement, as seen from the exterior region of the extended plane. The inner horizon confinement is a condition involving, in general, the entire extended plane; therefore, we also addressed this problem in the case of naked singularities and, in particular, in the bottleneck region of the extended plane, which is characterized by the horizon remnants region in each **NS** geometry, as seen in Fig.(2). It turned out that the conditions are similar to the case of the equatorial plane ($\sigma = 1$), if we consider the quantities parameterized by $\mathcal{A} \equiv a\sqrt{\sigma}$ —Sec. (B) and Fig. (5). We studied in detail black hole spacetimes. The confinement of the inner horizon was discussed in various parts of this work, for example, in Fig. (7) by considering the dependence on the plane σ and different parametrizations for the **MBs**. We proved, however, that the confinement can be overcome by the horizons replicas (leading to "frequencies extraction" through bundles in the outer region). There are solutions with frequencies equal to the inner (and outer) horizon, which are regulated by constraints on $\mathcal{A} = a\sqrt{\sigma}$.

Horizons replica Our study led to the introduction of the horizon replicas by considering the bundle orbits r in a specific geometry, other than that of **BH** horizons, but characterized by photons with orbital frequency equal to the (inner or outer) horizon frequency of the **BH** spacetime. In fact, this constitutes an aspect of information extraction of the **BH** properties into the exterior region of the extended plane. Examples of replicas are given in Figs (9). The existence of horizon replicas depends on the angle ($\sigma \in [0, 1]$) with respect to the rotational axis, while the frame-dragging of the ergoregion plays a limited role in this aspect of the analysis. The frame-dragging is related to the bending (curvature) of the curves in the positive section of the extended plane. This aspect was first evidenced in [21], where it was proved that the frame dragging affects the bending of the **MBs** curves in the extended plane. This result was obtained by the comparing the same situation in the static Schwarzschild and Reissner-Nordström geometries and by analyzing the balance between the effects of the electric charge (the dimensionless parameter Q/M related to the sphericity and staticity of the geometry in the sense described in [21]) and the rotational charge (the spin a/M) of the Kerr-Newman geometries. We could say that frame-dragging "closes" the **MBs** curves on the equatorial plane, whereas they are open for large spin and close to the rotational axis (small $\sigma \in [0, 1]$)—see Figs 13, 12, 14, and 16. We also proved that replicas reveal to be tools for the exploration of the region closed to ($\theta \approx 0, \sigma \approx 0$).

Extracting information From the observational view-point, we established that the rotational axis of a Kerr **BH** may have important implications for the knowledge of spacetimes structures closed to the singularity and horizons. The other significant aspect of the horizons confinement concerns the intriguing possibility of extracting information from counter-rotating orbits (negative frequencies with respect to the positive frequencies in the positive section of the extended plane), which we analyzed considering a supplement of the extended plane as seen in Fig. (27).

Significance of the extended plane The introduction of an extended plane for the representation of Kerr solutions has proved to be very significant since it leads to the establishment of a **BHs**–**NSs** connection and allows us to highlight important properties of the Kerr geometries and to formulate an alternative definition of the horizons for the Kerr geometries.

NSs, bottleneck and extended plane We pointed out that **MBs** and horizon remnants of the bottleneck region ($\mathcal{A} \in [M, 2M]$) on the extended plane appear to be related to the concept of spacetime pre-horizon regimes, indicating the existence of detectable mechanical effects allowing circular orbit observers to recognize the close presence of an event horizon. Pre-horizon regimes were introduced in [8] and worked out for the Kerr geometry in [9, 13]. A rather intriguing implication of this property is that an object like a gyroscope could observe a connected phenomenon and interpret it as a *memory* of the static (Schwarzschild-like) case in the Kerr metric—[11]. This interpretation could be perfectly fitted in an extended plane representation of the Kerr metric family, providing the interpretation of a (black hole) spacetime as a line of the plane as illustrated in Fig. (2). The concept of remnants evokes a sort of spacetime "plasticity" (or memory), which naturally can be read through the concept of the extended plane. Actually, we consider the entire family of solutions as a *unique geometric object*, and we propose a metric representation where we consider a spacetime as a single part of this plane. The relevance of this new representation, together with the possible conceptual significance, lies in its usefulness. In this new framework, we found several properties of the spacetime geometries: considering the Kerr family as a single object, the geometric quantities (for example, the horizons) defined for a single

solution acquire a completely different significance, when considered for the entire family. The naked singularity solutions, for example, play a specific role in the construction of the horizon curve on the extended plane, in the sense of the tangency property. Moreover, these structures could play an important role for the description of the black hole formation and for testing the possible existence of naked singularities. Horizon remnants could be of relevance during the gravitational collapse [5, 10, 12, 14]. Similar interpretations have been presented in [8, 9, 11, 13], by using the concept of pre-horizons, and in [32], by analyzing the so-called whale diagrams. We note that the physical evolution of the Kerr spacetime, during unchanged symmetry process stages, have to occur along parts of the extended plane. This also leads to an analysis of the causal structure as determined by stationary observers of the Kerr geometries. (For an analysis of gravitational instabilities and unstable axisymmetric modes in Kerr spacetimes, we refer to [15].)

MBs frequencies and horizons frequencies Finally, a further relevant aspect, very closely connected to the spacetime thermodynamical properties, concerns the horizon frequencies, which we proved are all and only all the bundle characteristic frequencies. For the horizon frequency $\omega_x \in \omega_H^\pm$ there is the set Γ_{ω_x} of Eq. (A7) of the **MBs**, which was considered in several parts of this analysis and, in particular, in Sec. (B). The extended plane is essentially equivalent to a function relating the frequency (bundle and horizon frequencies) to the (bundle origin) spin. Then, an important part of this analysis fixes also the **MBs** characteristic frequencies in relation to the photon orbital frequency and the horizons frequencies—see Eq. (A8) and Fig. (14). Notably, the **MBs** associated to the extreme Kerr **BH** corresponds to a regular curve, tangent to the horizon with bundle origin $a_0 = 2M$ when $\sigma = 1$; otherwise, it corresponds to the class $\Gamma_{a_g=M}$ of bundles with characteristic frequency $\omega_b = 1/2$ and tangent radius $r_g = a_g = M$. Thus, according to Eq. (12), the origin a_0 of each **MB** of $\Gamma_{a_g=M}$ is $a_0 = 2/\sqrt{\sigma}$ ($A = 2M$); then, the minimum value of the bundle origin a_0 in $\Gamma_{a_g=M}$, which is used to construct the limiting case of the extreme Kerr **BH** horizon, is the **NS** with $a_0 = 2M$ occurring for $\sigma = 1$ —Fig. (5).

BHs thermodynamics and NSs Conditions relating the tangent point a_g to the origin spin a_0 are given in Eq. (12). In this sense, **NSs** are “necessary” for the construction of horizons. Properties of horizons and bundles and different frequency relations are given in Sec. (B2 a), considering some notable frequency ratios related to the bundles of the classes Γ_x . On the other hand, we had pointed out in [21] the horizon frequency relations through the metric bundles for $\sigma = 1$, that is, the bundles of Γ_σ for $\sigma = 1$. (The horizons and, therefore, the tangency frequencies are obviously independent of σ since horizons are represented by spheres on the extended plane). The possible thermodynamic implications of the results discussed here, particularly, in relation to the possibility of formulating the **BH** thermodynamic laws in terms of metric bundles are the focus of a planned future work, where we also exploit the several symmetries found on the extended plane in the **BH** representation of Fig. (2).

Final remarks

- Significant for the transformations from one solution to another, **MBs** represent a global frame for the analysis of **BHs**. Extended planes and metric bundles allow us to connect different points of one geometry, but also different Kerr geometries, providing a new and global frame for the interpretation of these metrics and, in particular, of **NSs** solutions. In this respect, **MBs** in the extended plane enlighten some properties of the horizons connecting different **BHs** and **NSs** geometries. In this context, it has to be seen the relevance of the horizon replicas, or the opposite effect of causal balls, which are defined after the horizon confinement. Through the notion of replication we highlight those properties of a **BH** horizon which can be replicated in other points of the same or different spacetimes; otherwise, there is a confinement. We proved this, for example, for a portion of the Kerr inner horizon curve. Replicas (and therefore the confinement) are studied with the analysis of self-intersections of the bundles curves in the extended plane, in the same geometry (horizon confinement) or intersection of bundles curves in different geometries. (Note that, from **MBs** definition, there are horizons replicas in different geometries.) Viceversa, a local causal ball, a concept related to the horizon confinement, as a region of the extended plane $\mathcal{P} - r$ where **MBs** are entirely confined, implies that there are no horizons replicas in any other region of the extended plane.
- **MBs** utility lies in enlightening spacetime properties emerging in the extended plane, related to the local causal structure and **BHs** thermodynamics. The fact that the bottlenecks and remnants, the pre-horizons regime and whale diagrams have a clear interpretation in terms of metric bundles adds a further significance to the use of **MSs** in the analysis of **NSs**. These structures essentially explicate some properties of the Killing horizons in axially symmetric spacetimes and event horizons in the spherically symmetric case. The horizons in this last case are limiting surfaces of the **MBs** in the extended plane. We note that the Kerr **MBs** and the extended

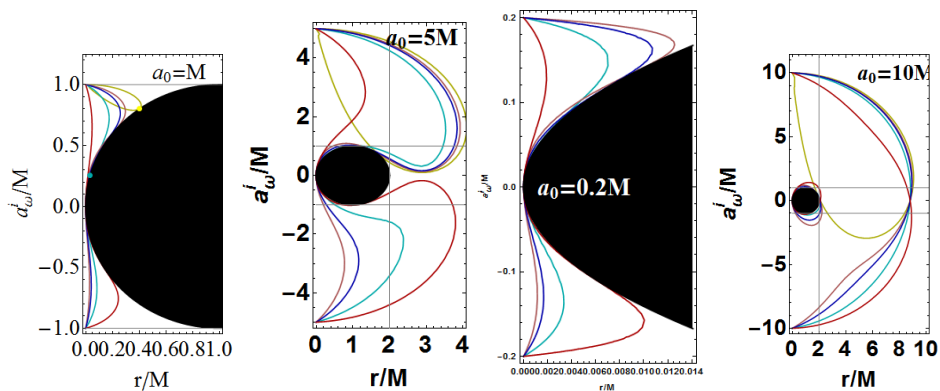


FIG. 12: Metric bundles Γ_{a_0} with equal origins a_0 , different planes σ and different frequencies $\omega_b = 1/a_0 \sin(\theta)$. The black region is the **BH** $a < a_{\pm}$ on the extended plane, gray region is the ergoregion. There $\theta = \pi/2$ (yellow curve), $\theta = \pi/12$ (cyan curve), $\theta = \pi/4$ (pink curve), $\theta = 2.2\pi$ (blue curve), $\theta = 3.82\pi$ (red curve). These results follow from the analysis of Eqs. (A1).

plane parametrization were conveniently settled using the dimensionless spin of the Kerr geometry a/M or $\mathcal{A} = a\sqrt{\sigma}/M$. In the more general case and, for example, in spherically symmetric spacetimes, this choice is not immediate. We see some aspects of this in [25].

- Investigating metric bundles we explore in an alternative way some aspects of the geometries defining the bundle as measured by an observer at infinity. As such, **MBs** are of importance for the analysis of **NSs** solutions, horizons and **BH** thermodynamics. One way to see the connection between **MBs** and **BHs** astrophysics (including **BHs** thermodynamics) passes through the appreciation that these conformal invariant structures are, in fact, expressed in terms of the light surfaces, particularly those light-surfaces from time-like stationary observers. The orbital light-like frequency $\omega(r)$, the bundle characteristic frequency, can be measured by an observer at a point r of the extended plane $\mathcal{P} - r$, where the **MBs** are defined as curves having equal limiting light-like orbital frequency, which is also an asymptotic limiting value for time-like stationary observers. These stationary observers and their limiting frequencies are related to the analysis of many aspects of **BHs** physics, such as **BH** images, and of several processes of energy extraction such as the jet emission and collimation, Blandford-Znajek process, accretion disks or of the Grad-Shafranov equation for the force free magnetosphere around **BHs**, where limiting frequencies (here the bundle frequencies) are used as limiting conditions.

Appendix A: Characteristics of the metric Killing bundles

In these appendix sections, we have included a detailed and extensive analysis of metric bundles.

a. Metric bundles Γ_x

In this section we study in details the **MBs** Γ_x for different quantities x as listed in Table (I), for each Γ_x we consider also some notable sets of **MBs** $\Gamma_{x,y}$ for different quantities y as defined in Sec. (II A). We conclude this subsection introducing the concept of *corresponding bundles* and with the investigation of the relation between origin spin and tangent spin

Metric bundles Γ_{a_0} with equal spin origin a_0 Metric bundles with equal spin origin a_0 have, according to Eq. (7), in general, different bundle frequencies ω_b and different tangent points at the horizon r_g ; consequently, they also have different tangent spins a_g for any polar plane θ (or $\sigma \in [0, 1]$). This case is studied in Figs (12). However, according to the relation $a_0(\omega, \sigma)$, the equal-origin bundles frequencies are $\omega(a_0) = \frac{1}{a_0\sqrt{\sigma}}$ with a minimum (in magnitude) $\omega(a_0) = 1/a_0$ on the equatorial plane. In this case the bundle is closed, as shown in [21]. Thus, $|\omega(a_0)| \in [1/a_0, +\infty[$.

The dependence of the tangent point r_g on the bundle origin a_0 changes with the polar angle θ . Explicitly, the tangent points r_g for bundles having the same origin spin a_0^M is $r_g(a_0^M)$, for a first fixed bundle with the same

origin frequency is $r_g(\omega_0^M)$ and, moreover, $a_g(a_0^M)$ is the tangent spin corresponding to the origin of the first bundle:

$$r_g(\omega_0^M) = \frac{2}{4(\omega_0^M)^2\sigma^{-1} + 1}, \quad r_g(a_0^M) = \frac{2}{\frac{4}{\sigma(a_0^M)^2} + 1}, \quad a_g(a_0) = \frac{4a_0^M\sqrt{\sigma}}{(a_0^M)^2\sigma + 4} \quad (\text{A1})$$

where $\omega_b(a_0^M) = \frac{1}{a_0^M\sqrt{\sigma}}$, and $a_0 = \frac{2\sqrt{r_g}}{\sqrt{\sigma(2-r_g)}}$.

Note that the definition $r_g(\omega_0^M)$ holds for the maximum origin, while $\omega_b(a_0^M)$ is obviously the frequency of the bundle with origin a_0^M ; consequently, it holds at each point of the bundle particularly at the tangency point and its origin located at a_0 .

The tangent spin has a maximum for σ and for a_0 at $\sigma = 4/a_0^2$ where $a_0 = M$. However, according to Eq. (8), the tangent point to the horizon is bounded in the range $r_g(\theta) \in [0, r_g^*] \in [0, 2M]$, where $r_g^* = r_g^*|_{\theta=\pi/2} = 2/4/(a_0^2) + 1$. The bundle frequency and its tangent point are fixed points under variations of the plane in $\sigma \in [0, 1]$.

We now consider some special cases of metric bundles with equal tangent spin a_g or radius r_g or plane σ . Some of these cases will be detailed below in dedicated paragraphs, in which we consider two bundles with $(a_0, \sigma, a_g, \omega_b)$ and $(a_0, \sigma_p, a_g^p, \omega_b^p)$, respectively.

Metric bundles with equal a_0 and a_g ($a_g = a_g^p$): In this case (A2)

- $a_0 \in]0, 2M[$, for $\sigma_p \in [0, 1]$ and $\sigma = \sigma_p$
- $a_0 > 2M$ (i) $\sigma_p \in \left[0, \frac{16}{a_0^4}\right]$, and $\sigma = \sigma_p$ (ii) $\sigma_p \in \left[\frac{16}{a_0^4}, \frac{4}{a_0^2}\right]$, and $\sigma \in (\sigma_p, \sigma_\ell^p)$;
- (iii) $\sigma_p = \frac{4}{a_0^2}$ and $\sigma = \sigma_p$, (iv) $\sigma_p \in \left]\frac{4}{a_0^2}, 1\right]$ and $\sigma \in (\sigma_p, \sigma_\ell^p)$

where $\sigma_\ell^p \equiv \frac{16}{a_0^4\sigma_p}$, frequency ratio $s = \frac{\omega_b}{\omega_b^p} \in \{1, \frac{\sqrt{\sigma_p}}{\sqrt{\sigma}} = \frac{4}{a_0^2\sigma} = \frac{a_0^2\sigma_p}{4}\}$ (A3)

Metric bundles with equal a_0 and σ : In this case $a_g = a_g^p$ and $\omega_b = \omega_b^p$

Metric bundles with equal a_0 and r_g (ω_b): In this case $\sigma = \sigma_p$ and $a_g = a_g^p$

Metric bundles with equal a_0 and a_g and r_g (ω_b): In this case $\sigma = \sigma_p$.

Metric bundles with equal a_0 and σ , or equal origin and tangent radius r_g (or frequency) are equal. In the case of equal origin and tangent spin a_g , except for the trivial case of coincidence of the bundle $\sigma = \sigma_p$, it is noteworthy that only two distinct bundles can exist for **NS** origins with spin $a_0 > 2M$ and large plane $\sigma_p > 4/a_0^2$, with a fixed ratio between the σ planes and the frequencies. In Sec. (B), we will particularly focus on the relations between the frequencies, which are the horizon frequencies ω_H^\pm (see also Figs 23). Note that the ratio in Eq. (A3) depends on the spin because it is parameterized by the bundle origin a_0 , which is related to the bundle frequency through σ .

Metric bundles Γ_σ on the same plane θ We focus on metric bundles on an equal plane σ . The case $\sigma = 1$ has been analyzed in detail in [21]. We will also take into account the results given in Eq. (A1). However, we present here some of the relations (A1) as follows:

Tangent radius $r_g(\omega_b) = \frac{2}{4\omega_b^2 + 1}$, $r_g(a_0) = \frac{2}{\frac{4}{a_0^2\sigma} + 1}$, (A4)

Tangent spin $a_g(\omega_b) = 4\sqrt{\frac{\omega_b^2}{(4\omega_b^2 + 1)^2}}$, $a_g(a_0) = \frac{4a_0\sqrt{\sigma}}{a_0^2\sigma + 4}$, (A5)

Bundle origin $a_0(\omega_b) = \frac{1}{\sqrt{\sigma}\omega_b}$, $a_0(r_g) = \frac{2\sqrt{r_g}}{\sqrt{2\sigma - r_g\sigma}}$, (A6)

where $r_g \in [0, 2M]$, $a_0 \in [0, +\infty[\cup]-\infty, 0]$, $a_g \in [0, M]$ $\omega_b = \omega_H^\pm \in]0, +\infty[$

See the Figs (5,1,4,13), where $(r_g(\omega_b)$ and $r_g(a_0))$ is the tangent radius as function of the bundle frequency ω_b and of the bundle origin spin a_0 , respectively. The radius $r_g(a_0)$ is maximum (for σ and a_0) at $a_0 = \sigma = 0$,

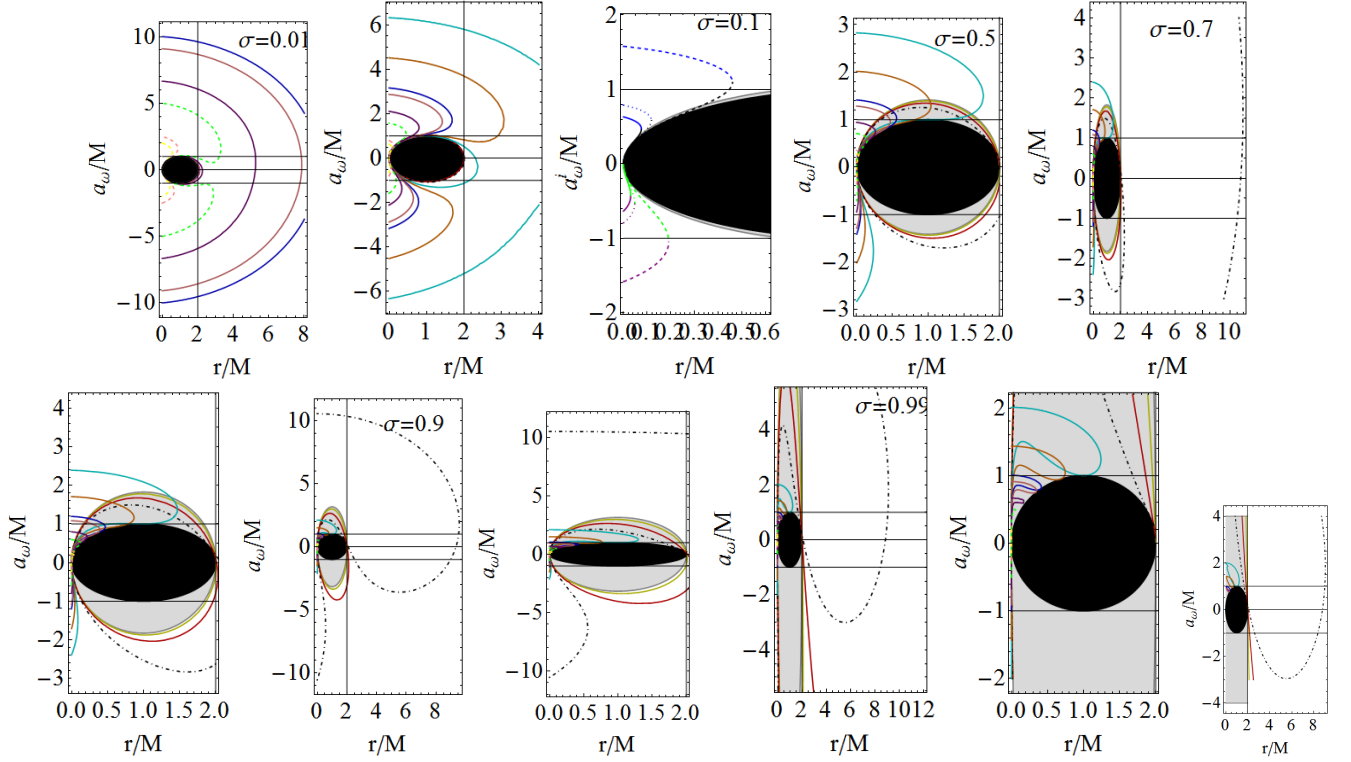


FIG. 13: Metric bundles Γ_σ for the same plane σ and different bundle frequencies $\omega_b \in \{0.01$ (yellow), $1/27$ (Red), 0.1 (dotted-dashed), 0.5 (cyan), 0.7 (orange), 1 (blue), 1.1 (pink), 1.5 (purple), 2 (green), 4 (dashed-pink), 5 (yellow-dashed)}. The black region represents a **BH** ($a < a_\pm$) on the extended plane. It follows the analysis of Eq. (A4).

where $r_g = 2M$. $(a_g(\omega_b), a_g(a_0))$ is the tangent spin as function of the bundle frequency ω_b and bundle origin spin a_0 , respectively. $(a_0(\omega_b), a_0(r_g))$ is the bundle origin spin as function of the bundle frequency ω_b and bundle tangent radius r_g , respectively. The function $a_g(\omega_b)$ has an extremum at $\omega_b = 1/2$, where $a_g(\omega_b) = 1$.

Metric bundles Γ_{ω_b} with equal bundle frequencies ω_b According to Eq. (A4), metric bundles characterized by the same frequency ω_b have the same point of tangency with horizon r_g and tangent spin a_g , but different origin spins $a_0(\omega_b, \theta)$ for different planes θ . The relation between the origins of the equal-frequency bundles ω_b and, therefore, also the same point of tangency (a_g, r_p) , is

$$\text{bundles with equal } \omega_b \text{ (} \mathbf{r}_g, \mathbf{a}_g \text{)} \quad \frac{a_0^p}{a_0} = \sqrt{\frac{\sigma}{\sigma_p}}, \quad \text{in particular } a_0^p = a_0 \quad \text{iff } \sqrt{\sigma} = \sqrt{\sigma_p} \quad (\text{A7})$$

This case is studied in Figs (14). This confirms that for each plane σ there is one and only one metric bundle associated with the horizon frequency ω_b and the pair (r_g, a_g) (recall that the tangent radius r_g and, therefore, the tangent spin a_g are determined by the bundle frequency only, while the bundle origin a_0 depends on the plane σ). In addition, on different planes, there may be different bundles all tangent to the point of the horizon with a radius r_g and frequency ω_b , but different a_0 for different σ , as follows from Eq. (A7). This relation implies the following fact: if the origin a_0 corresponds to a **BH**, (i.e. $a_0 \in [0, M]$), it is always tangent to the inner horizon (this will be proved explicitly later especially in Sec.B). Then, a bundle with the same frequency as the inner horizon and therefore the same point of tangency can be generated by an origin a_0^p in **NS** related to the frequency by $a_0^p = a_0 \sqrt{\sigma/\sigma_p}$ if $\sqrt{\sigma_p} \leq \mathcal{A}_0 \equiv a_0 \sqrt{\sigma}$. If $\sqrt{\sigma_p} = \mathcal{A}_0$, then a_0^p is always tangent to the point of the horizon that corresponds to the extreme **BH**. Particularly, for the equatorial plane where $\sigma = 1$ and $a_0^p = a_0/\sqrt{\sigma_p}$, we conclude that for a fixed point of tangency the *minimum* origin spin occurs *always* on the equatorial plane; every other bundle has a higher origin. Then, the bundle with origin in $a_0 = M$ on the equatorial plane has other bundles with equal tangent point necessarily located in the **NS** region with $a_0^p = 1/\sqrt{\sigma_p}$.

Metric bundles Γ_{a_g} with equal bundle tangent spin a_g : Construction of horizons We focus on the case of metric bundles with the same tangent spin a_g . This condition allows us to construct the horizons in the

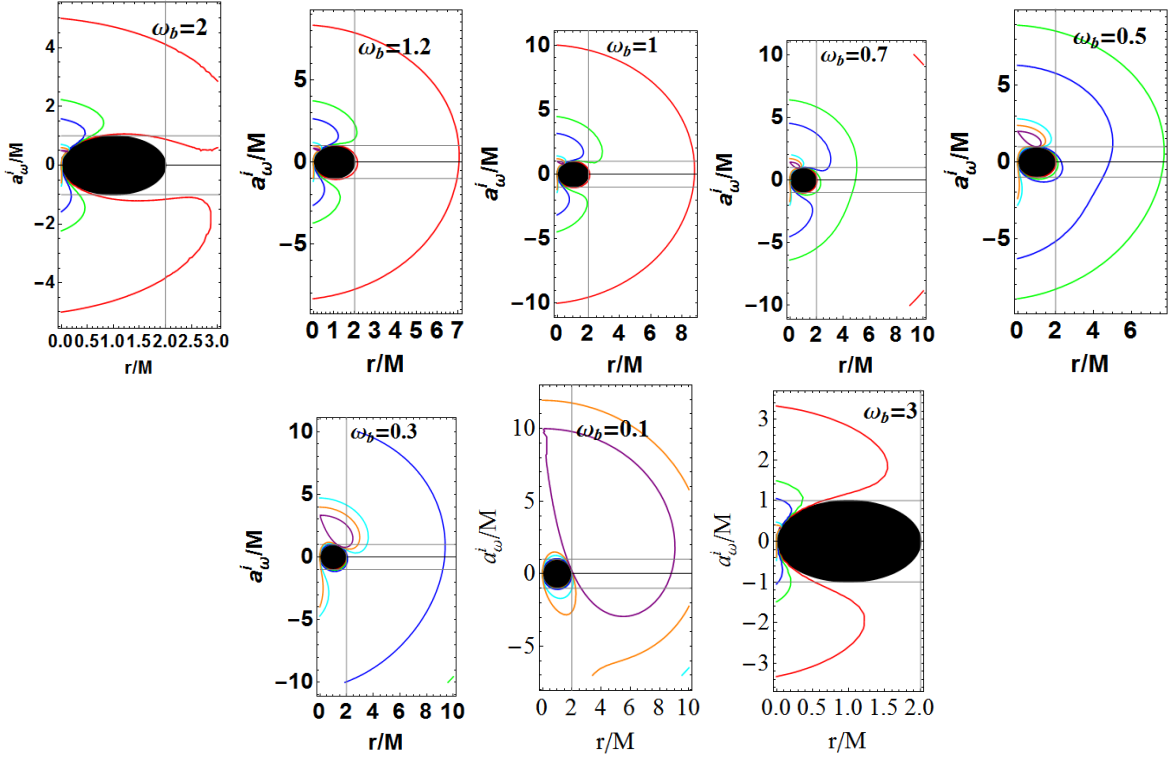


FIG. 14: Metric bundles Γ_{ω_b} with the same frequency ω_b and, therefore, also the same spin tangent a_g and tangent radius r_g . The bundle origins a_0 depend on the plane σ : the blue curve is for $\sigma = 0.1$; cyan curve is for $\sigma = 0.5$, green is for $\sigma = 0.05$; orange curve $\sigma = 0.7$, purple curve is $\sigma = 1$, red curve is $\sigma = 0.01$. The black region corresponds to a **BH** ($a < a_{\pm}$) on the extended plane. It follows from the analysis of Eq. (A7)

extended plane corresponding to a **BH** with with spin a_g . We recall that if two metric bundles have the same spin tangent a_g , then irrespectively of the plane σ or origin a_0 , they can have either **(1)** the same frequency ω_b , i.e., they belong to the family Γ_{ω_b} studied in Eq. (A7), or **(2)** different ω_b^1 ; in any case, it holds that $(\omega_b(a_g), \omega_b^1(a_g)) = \omega_H^{\pm}(a_g)$, that is, they must both have one of the horizon frequencies with spin **BH** spin a_g .

To obtain the relation between these bundles, we use Eq. (A4). We divide the problem by considering **(1)** firstly, a fixed spin a_g with equal σ , and then **(2)** a fixed a_g with arbitrary σ . This case is studied in Figs (16). For fixed spin tangent a_g , the two tangent radii are obviously $r_g = r_{\pm}(a_g) = 1 \pm \sqrt{1 - a_g^2}$, which coincide only for extreme **BH** case $a_g = M$. As this a notable case, we will analyze it separately. The metric bundles with the same point of contact $p_g = (a_g, r_g)$ have the same frequency ω_b , but pertain to different planes σ and origins a_0 ; the *larger* origin spin (for fixed frequency) corresponds to the equatorial plane ($\sigma = 1$). Thus we obtain a family of metric bundles with the same (a_g, ω_b, r_g) , but different $a_0(\sigma)$ for different σ ; each σ corresponds to one and only one bundle with (a_g, ω_b, r_g) .

For fixed σ , we now consider metric bundles with equal (a_g, ω_b) which have equal r_g related by the horizon curve, i.e., $r_g^{\pm} = 1 \pm \sqrt{1 - a_g^2}$. The bundle frequencies (ω_b^1, ω_b) and the bundle origins (a_0^1, a_0) are related as follows

$$\text{Metric bundles with equal } (a_g, \sigma) : \omega_b^1 = \frac{1}{4\omega_b}, \quad a_0 = \frac{1}{\omega_b\sqrt{\sigma}}, \quad a_0^1 = \frac{4\omega_b}{\sqrt{\sigma}} = 4\omega_b^2 a_0 = \frac{4}{a_0\sigma} \quad (\text{A8})$$

$$\text{from which} \quad a_0^1 a_0 = \frac{4}{\sigma}, \quad \frac{a_0^1}{a_0} = 4\omega_b^2$$

$$\text{Metric bundles with equal } (a_g, \omega_b, r_g) : a_0^c = \frac{1}{\omega_b\sqrt{\sigma}} = \frac{a_0\sqrt{\sigma}}{\sqrt{\sigma_c}} \quad \text{from which} \quad \frac{a_0^c}{a_0} = \sqrt{\frac{\sigma}{\sigma_c}}. \quad (\text{A9})$$

The behavior of these quantities is illustrated in Fig. (15). It is clear that for the class (A8), composed by metric bundles with equal (a_g, σ) , the two bundles have tangent points on the horizon $(r_g, r_g^1) = (r_-(a_g), r_+(a_g))$,

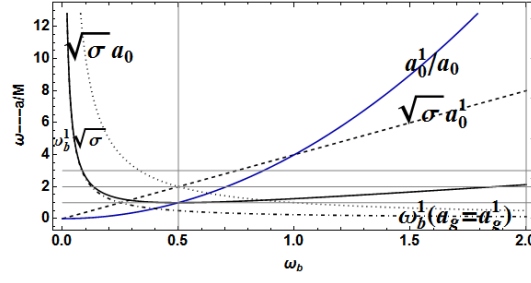


FIG. 15: The black curve is $\omega_b^1(\omega)$ from Eq. (A10), the dashed curve is $a_0(\omega_b)\sqrt{\sigma}$ for equal (a_g, σ) of Eq. (A8), the blue curve is a_0^1/a_0 for equal (a_g, σ) from Eq. (A8), the dotted curve is for $a_0\sqrt{\sigma}$ for equal (a_g, σ) of Eq. (A8), the dotted-dashed curve is $\omega_b^1(\omega_b)$ of Eq. (A11) for $a_g(\omega_b^1) = a_g^1(\omega_b)$.

generating in this way the horizon of the **BH** spacetime with spin a_g . We will see also more details below.

Corresponding bundles As studied in [21], there are corresponding bundles with $a_0^1 = a_g$: the tangent point of a bundle is the origin of a second bundle with $a_0^1 = a_g$, which must have a **BH** origin. Then, we can identify an entire class of corresponding bundles Γ_{a_g} with the same tangent spin, studied in Eq. (A8), and the class $\Gamma_{a_0^1}$ of metric bundles with the same origin, studied in Eq. (A1). The frequencies of these bundles are related by

$$\text{Frequency relations for corresponding bundles } a_0^1 = a_g: \quad \omega_b^p = \frac{4\omega_b^2 + 1}{4\sqrt{\sigma}\omega_b^2} \quad (\text{A10})$$

See Fig. (15). There is an extremum at $\omega_b^p = 1/\sqrt{\sigma}$ for $\omega_b = 1/2$. In general, the following relations hold:

$$\text{Corresponding metric bundles } a_0^1 = a_g: \quad (\text{A11})$$

$$\text{It holds } a_g(\omega_b^1) = a_g^1(\omega_b), \quad \text{for } \omega_b^1 = \pm \frac{1}{4(\omega_b)}.$$

$$\text{It holds } a_g(a_0^1) = a_g(a_0), \quad \text{and } \sigma = \sigma_1 \quad \text{for } a_0 = \frac{4}{a_0^1\sigma} \quad \text{and}$$

$$\sigma \neq \sigma_1 \quad \text{for } a_0 = \frac{4}{a_0^1\sqrt{\sigma}\sigma_1} \quad \text{and } a_0 = \frac{a_0^1\sqrt{\sigma_1}}{\sqrt{\sigma}}.$$

$$\text{It holds } a_g(a_0, \sigma) = a_g^1(a_0, \sigma_1) \quad \text{for } \sigma_1 = \frac{16}{a_0^4\sigma}.$$

See Fig. (15). The tangent radii for these bundles are

$$\text{Tangent radii } r_g(\omega_b) = r_b \quad \text{for } a = \# \frac{4\omega_b}{4\omega_b^2 + 1}, \quad \text{where } \flat = \pm, \quad \# = \pm, \quad (\text{A12})$$

$$r_g(\omega_b) = r_g(\omega_b^p) \quad \text{for } \omega_b^p = \pm\omega_b; \quad r_g(a_0) = r_b \quad \text{for } a = \# \frac{4a_0\sqrt{\sigma}}{a_0^2\sigma + 4}, \quad (\text{A13})$$

$$r_g(a_0^1, \sigma^1) = r_g(a_0, \sigma) \quad \text{for } a_0^1 = \pm \frac{a_0\sqrt{\sigma}}{\sqrt{\sigma_1}}$$

(the use of \flat and $\#$ for the sign convention means that there is no correspondence between the two options). The following special points determine some particular values of the bundles:

$$a_g = M \quad \text{for } \omega_b = \pm \frac{1}{2}, \quad a_g = M \quad \text{for } a_0^2 = \frac{4}{\sigma}, \quad \text{and } a_g(a_0 = M) = \frac{4\sqrt{\sigma}}{\sigma + 4}, \quad a_g(0) = 0. \quad (\text{A14})$$

$$r_g = M \quad \text{for } \omega_b = \pm \frac{1}{2} \quad \text{and } r_g(a_0) = M \quad a_0 = \frac{2}{\sqrt{\sigma}}.$$

$$\text{For } a_0 = M \quad \text{it holds } \omega \rightarrow \frac{1}{\sqrt{\sigma}} \quad \lim_{a_0 \rightarrow +\infty} a_g = \lim_{a_0 \rightarrow +0} a_g = \lim_{a_0 \rightarrow +\infty} \omega_b = 0, \quad \lim_{a_0 \rightarrow +0} \omega_b = \infty$$

$$\lim_{a_0 \rightarrow +0} r_g = 0, \quad \lim_{a_0 \rightarrow +\infty} r_g = 2M, \quad \text{and } r_g = 2M \quad \text{for } \omega_b = 0,$$

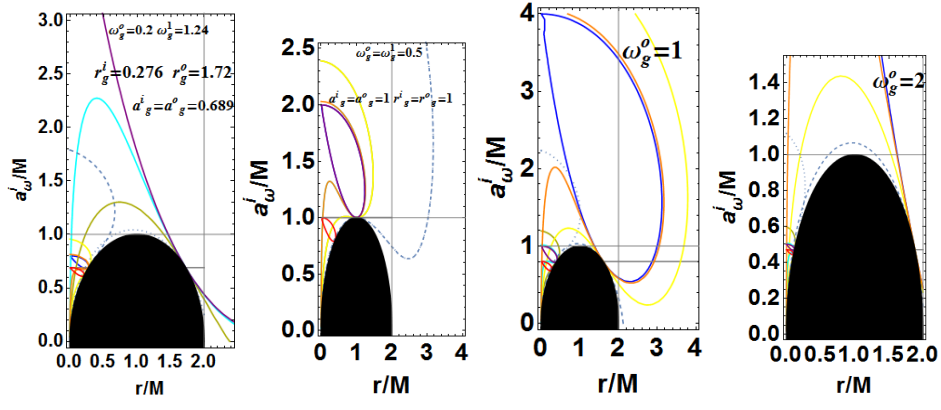


FIG. 16: Horizon construction: metric bundles Γ_{a_g} with equal tangent spin a_g and tangent frequencies $\omega_g = \omega_b$ and, consequently, equal tangent radius r_g . Construction of horizons $r_+ = r_g^o$ and $r_- = r_g^i$ for a spacetime with $a = a_g$ through the corresponding bundle $a_g^1 = a_g^2$ is also shown as the metric bundles with origin $a_g^i = a_0$. The black region is a **BH** on the extended plane. Purple and blue curves are for $\sigma = 1$; orange and cyan curves are for $\sigma = 0.97$, darker-yellow and yellow curves are for $\sigma = 0.7$, dotted and dashed curves are for $\sigma = 0.2$, and the red curve is for $\sigma = 1$. It follows from the discussion of Eqs. (A8,A10,A11,A12,A14).

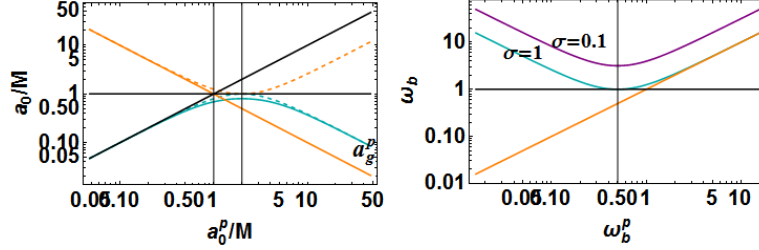


FIG. 17: Analysis of Eq. (A15). Left panel: for $\sigma = 1$, a_g^p of the corresponding bundle (cyan), origin of the corresponding **MBs** (cyan, dashed), frequency ($1/a_0^p$) (orange), frequency of the corresponding **MBs** (orange dashed), origin a_0^p (black) as function of a_0^p . The right panel illustrates the frequencies relations ω_b^p as functions of the bundle frequencies of Eq. (A15) for different planes σ . The orange line is the $\omega_b = \omega_b^p$.

see Fig. (16). These limiting frequencies will be found also in the frequency relations of Sec. (B).

On the relation between origin spin and tangent spin Consider the origin frequency ω_0 , associated with a spacetime with origin spin coincident with the tangent spin ($a_0 = a_g$) of a bundle with frequency ω_b^p , plane σ_p and origin a_0^p , there is then

$$\begin{aligned} \text{for } \sigma = \sigma_p \quad \omega_0^\pm(a_g) &= \frac{1}{a_0^p \sigma} + \frac{a_0^p}{4}, \quad \omega_0^\pm(a_g) = \frac{4(\omega_b^p)^2 + 1}{4\sqrt{\sigma}\omega_b^p}, \quad \text{where } a_g = a_g(a_0^p) \\ \sigma \neq \sigma_p \quad \omega_0^\pm(a_g) &= \frac{a_0^p}{4} \sqrt{\frac{\sigma_p}{\sigma}} + \frac{1}{a_0^p \sqrt{\sigma\sigma_p}}, \quad \text{where the tangent spin of the bundle with origin in } a_g \text{ is} \\ a_g^p &= \frac{4a_0^p \sqrt{\sigma\sigma_p} [(a_0^p)^2 \sigma_p + 4]}{(a_0^p)^2 \sigma_p [(a_0^p)^2 \sigma_p + 4\sigma + 8] + 16}. \end{aligned} \quad (\text{A15})$$

In this way, we also obtained a relation between the origins (a_0, a_0^p) and the characteristic frequencies of the two corresponding **MBs**. The relation between the frequencies (ω_b, ω_b^p) is clearly independent of the plane σ_p , because it is included in the form of ω_b^p in terms of the origin spin. The tangent spin a_g^p has a maximum in terms of the first **MB** origin as a_0 as $\sigma_p = 4/(a_0^p)^2$ —see Fig. (17).

Appendix B: Horizon frequencies as bundle frequencies

The fact that the bundle frequency ω_b coincides with the horizon frequencies $\omega_H^\pm(a_g)$ with spin a_g and, consequently, each photon orbital frequency, $\omega_+(a)$ or $\omega_-(a)$, at any point (r, a, σ) and any azimuthal angle $\varphi = \text{constant}$ in any geometry a of the bundle a_ω^\pm is a horizon frequency in the extended plane, allows us to analyze the bundle properties and, therefore, the Kerr spacetime causal structure in terms of horizon frequencies⁸.

This analysis also allows us to better understand the **MBs** meaning and specifically the relations between the origin a_0 and the bundle tangent spin a_g as given in Eqs. (9) and (12). The relation $a_g(a_0)$ given in Eq. (9), as function of $\mathcal{A} \equiv a\sqrt{\sigma}$, is similar to that of the case $\sigma = 1$ as follows from Fig. (5). Consequently, all the results concerning (a_g, r_g, ω_b) obtained for the equatorial case are valid also for $\sigma \in]0, 1[$, in terms of $\mathcal{A} \equiv a\sqrt{\sigma}$; see Eq. (12) and Fig. (5).

In [21], we demonstrated that for $\sigma = 1$:

- **MBs** with **BH** origins $a_0 \in [0, M]$ are *all* tangent to the inner horizon and, therefore, have tangent spin $a_g \in [0, 0.8M]$ and tangent radius $r_g \in [0, 2/5M]$ with frequencies $\omega_b = \omega_H^- \geq 1$ —see Fig. (21). These **MBs** are *all confined* in the region of the extended plane upper-bounded by the inner horizon (because $a_0 \geq a \geq a_g$ for any spin a of the bundle)—(see the **BB** model of [21]).
- **MBs** with **WNS** origins $a_0 \in [M, 2M]$ can be used to construct only a portion of the inner horizon with $a_g \in [0.8M, M]$, $r_g \in [2/5M, M]$, and $\omega_b \in [0.5, 1[$. These bundles are made of **NSs** and **BHs**.
- Metric bundles with strong naked singularities origins (**SNSs**), $a_0 > 2M$, can be used to construct only the outer horizon on the extended plane.

These results have some remarkable implications:

(1) On the equatorial plane and, more generally, for sufficiently large values of $\sigma \in [0, 1]$, **MBs** with **BH** origins are *all confined* in the inner region of the extended plane (*bundles confinement*)—see Fig. (2). Consequently:

(2) All the frequencies $\omega_b \geq 1$ belonging to these bundles cannot be found in the **NS** regime nor in the outer region ($r > r_+$) on the extended plane for large values of σ (*frequencies confinement*). Results (1) and (2), therefore, hold if we consider the variable $\mathcal{A}_0 = a_0\sqrt{\sigma}$.

(3) The bottleneck region of Fig. (2), including **NS** metric bundle origins $\mathcal{A}_0 \equiv a_0\sqrt{\sigma} \in [M, 2M]$, with bundle characteristic frequencies $\omega_b \in [0.5, 1[$ remain confined to the **BH** inner region or to the **NS** region, i.e., they are outside the region $r > r_+$ and $a \in [0, M]$, for large values of σ .

(4) All **MBs** with an origin spin of a **NS** have characteristic frequencies of the outer horizon on the extended plane, *apart* from the *bottleneck* region ($\mathcal{A}_0 \in [M, 2M]$), where **MBs** have the frequencies of the inner horizon. We can see this relation, in terms of \mathcal{A} between tangent spin and tangent radius also in Fig. (19). As it is clear from the analysis of Sec. (B), there are bundles (and therefore orbits) with characteristic frequencies equal to the outer horizon frequencies, which are located in the inner region of the extended plane. Vice versa, outer horizon frequencies and are all and only those of **NS** origins $\mathcal{A}_0 = a_0\sqrt{\sigma} \geq 2M$ for *any* plane σ (thus, $a_0 \geq 2M/\sqrt{\sigma} \geq 2M$).

The results (4) imply that the outer horizon can be constructed only by strong naked singularity origins with $\mathcal{A}_0 \geq 2M$ and, therefore, with $a_0 \geq 2M/\sqrt{\sigma} \geq 2M$.

More precisely, concerning the inner horizon confinement, as the relations $a_g(a_0, \sigma)$, $r_g(a_0, \sigma)$ and $\omega_b(a_0, \sigma)$ can be read as $a_g(\mathcal{A}_0)$, $r_g(\mathcal{A}_0)$ and $\omega_b(\mathcal{A}_0)$, then all the relations between these quantities valid for the equatorial plane $\sigma = 1$, hold also for any $\sigma \neq 0$ (from the symmetry properties it follows also the scheme presented in Fig. 2). On the contrary, the quantity $\mathcal{L}_\mathcal{N}$ cannot be written as a function of \mathcal{A} only, the explicit expression for the **MBs** given in Eq. (C1), or for frequencies given in Eq. (6). Therefore, they do not depend only on the variable \mathcal{A} , but depend explicitly on the plane $\sigma \in [0, 1]$. This has important consequences for the confinement of **MBs** tangent to the inner horizon and of the inner horizon frequencies. For each point $r_g \in a_-$, tangent point belonging to the inner horizon on the extended plane, it is possible to find a plane $\sigma < \sigma_{descr}$ such that solutions of the condition $\mathcal{L} \cdot \mathcal{L} = 0$ exist for $a \in [0, M]$ and $r > M$, with $\omega_b \geq 0.5$ and, particularly, $\omega_b \geq 1$ (frequency range of the inner horizon $a_g < M$, $r < M$ and $a_g < 0.8M$, $r < 2.5M$). This condition, moreover, had already been discussed differently in Eq. (25). This result implies that there are no orbits confined in the inner horizon and that close to the rotational axis $\sigma \ll 1$, for any spacetime a it is possible to find an orbit in the outer region, $r > r_+$, with frequency equal to that of the internal horizon for a close to the rotation axis, see also Figs 8, 13, 12, 14, and 16.

⁸ More precisely, we can characterize the spacetime causal structure by using the fact that the condition $\mathcal{L} \cdot \mathcal{L} = 0$ determines lightlike, causal, boundary delimiting stationary observer orbits.

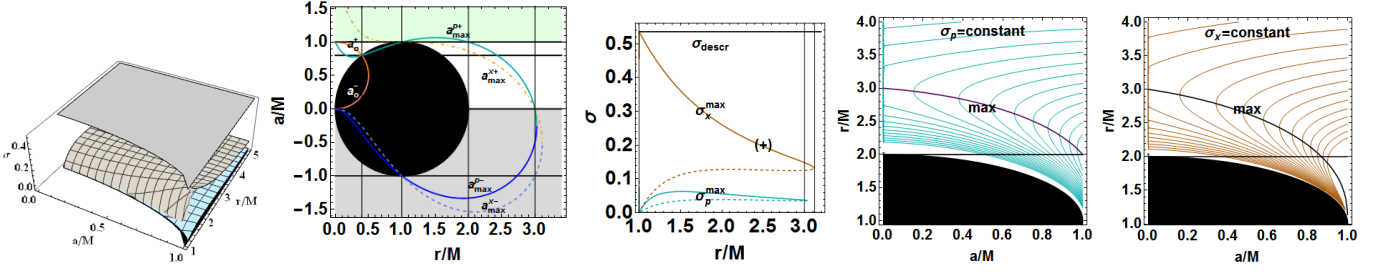


FIG. 18: Analysis of Eqs. (B1) and (B2) on the confinement of the metric bundles with a frequency equal to that of the internal horizon $\omega_{\bar{H}}$ on the extended plane. This topic is also addressed in Eq. (25). It is shown that it is always possible to find bundle frequencies $\omega > 1$ (equal to the inner horizon frequencies) in the exterior region as in Fig. (2) for large spin a and small σ . The frequency $\omega_b \geq 1$ refers to $a_g \in [0, 0.8]$, and $\omega_b \in [0.5, 1[$ is related to $a_g \in]0.8, 1[$. Left panel: 3D plot of planes $\sigma_p < \sigma_x$ as functions of $a \in [0, M]$ and $r > M$. Planes $\sigma \in \{0, 1\}$ are also shown. Second panel: black region is the **BH** on the extended plane, the gray region contains negative values of frequencies (corresponding to retrograde motion or $a < 0$). The maximum values of $\sigma_p < \sigma_x$ are also shown. Third panel: maximum values of $\sigma_p < \sigma_x$ for positive and negative a are shown as functions of r/M . The value σ_{descr} as in Eq. (25) and Fig. (10) is also shown. Fourth and fifth panels: planes $\sigma_p = \text{constant}$ and $\sigma_x = \text{constant}$ for $(a/M, r > r_+)$

More in detail, we have that

$$\text{(SBH)} \quad \mathcal{L} \cdot \mathcal{L} = 0, \quad \text{for} \quad (1) \quad a \in]0, M], \quad r \geq M, \quad \sigma \in]0, 1], \quad (2) \quad \omega > 1 \quad \text{for} \quad (B1)$$

$$\omega = \omega_- \quad \sigma \in]0, \sigma_p[\quad \text{and} \quad \bullet \quad r \in]M, 2M], \quad a \in]a_{\pm}, M] \quad \text{or} \quad \bullet \quad r > 2M, \quad a \in]0, M].$$

$$\text{(WBH)} \quad \mathcal{L} \cdot \mathcal{L} = 0, \quad \text{for} \quad (1) \quad a \in]0, M], \quad r \geq M, \quad \sigma \in]0, 1], \quad (2) \quad \omega \in [1/2, 1] \quad \text{for}$$

$$\omega = 1/2 \quad \text{for} \quad a = M \quad r = M,$$

$$\omega = \omega_- \quad \sigma \in [\sigma_p, \sigma_x] \quad \text{and} \quad \bullet \quad r \in]M, 2M], \quad a \in]a_{\pm}, M] \quad \text{or} \quad \bullet \quad r > 2M, \quad a \in]0, M].$$

$$\text{where} \quad \sigma_p \equiv \frac{1}{2} \left[\frac{a^4 + a^2(2r^2 + 1) - 4ar + r^4}{a^4 + a^2(r-2)r} - \sqrt{\frac{[(a-1)a + r]^2 [a^2(a+1)^2 + 2a(a+1)r^2 - 8ar + r^4]}{a^4 \Delta^2}} \right]$$

$$\sigma_x \equiv \frac{1}{2} \left[\frac{a^4 + 2a^2(r^2 + 2) - 8ar + r^4}{a^4 + a^2(r-2)r} - \sqrt{\frac{[(a-2)a + r]^2 [a^2(a+2)^2 + 2a(a+2)r^2 - 16ar + r^4]}{a^4 \Delta^2}} \right].$$

The frequency $\omega_b \geq 1$ refers to $a_g \in [0, 0.8M]$, $\omega_b \in [0.5, 1[$ refers to tangent spins $a_g \in]0.8M, M]$. This analysis is in agreement with Sec. (III) and particularly Eq. (25), as can be seen also from Fig. (10), where it is clear the role of $\sigma_{descr} \geq \sigma_x \geq \sigma_p > 0$. There are maximum points for (σ_p, σ_x) as functions of r/M :

$$\partial_r \sigma_p = 0, \quad \text{for} \quad a_{\max}^{\pm} \equiv \frac{1}{r+1} - \frac{1}{2} \pm \frac{\sqrt{r[r(13-4(r-2)r)-2]+1}}{2\sqrt{(r+1)^2}}, \quad a_o^{\pm} \equiv \frac{1}{2} \left(1 \pm \sqrt{1-4r^2} \right) \quad (B2)$$

$$\partial_r \sigma_x = 0, \quad \text{for} \quad a = a_o^{\pm}, \quad \text{and} \quad a_{\max}^{x\pm} \equiv \frac{2}{r+1} - 1 \pm \frac{\sqrt{1-r[r((r-2)r-4)+2]}}{\sqrt{(r+1)^2}},$$

–see Fig. (18).

Before moving on to the analysis of frequencies, we conclude this part by considering the tangent lines to the horizon curve on the extended plane, which also provide the transformations used in the scheme of Fig. (2). Note that as they relate a_g and r_g to a_0 , then these relations can be parameterized in terms of the variable $\mathcal{A} \equiv a\sqrt{\sigma}$. Therefore,

$$\mathcal{A}_0(r) \equiv \mathcal{A}_0 - \frac{\mathcal{A}_0}{2}r, \quad \mathcal{A}_r^*(r) \equiv \frac{2}{\mathcal{A}_0}r, \quad \mathcal{A}_{tangent}(r) \equiv -\frac{\left[\sqrt{\frac{\mathcal{A}_0^2}{(\mathcal{A}_0^2+4)^2} (\mathcal{A}_0^4 - 16)} \right]}{4\mathcal{A}_0^2}r + \frac{(\mathcal{A}_0^4 - 16) \sqrt{\frac{\mathcal{A}_0^2}{(\mathcal{A}_0^2+4)^2} + 8\mathcal{A}_0}}{2(\mathcal{A}_0^2 + 4)},$$

$$\text{and} \quad \mathcal{A}_0(r) = \mathcal{A}_r^*(r) \quad \text{for} \quad r = r_g; \quad \mathcal{A}_0(r) = \mathcal{A}_{tangent}(r) \quad \text{for} \quad r = r_g \quad \text{or} \quad \mathcal{A}_0 = -\frac{2}{\sqrt{3}},$$

$$\text{and} \quad \mathcal{A}_{tangent}(r) = \mathcal{A}_r^*(r) \quad \text{for} \quad r = r_g \quad \text{or} \quad \mathcal{A}_0 = -2\sqrt{3}, \quad (B3)$$

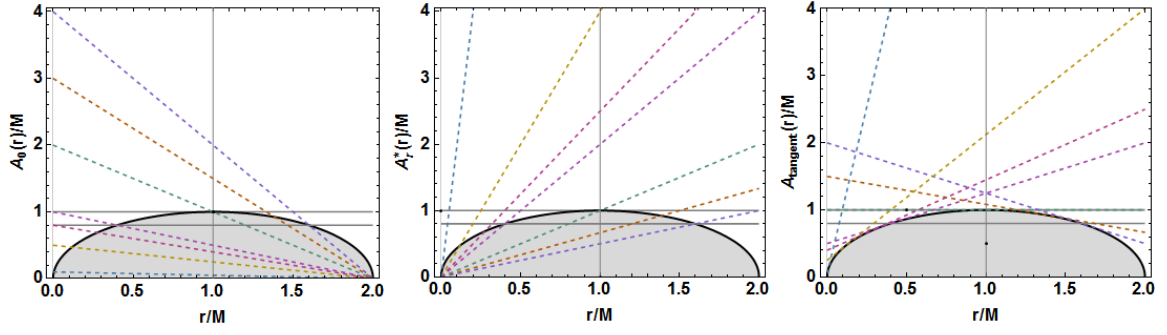


FIG. 19: Gray region is the black hole on the extended plane. Here $\mathcal{A} \equiv a\sqrt{\sigma}$. The relations between tangent spin and origin spin of the bundles are shown—see Eq. (B3). Third panel defines the interior region and the bottleneck region of Fig. (2).

see Fig. (19).

1. On the bundle frequency relations

In the following we consider the frequency relations among metric bundles. We start by considering the following quantities

$$s \equiv \frac{\omega_H^+}{\omega_H^-} = \frac{r_-}{r_+} = \frac{1}{4(\omega_H^-)^2} = 4(\omega_H^+)^2 \quad \text{see also Eq. (A8)}. \quad \text{It holds} \quad \omega_H^+ \omega_H^- = \frac{1}{4} \quad r_+ r_- = a^2 \quad \text{and} \quad (\text{B4})$$

$$\partial_a^{(2)} \ln s = 0 \quad \text{for} \quad a = a_\partial \equiv \frac{1}{\sqrt{2}} \quad \text{where} \quad s_\partial = 3 - 2\sqrt{2} \approx 0.171573, \quad (\ln s_\partial \approx -1.76275), \quad (\text{B5})$$

We see that $s = 1/4$ (and then $s = 4$) is a remarkable frequency ratio (note that for a fixed tangent spin a_g , the inequality $s \leq 1$ is valid). This quantity is shown in Fig. (24). The spin a_∂ provides a remarkable frequency ratio for the physics of black holes; this is a saddle point of the function $\ln s$ for a . Clearly, s is minimal in the limiting spherically symmetrical case where $a = 0$ and $s = 0$. We also note that, from the analysis of the previous sections, it is evident that, for small values of σ ($\sigma < \sigma_{descr} < 0.5$) and, in general, for large spins a/M , the inner horizon frequencies can exist on orbits of the outer region—see particularly Fig. (7).

Note that if there would be no outer orbits (orbits in the exterior region $r > r_+$ of the extended plane) with frequency equal to the inner horizon frequency ω_H^- , it would imply that there are not metric bundles tangent to the inner horizons in the exterior region; therefore, the **MBs** tangent to the inner horizon would be all confined in the interior region. This is also the problem addressed in Sec. (III). To understand the relations between different bundle frequencies as horizon frequencies for **MBs** of the classes $(\Gamma_{a_g}, \Gamma_{r_g}, \Gamma_{a_0})$ at equal a_g, r_g , or a_0 respectively, it is convenient to study the frequency ratio $s = (\omega_b/\omega_b^1)$. The parameter s is also understood, in general, as the bundle frequency ratio, in which case the dependence from a in (ω_b, ω_b^1) will obviously be different. This allows us to consider both s and $1/s$ as ratios. It can also be considered as a wave signal $\phi_H^\pm(t)$ with frequencies $\omega_b = \omega_H^\pm$, respectively, that gives an immediate impression of the photon frequency difference in those orbits and geometries included in the metric bundles—Figs 25 and 26.

It is clear that the ratio s is a function of the tangent spin $a_g \in a_\pm$. **MBs** tangent to the inner horizon on the extended plane will always have a greater characteristic frequency $\omega_b = \omega_H^-(a_g)$ than *any* **MB** tangent to the outer horizon—see also Figs (5) and (4). However, we can express this ratio in terms of the bundle origins to enlighten the relation between different **MBs** frequencies related by Eq. (9) and Eq. (12). In Sec. (B 2 a), we analyze particular cases.

We now go back to the frequency analysis, introducing the following “resonance” solutions:

$$a_\beta^i : \quad \omega_H^\pm(a_\beta^i) = s\omega_H^\mp(a) \quad \text{where} \quad a_\beta^i \equiv \frac{2as[r_-(a)s^2 + r_+(a)]}{a^2(s^2 - 1)^2 + 4s^2}, \quad (\text{B6})$$

$$a_\beta^{ii} : \quad \omega_H^\pm(a_\beta^{ii}) = s\omega_H^\pm(a) \quad \text{where} \quad a_\beta^{ii} \equiv \frac{2as[r_+(a)s^2 + r_-(a)]}{a^2(s^2 - 1)^2 + 4s^2}, \quad (\text{B7})$$

$$\text{then} \quad a_\beta^i = a_\beta^{ii} \quad \text{for} \quad \lambda = \pm 1 \quad \text{or} \quad \lambda = 0 \quad \text{where} \quad \lambda = \{a/M, s\}. \quad (\text{B8})$$

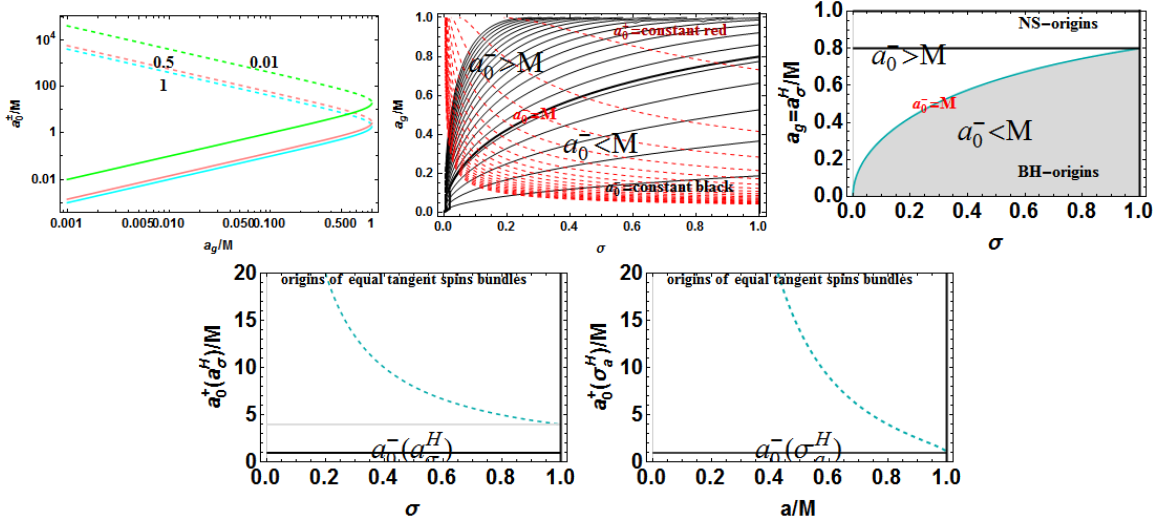


FIG. 20: Study of origins a_0^\pm in terms of the outer and inner horizon frequency. See Sec. (B) and Eqs. (B16) and (B18). Upper panels left: plots of the bundle origin a_0^\pm as functions of the tangent spins a_0 on the outer and inner horizon, respectively, for different planes σ . The logarithm plot shows the logarithm identity as discussed in the text. Here $a_0^+ > a_0^-$ and $a_0^+ = a_0^-$ for tangent spin in $a_g = M$. Bundle tangent spin a_g as horizon spins a_\pm .

Note that the equations with solutions $a_\beta = (a_\beta^i, a_\beta^{ii})$ allow us to analyze and characterize separately both the solutions for (s, s^{-1}) since $a_\beta^i(s) = a_\beta^{ii}(1/s)$ —see Fig. (24).

The spins $a_\beta = (a_\beta^i, a_\beta^{ii})$ have a maximum with respect to the spin $a = a_g \in [0, M]$ for $a_f(s)$, which is a function of s as:

$$a_f(s) \equiv \pm \frac{2s}{(s^2 + 1)} : \quad \partial_a a_\beta = 0, \quad \text{where } a_\beta = (a_\beta^i, a_\beta^{ii}), \quad \text{and} \quad (\text{B9})$$

$$a_\beta^{ii}(a_f) = \frac{s^4 + \left[\sqrt{(s^2 - 1)^2 + 2} \right] s^2 - \sqrt{(s^2 - 1)^2 + 1}}{2(s^4 + 1)}, \quad a_\beta^i(a_f) = \frac{s^4 - \left[\sqrt{(s^2 - 1)^2 - 2} \right] s^2 + \sqrt{(s^2 - 1)^2 + 1}}{2(s^4 + 1)},$$

—see Fig. (24). The following remarkable feature clarifies some significant aspects of the metric bundles:

$$\text{there is (1) } a_f(s) = a_g(a_0, \sigma) \text{ for } s \rightarrow \frac{2}{a_0 \sqrt{\sigma}}, \text{ and (2) } a_f(s) = a_g(\omega_b) \text{ for } s \rightarrow 2\omega_b \quad (\text{B10})$$

where $a_g(a_0, \sigma)$ and $a_g(\omega_b)$ are defined in Eq. (9)—see Fig. (24). These relations ensure that the maximum point spin $a_f(s)$ of Eq. (B9) is the tangent spin a_g (that is the horizon a_\pm on the extended plane) for fixed frequency ratios s that are twice those of the bundle or, equivalently, which depend on the bundle spin origin (in all the analysis of Eq. (B10) we are considering equal spin a). Clearly, $a_f(s)$ is invariant under the transformation $s \rightarrow 1/s$, i.e., $a_f(s) = a_f(s^{-1})$. The maximum $a_\beta(a_f)$ obviously presents the discriminating value $s = \pm 1$. This is also clear from Fig. (24). We are particularly interested in the integer values of s , considering then the symmetries under the transformation $s \rightarrow 1/s$.

Similarly, both $a_\beta = (a_\beta^i, a_\beta^{ii})$ have a maximum for the value:

$$s_\beta^\pm \equiv \sqrt{\frac{2r_\pm}{a^2} - 1} = \sqrt{\frac{4\omega_H^\mp}{a} - 1}. \quad (\text{B11})$$

The function $s_\beta^\pm = s$ coincides, in fact, with the solution of $a = a_f$ of Eq. (B9); this is also clear from the three-dimensional plots of Fig. (24). Moreover, the following bi-logarithmic identity holds $\ln s_\beta^+(\ln a) = -\ln s_\beta^-(\ln a)$ (i.e., under the transformation $a \rightarrow \ln s$ and $a \rightarrow \ln a$). This identity will be found in many of the quantities related to the horizon frequencies we analyze in this section. This is also clear from the bi-logarithmic plots.

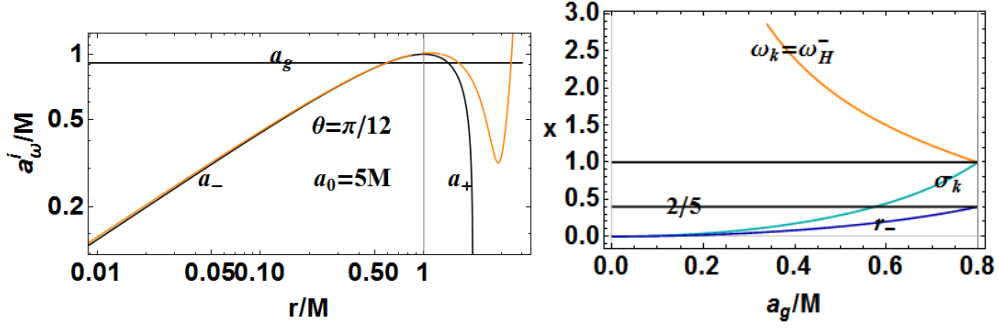


FIG. 21: Left: metric bundle for the origin spin $a_0 = 5M$ and plane $\theta = \pi/12$. The black line is the tangent spin of the bundle (orange) to the horizon curve a_{\pm} (black) on the extended plane. It shows also the existence of minimum of the bundle curve with spin lower than the tangent spin. The full extension of this bundle is depicted in Fig. (12). Right panel: limiting plane σ_k , frequency $\omega_k = \omega_H^-$ (inner horizon frequency on the extended plane), the inner horizon r_- as function of the tangent spin a_g . Based on the analysis of Eqs. (B12) and (B13).

2. Origin and tangent spins relations: metric bundles confinement

With regard to the relation between the origin-spin a_0 and the tangent-spin a_g , we analyze the conditions on the **MBs** origin for the metric bundle to be tangent to the inner horizon $r_g = r_-$ (equivalently, $\omega_b = \omega_H^-$) or the outer horizon $r_g = r_+$ (equivalently, $\omega_b = \omega_H^+$) on the extended plane. Particularly, we discuss the conditions for the **MBs** tangent to the inner horizon curve to remain confined in the inner region of the extended plane, bounded by the inner horizon, where $a \in [0, M]$ and $r \in [0, M]$.

The situation for $\sigma = 1$, equatorial plane, was analyzed in [21]. For a general plane the situation is analogue to the equatorial plane, if we consider the variable $\mathcal{A} = a\sqrt{\sigma}$ as shown in Fig. (5). We know that the **MBs** (and therefore the bundle frequencies) with tangent $a_g \in [0, 0.8]$, $r_g \in [0, 2/5]$ and $\omega_b \geq 1$, origin $\mathcal{A}_0 = a_0\sqrt{\sigma} \in [0, M]$ remain confined for large σ or, equivalently, $a_0 \in [0, 1/\sqrt{\sigma}] \supseteq [0, M]$; the bottleneck region with $\mathcal{A}_0 = a_0\sqrt{\sigma} \in]M, 2M]$ or, equivalently, $a_0 \in [1/\sqrt{\sigma}, 2/\sqrt{\sigma}] \supseteq]M, 2M]$, where $a_g \in]0.8M, M]$, $r_g \in]2M/5, M]$ and $\omega_b \in [0.5, 1[$. Then, depending on the value of σ , they are confined to the exterior region of the extended plane ($a \in [0, M] \cup r > r_+$), i.e., there are no photon orbital frequency equal to the inner horizon for $r > r_+$. We point out, however, that the analysis of Sec. (III) was based on the condition $a < M$ because it is related to the tangent spin $a_g = a < M$.

In general, however, **MBs** spins a satisfy the relation $a_g \leq a_0 > 0$; therefore, on the equatorial plane, there is $a_g \leq a \leq a_0 > 0$, that is, the origin spin is a supremum of the **MBs** spins. We should note that some with **MBs** origin $a_0 > 0$ have, for some plane σ solutions ($r = 0, a = 0$) and different maximum points, which are evident from Figs 13,12,14, and 16. We do not consider here these situations focusing specifically on the relation between the bundle origin spin a_0 and the tangent spin a_g , where the relationship $a_g < a_0$ holds. This problem concerns the following three aspects of the metric bundle properties: **(1)** the confinement of bundles in the region of the inner horizons, **(2)** the presence of mixed **NS** and **BH** bundles, depending on the origin (or tangency spin) and **(3)** the number of orbits for a given spacetime with the same frequency of the inner horizons, that is, the intersection of the horizontal lines of the extended plane $a = \text{constant}$ (this problem concerns the curvature of the bundle solutions on the extended plane). We see an example of bundles with extremum in Fig. (21).

The following property, however, holds

Confinement I: There are *no* solutions of the equation $\mathcal{L} \cdot \mathcal{L} = 0$ in the following case: (B12)

$$\sigma \in [0, 1], \quad r \geq 0, \quad a > M, \quad (1) \quad 0 < \frac{1}{\sqrt{\sigma}\omega} \leq 1, \quad (2) \quad \omega > \frac{1}{2}$$

Confinement II: There are *no* solutions of the equation $\mathcal{L} \cdot \mathcal{L} = 0$ in the following case:

$$\sigma \in [0, 1], \quad r \geq M, \quad 0 < a < M, \quad (1b) \quad 0 < \frac{1}{\sqrt{\sigma}\omega} \leq 2, \quad (2b) \quad \omega > \frac{1}{2}$$

The condition **(1)** on $\sqrt{\sigma}\omega$ means the **BH** origin $a_0 \in]0, M]$; the condition **(2)** on the frequency requires that $\omega = \omega_H^-$, that is, the inner horizon frequency on the extended plane ($\omega = 1/2$ for $a_g = M$). Finally, the condition $a > M$ is the assumption that **MBs** with origin in **BH** $a_0 \in \text{BH}$ are *not* confined in the **BH** region, which means that $a > M$. This case does not occur under those conditions. This demonstrates the *confinement* of the **MBs** occurs in the interior region, if the origin is $a_0 \in]0, M]$. These confined **MBs** with origin in the **BH** region have tangent spin

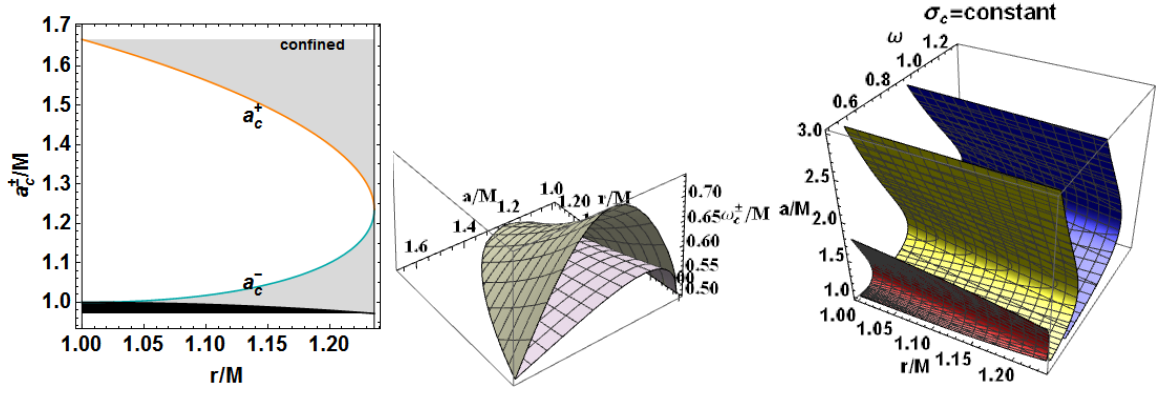


FIG. 22: Confinement of the inner horizon frequencies based on the analysis of Eq. (B15). Left: limiting spins a_c^\pm as functions of r/M . Center: limiting frequencies ω_c^\pm as functions of r/M and a/M . Right: plane solution $\sigma_c = \text{constant}$ for a/M and r/M and frequency ω (blue is for $\sigma = 0.1$, yellow is for $\sigma = 0.3$, red for $\sigma = 0.9$).

$a_g/M \in [0, 4/5]$. Specifically,

$$a_g \in]0, 4M/5[\quad \text{and} \quad \sigma \in [\sigma_k, 1] \quad \text{where} \quad \sigma_k \equiv \frac{8}{a_g^2} - 8\sqrt{\frac{1}{a_g^2} \left(\frac{1}{a_g^2} - 1 \right)} - 4 \quad \text{and} \quad (B13)$$

$$\omega = \omega_k \equiv \frac{a_g \sqrt{\frac{1}{a_g^2} - 1} + 1}{2a_g}, \quad r_g \in]0, 2M/5] \quad (\text{for } a_g = \frac{4M}{5}, \quad \sigma = 1, \quad \omega = 1) \quad (B14)$$

–Fig. (21).

Therefore, this has the important consequence that if the origin is $a_0 \in \mathbf{BH}$, then the metric bundle will be confined in the \mathbf{BH} region for *any* plane $\sigma \in]0, 1]$. The outer horizon on the extended plane is generated *only* by \mathbf{NS} bundle origins with $a_0 > 2M$. Viceversa, according to the value of the plane σ , the inner horizon can be generated either by \mathbf{NS} or only by \mathbf{BH} origins (as it was also for the $\sigma = 1$ case), \mathbf{BH} origin \mathbf{MBs} generate *only* the inner horizon on the extended plane. This holds also according to $a_0 > a_g(a_0, \sigma)$, which is always verified. The \mathbf{MBs} with \mathbf{NS} origins, tangent to the inner horizon can also be at $a_0 > 2M$: $\mathcal{A}_0 > 2M$ generate only the outer horizon, viceversa $\mathcal{A}_0 < 2M$ generate only the inner horizon, as $\mathcal{A} = a\sqrt{\sigma}$; this implies $a_0 > 2/\sqrt{\sigma} \geq 2$ (equivalently, $\sqrt{\sigma} > 2/a_0$ with $a_0 \geq 2$) with $\sigma \in [0, 1]$, for the construction of only the outer horizon. For the inner horizon, there is $a_0 < 2/\sqrt{\sigma} \geq 2$ (equivalently, $\sqrt{\sigma} < 2/a_0$) thus there is no upper limit for a_0 ; it can be larger, depending on how close the orbit r is to the rotation axis ($\sigma \approx 0$), whereas the bottom limit is 2, i.e., for $a_0 < M$; in particular, the origin is always in the \mathbf{BH} region. Therefore, portions of the internal horizon are generated by different \mathbf{BH} origins in agreement also with the analysis of [21]. We shall investigate these limits more precisely below.

There are solutions of the condition $\mathcal{L} \cdot \mathcal{L} = 0$ in the following cases:

$$\sigma \in]0, 1], \quad a > M, \quad 1 < \frac{1}{\sqrt{\sigma}\omega} \leq 2, \quad \omega > \frac{1}{2}, \quad r > M \quad \text{more precisely,} \quad \frac{r}{M} \in]1, \sqrt{5} - 1[\quad a \in]a_c^-, a_c^+[\quad \omega \in [\omega_c^-, \omega_c^+[,$$

$$\text{where} \quad a_c^\mp \equiv \frac{4}{r+2} \mp \sqrt{\frac{-r^4 - 2r^3 + 4r^2}{(r+2)^2}}, \quad \omega_c^- \equiv \frac{2a}{a^2(r+2) + r^3} + \sqrt{\frac{r^2\Delta}{[a^2(r+2) + r^3]^2}}, \quad (B15)$$

$$\omega_c^+ \equiv \frac{1}{2} \left[\frac{4ar}{a^4 + 2a^2(r^2 - 2) + r(r^3 - 4r + 8)} + \sqrt{\frac{a^2\Delta(a^2 + r^2 - 4)^2}{[a^4 + 2a^2(r^2 - 2) + r(r^3 - 4r + 8)]^2}} \right],$$

$$\sigma_c \equiv \frac{a^4\omega^2 + 2a^2r^2\omega^2 + a^2 - a^2\omega^2\Delta\sqrt{\frac{[a - \omega(a^2 + r^2)]^2[\omega^2(a^2 + r^2)^2 + 2a\omega[a^2 + (r-4)r] + a^2]}{a^4\omega^4\Delta^2}} - 4ar\omega + r^4\omega^2}{2a^2\omega^2\Delta},$$

–Fig. (22). Firstly, we made use of the recursive relation considered in [21] and Eqs. (A10) and (A15) to study the corresponding \mathbf{MBs} with $a_0^p = a_g$, i.e., the origin of the second bundle is the tangent spin of the first bundle. This analysis also shows another aspect of the confinement of metric bundles. From the condition $a_g < a_0$, it follows that the spin $a_g^{(1)}(a_g)$ corresponds to a \mathbf{BH} . Consider the origins a_0^\pm of the \mathbf{MBs} tangent to the inner and outer horizons,

respectively, and we express them in terms of the tangency frequency. Then,

$$a_0^\pm \equiv \frac{1}{\omega_H^\pm \sqrt{\sigma}}, \quad \text{where } a_0^+ \geq a_0^-. \quad (\text{B16})$$

Outer horizon tangency:

$$a_0^+ \geq 2M \quad \text{for any } a_g \in]0, M] \quad \text{and } \sigma \in]0, 1], \quad (a_0^+ = 2M) \quad \text{for } a_g = M$$

Inner horizon tangency:

$$\bullet \quad a_0^- = 1 \quad \text{for } a_g = a_\sigma^H, \quad \bullet \quad a_0^- > M \quad \text{for } a_g \in]a_\sigma^H, M], \quad \bullet \quad a_0^- \in]0, M[\quad \text{for } a_g \in]0, a_\sigma^H[.$$

Equivalently

- $a_0^- = M$ for $a_g/M \in]0, 4/5]$ and $\sigma = \sigma_a^H$,
- $a_0^- > M$ for $a_g/M \in]0, 4/5[$ and $\sigma \in]0, \sigma_a^H[$, $a_g/M \in]4/5, 1]$ and $\sigma \in]0, 1]$
- $a_0^- \in]0, M[$ for $a_g/M \in]0, 4/5]$ and $\sigma \in]\sigma_a^H, 1]$,

$$\text{where } a_\sigma^H \equiv 4\sqrt{\frac{\sigma}{(\sigma+4)^2}} < \frac{4}{5} = 0.8, \quad \sigma_a^H \equiv \frac{4(2r_- - a^2)}{a^2},$$

(we consider mainly $a \geq 0$ and $\sigma \geq 0$)—Figs (20)–(23). The spin $a_0^+(a_g^H)$ is the origin of the bundle tangent at a_σ^H to the outer horizon on the extended plane of a **BH** spacetime with spin a_g^H ; the origin of the bundle relative to the construction of the inner horizon, $r_-(a_\sigma^H)$ is obviously, in agreement with Eq. (B17), $a_0^-(a_\sigma^H) = M$, where

$$a_0^+(a_\sigma^H) \equiv \frac{(\sigma+4) \left[\sqrt{\frac{(\sigma-4)^2}{(\sigma+4)^2} + 1} \right]}{2\sigma}, \quad a_0^-(a_\sigma^H) = M; \quad a_0^+(\sigma_a^H) \equiv \frac{a}{r_- \sqrt{\frac{2r_- - a^2}{a^2}}}, \quad a_0^-(\sigma_a^H) = M \quad (\text{B18})$$

—Fig. (20). We note that these relations depend on the plane σ (dependence on the origins \mathcal{A}_0). Note also that $a_0^+(a_\sigma^H) = 4M$ for $\sigma = 1$ where $a_\sigma^H/M = 4/5$. Clearly, $a_0^\pm(a_g)$ is the inverse function of $a_g(a_0, \sigma)$ represented in Fig. (5) and studied in different parts of this article. We have already seen that this function can be set for variable $\mathcal{A} \equiv a\sqrt{\sigma}$. Now, the explicit form of $a_0(a_g)$ under the restriction $a_0 > 0$ is

$$a_0^\mp(a_g) \equiv \sqrt{\frac{4(2-a_g^2)}{\sigma a_g^2} \mp 8\sqrt{\frac{1-a_g^2}{a_g^4 \sigma^2}}}, \quad (\text{equivalently } a_0^\mp = \frac{2r_\mp(a_g)}{a_g \sqrt{\sigma}}), \quad \text{where} \quad (\text{B19})$$

$$\sigma = 0 \quad a_g = 0, \quad a_0 > 0; \quad a_g = 1 \quad a_0 = \frac{2}{\sqrt{\sigma}}, \quad \frac{a_0^-(a_g)}{a_0^+(a_g)} = \sqrt{-\frac{4[r_+(a_g)+1]}{a_g^2} + \frac{8r_+(a_g)}{a_g^4} + 1}, \quad \text{and}$$

$$\bullet \quad \partial_{a_g}^{(2)} a_0^+(a_g) = 0 \quad \text{for } a_g = \frac{\sqrt{3}}{2}, \quad \text{where } \left(\omega_H^- = \frac{\sqrt{3}}{2}, \omega_H^+ = \frac{1}{2\sqrt{3}} \right), \quad \mathbf{s} = \frac{\omega_{\mathbf{H}}^+}{\omega_{\mathbf{H}}^-} = \frac{\mathbf{1}}{\mathbf{3}} = \frac{\mathbf{a}_0^-}{\mathbf{a}_0^+} \quad \text{and}$$

$$a_0^\mp = \frac{2\sqrt{\frac{5}{\sigma} \mp 4\sqrt{\frac{1}{\sigma^2}}}}{\sqrt{3}}, \quad \text{for } \sigma = 1 \quad \left(a_0^- = \frac{2}{\sqrt{3}}, a_0^+ = 2\sqrt{3} \right), \quad \text{and}$$

$$\bullet \quad \partial_{a_g}^{(2)} a_0^-(a_g) = 0 \quad \text{for } a_g = \frac{1}{\sqrt{2}}, \quad \text{where } \omega_H^\mp = \frac{1}{2} \pm \frac{1}{\sqrt{2}}, \quad \mathbf{s} = \frac{\omega_{\mathbf{H}}^+}{\omega_{\mathbf{H}}^-} = \mathbf{3} - 2\sqrt{2} = \frac{\mathbf{a}_0^-}{\mathbf{a}_0^+} \quad \text{and}$$

$$a_0^\mp = 2\sqrt{\frac{3}{\sigma} \mp 2\sqrt{2}\sqrt{\frac{1}{\sigma^2}}}, \quad \text{for } \sigma = 1 \quad a_0^\mp = 2\sqrt{3 \mp 2\sqrt{2}} \quad (\text{B20})$$

—Fig. (23). The origin spin $a_0 = 2/\sqrt{\sigma}$ is a limiting value that is often found in this analysis as this is related to the extreme Kerr geometry. Other remarkable spins are $a_g = \sqrt{3}/2$ and $a_g = 1/\sqrt{2}$. Notably these are independent from the plane σ ; furthermore, we recall that these spins correspond to particular bundle frequencies and particular frequency ratios. It is important to note that the ratio $a_0^-(a_g)/a_0^+(a_g)$, that is, the bundle spin origins related to the construction of the inner and outer horizon of the same geometry with spin a_g (the tangent spin of the two bundles) is *independent* of the plane σ .

These relations allow us to establish for a given tangent spin if the origin is a **BH** or a **NS** and, vice versa, given a bundle origin we can establish the tangent spin a_g . Obviously, there is always $a_g \in \mathbf{BH} \equiv [0, 1]$. However, as was the case in the equatorial plane studied in [21], there are particular classes of **BHs** and **NSs**.

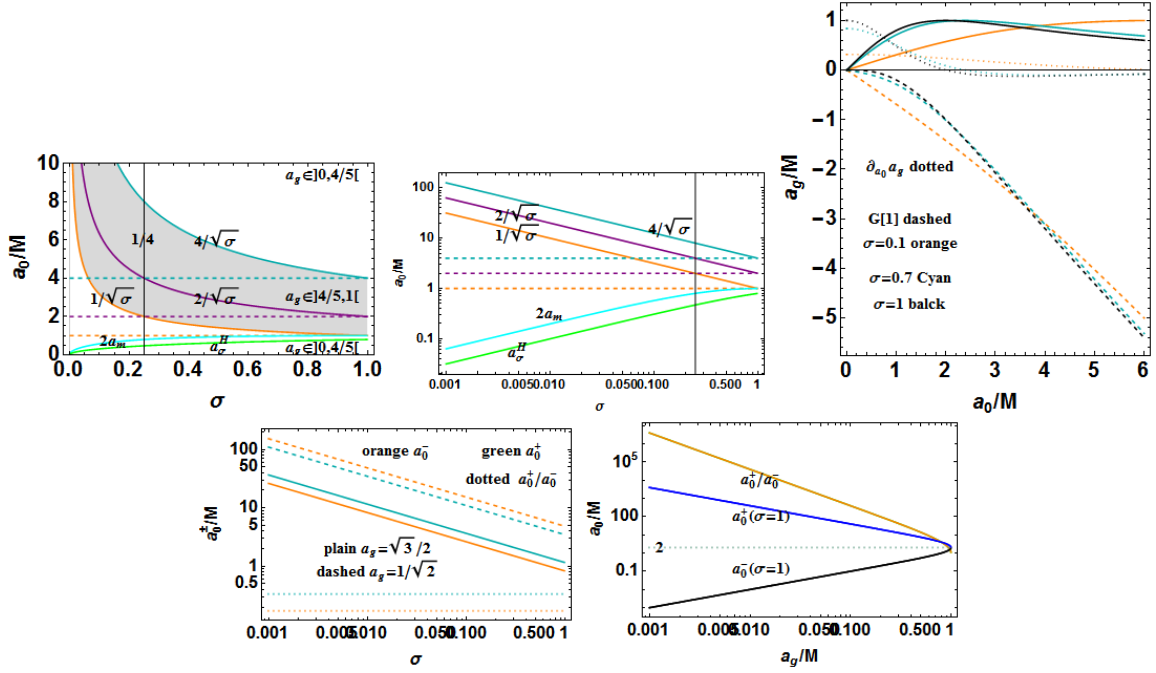


FIG. 23: Upper line. Left panel: relation $a_0(a_g)$ and regions **BH-NS** origin a_0 to **BH** tangent spins a_g as function of the plane $\sigma \in [0, 1]$. The limiting values $a_0 \in \{1, 2, 4\}$ are shown explicitly. In the gray region a_0 corresponds to $a_g \in [0.8M, M]$. It refers to the analysis of Eqs. (B21, B22) and (B16). Center panel: logarithmic plot shows the logarithm identity discussed in the text. Right panel: tangent spin $a_g(a_0)$ and bundle origin spin for different planes σ , dotted line is the a_g gradient. Dashed curve is $G[1] \equiv a_g(a_0) - a_0$ for different a_0 . Crossing a_g curves represent bundles with equal tangent spin a_g and origin a_0 , consequently, with different planes σ and eventually different frequencies $\omega_H^+(a_g)$ or $\omega_H^-(a_g)$ –see Eq. (A2). The origins are related to the frequencies and planes by $a_0 = 1/(\omega_b \sqrt{\sigma})$, it follows for two bundles planes $\sigma_p = \frac{16}{a_0^4 \sigma}$ or $\sigma = \sigma^p$ with frequencies related by $\omega_b^p/\omega_b = \sqrt{\sigma}/\sqrt{\sigma^p}$. This is also related to bundle frequency ratios $s = \omega_b^p/\omega_b = \sqrt{\sigma}/\sqrt{\sigma^p}$. Based upon the analysis of Eq. (B19).

We see that a_0^+ , i.e., the origin of the **MBsf** tangent to the outer horizon is necessarily a **NS** in agreement also with Eq. (12). Therefore, for each plane σ the outer horizon is built by **MBs** with **NS** origins and particularly for $a_0 > 2M$. In the case of the inner horizon, as it was for $\sigma = 1$, for $a_g \in]0.8M, M[$ there is a **NS** origin $a_0 \in]M, 2M[$ for any plane. Therefore, the portion $a_g \in]0.8M, M[$ of the inner horizon is always constructed by bundles with **WNS** spin origin $a_0 \in]M, 2M[$ for any plane. For $a_g < 0.8M$ there may be **BH** or **NS** origins, depending on the plane (if the angles are considerably small).

In other words, if a_0 is a **BH**, then the tangent point is certainly a **BH** with $a_g \in [0, 0.8M]$. An extreme spacetime $a_g = M$ corresponds to an origin $a_0 = 2/\sqrt{\sigma}$; particularly, if $a_g \in]0, 0.8M[$, then $a_0 \in]0, 0.8M[$ and, viceversa, for the range $]0, 0.8M[$ the bounding range for the spin is $a \in \{a_0, a_g\}$, which confines the **MBs** in the region bounded by the inner horizon—see also[21].

Then,

- $a_0^- > 2M$ for $a_g \in]2a_m, M[$; • $a_0^- \in]M, 2M[$ for $a_g \in]a_\sigma^H, 2a_m[$; • $a_0^- \in]0, 1[$ for $a_g > a_\sigma^H$

where $\frac{a_m}{M} \equiv \sqrt{\frac{\sigma}{(\sigma+1)^2}}$. It holds $\partial_x a_g = 0$ for $a = \frac{2}{\sqrt{\sigma}}$ where $x \in \{a_0, \sigma\}$, (B21)

(we note that $a_g \neq A \equiv a\sqrt{\sigma}$, and $a_g = A$ only for $\sigma = 0$ and $a_g \neq a_0$)—Fig. (23).

Then, $a_0^{(1)} = a_g \in]0.8M, M[$ (implying a **NS** bundle origin a_0 according to Eq. (B17), if $a_0 \in]1/\sqrt{\sigma}, 4/\sqrt{\sigma}[$, and for $a_0 = 2/\sqrt{\sigma}$ we obtain that $a_g = M$. Otherwise, we have that $a_0^{(1)} = a_g \in]0, 0.8M[$, if $a_0 \in]0, 1/\sqrt{\sigma}[$ and $a_0 > 4/\sqrt{\sigma}$, that is, a **BH** and **NS** origin—see Fig. (23). We see below some essential features of the bundles concerning the relation

$a_g(a_0)$:

BH origins $a_0 \in]0, M[$ then • $a_g \in]0, 0.8M[, (r_g = r_- \in]0, 0.5M[$ (B22)

NS origins $a_0 > M$

• $a_g \in]0.8M, M[$ for **(i)** $a_0 \in]M, 2M[$ $\sigma \in]1/a_0^2, 1]$,

(ii) $a_0 \in [2M, 4M[$ $\sigma \in]1/a_0^2, 1]$; **(iii)** $a_0 \geq 4M$ $\sigma \in]1/a_0^2, 16/a_0^2[$

equivalently $a_0 \in]1/\sqrt{\sigma}, 4/\sqrt{\sigma}[$

• $a_g \in]0, 0.8M[$ for **(i)** $a_0 \in]M, 4M[$ $\sigma \in]0, 1/a_0^2[$, **(ii)** $a_0 > 4M$, $\sigma \in]0, 1/a_0^2[\cup \sigma \in [16/a_0^2, 1]$,
equivalently $a_0 \in]1, 1/\sqrt{\sigma}[\cup a_0 > 4/\sqrt{\sigma}$

Inner horizon tangency: $a_g \in]0, M[$ $r_g = r_- \in]\sqrt{a_g^2\sigma}/2, 1[$ $a_0 = 2r_g/a_g\sqrt{\sigma}$

–Figs (23,24,26).

a. Relations between the frequencies of particular bundles seen as horizon frequencies

We now focus on particular pairs of bundles, introduced in Eq. (A11), which are related through their frequencies. Following the considerations of Sec. (B), we know that each photon orbital frequency at any point of any Kerr (**NS** or **BH**) geometry is a horizon frequency ($\omega_H^\pm(a_g), \omega_H^\pm(a_g^p)$), where (a_g, a_g^p) are the tangent spins of two bundles crossing in the point \bar{r} . Therefore, the following relations hold

Metric bundles with equal (a_g, σ) : $\omega_b^1 = \frac{1}{4\omega_b} = \frac{a}{2r_\pm}$ respectively for $\omega_b = \omega_H^\mp$ –see Eq. (A8) (B23)

corresponding bundles $a_0^1 = a_g$: $\omega_b^1 = \frac{1}{4\sqrt{\sigma}\sqrt{\frac{\omega_b^2}{(4\omega_b^2+1)^2}}} = \frac{1}{a\sqrt{\sigma}} = \frac{1}{\mathcal{A}}$ for $\omega_b = \omega_H^\mp$, see Eq. (A10)(B24)

Bundles with equal ω_b $(\mathbf{r}_g, \mathbf{a}_g)$ $a_0^p = a_0\sqrt{\frac{\sigma}{\sigma_p}}$ ($\mathcal{A}_0^p = \mathcal{A}_0$), $\omega_H^\pm = \frac{1 \mp \sqrt{1 - \frac{a_0^2\sigma}{\sigma_p}}}{2a_0\sqrt{\frac{\sigma}{\sigma_p}}}$ see Eq. (A7)

Tangent spin $a_g = \frac{4\mathcal{A}_0}{\mathcal{A}_0^2 + 4}$ see Eqs (9,A1,A5,A13) $\omega_H^\mp(a_g) = \frac{\mathcal{A}_0^2 \pm \sqrt{(\mathcal{A}_0^2 - 4)^2 + 4}}{8\mathcal{A}_0}$ (B25)

Bundle origin $a_0 = \frac{1}{\sqrt{\sigma}\omega_b}$. For $\omega_b = \omega_H^-$ $a_0 = \frac{2a}{r_+\sqrt{\sigma}}$. For $\omega_b = \omega_H^+$ $a_0 = \frac{2r_+}{a\sqrt{\sigma}}$. (B26)

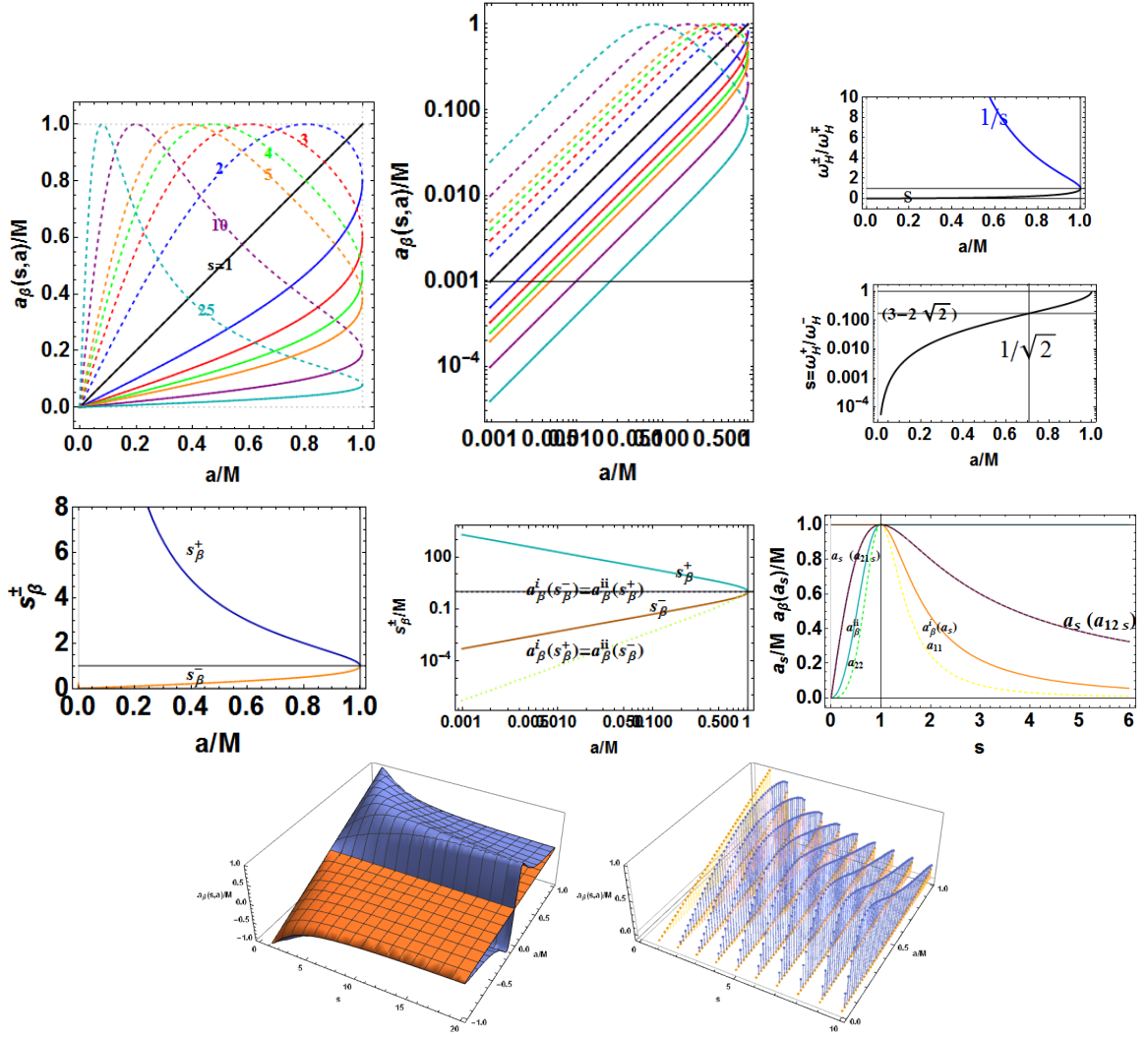


FIG. 24: Upper line. Left panel: spins $a_\beta = \{a_\beta^i, a_\beta^{ii}\}$ of Eq. (B6) for different resonance solutions $s \equiv \omega_H^+/\omega_H^-$ as functions of the tangent spin a of the second frequency bundle ω_H^\pm , in accordance with Eq. (B6). The identity for $s = 1$ and the symmetry for $s \rightarrow 1/s$ are shown. Note the behavior as s increases. Plots provide also the classes of metric bundles with same resonant frequencies. The situation for a fixed **BH** geometry with spin a_g is described by vertical $a_g = \text{constant}$ line of the graph (which is clearly independent of the plane σ). Central panel: logarithmic plot shows the logarithmic identities discussed in the text (generally in the form $\ln Q_1(\ln q_1) = -\ln Q_2(\ln q_2)$ for any quantities $\{Q_1, Q_2, q_1, q_2\}$). Right panel: $s(a_g)$ as function of the bundle tangent spin—Eq. (B4). Note the relation between (s, s^{-1}) and the role of the saddle point $a_\partial = M/\sqrt{2}$. Here $s = 1$ for $a_g = M$. Center panel line. Left: ratios s_β^\pm of Eq. (B11) as functions of the tangent spin a_g/M and maximum of $a_\beta = (a_\beta^i, a_\beta^{ii})$ with respect to s . The role of $s = 1$ for $a = M$ and the symmetries of $(s_\beta^+, 1/s_\beta^-)$ are explicitly shown. Center panel: di-logarithmic plot of s_β^\pm and the functions $(a_\beta^i, a_\beta^{ii})$ on s_β^\pm . Right panel: maximum spin $a_f(s)$ of Eq. (B10) as function of s . The spins maximum $a_\beta(a_f)$, Eq. (B10), and $a_{11} = a_\beta^i(a_\beta^i)$, $a_{22} = a_\beta^{ii}(a_\beta^{ii})$, $a_{12} = a_\beta^i(a_\beta^{ii})$, $a_{21} = a_\beta^{ii}(a_\beta^i)$ are also shown, where $a_{12} \cup a_{21} = a_f$. Bottom panel lines: 3D plots of a_β^\pm as functions of $a_g \in [-M, M]$ and s (left panel) for $s \in \mathbb{N}$ (right panel).

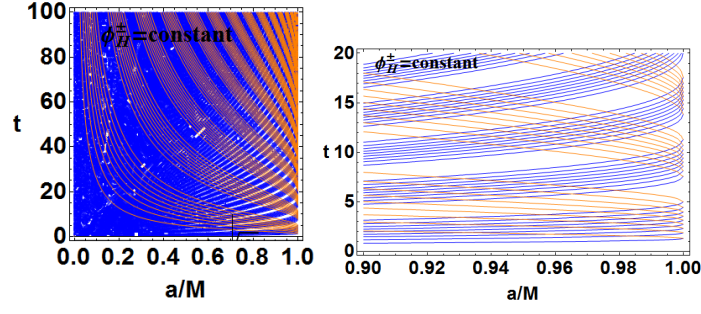


FIG. 25: Function $\phi_H(\omega_H^\pm t) = \text{constant}$ in the plane $(t, a/M)$. ω_H^\pm are the frequencies of the outer and inner horizons, respectively. Based on the analysis of Sec. (B). See also Figs (26).

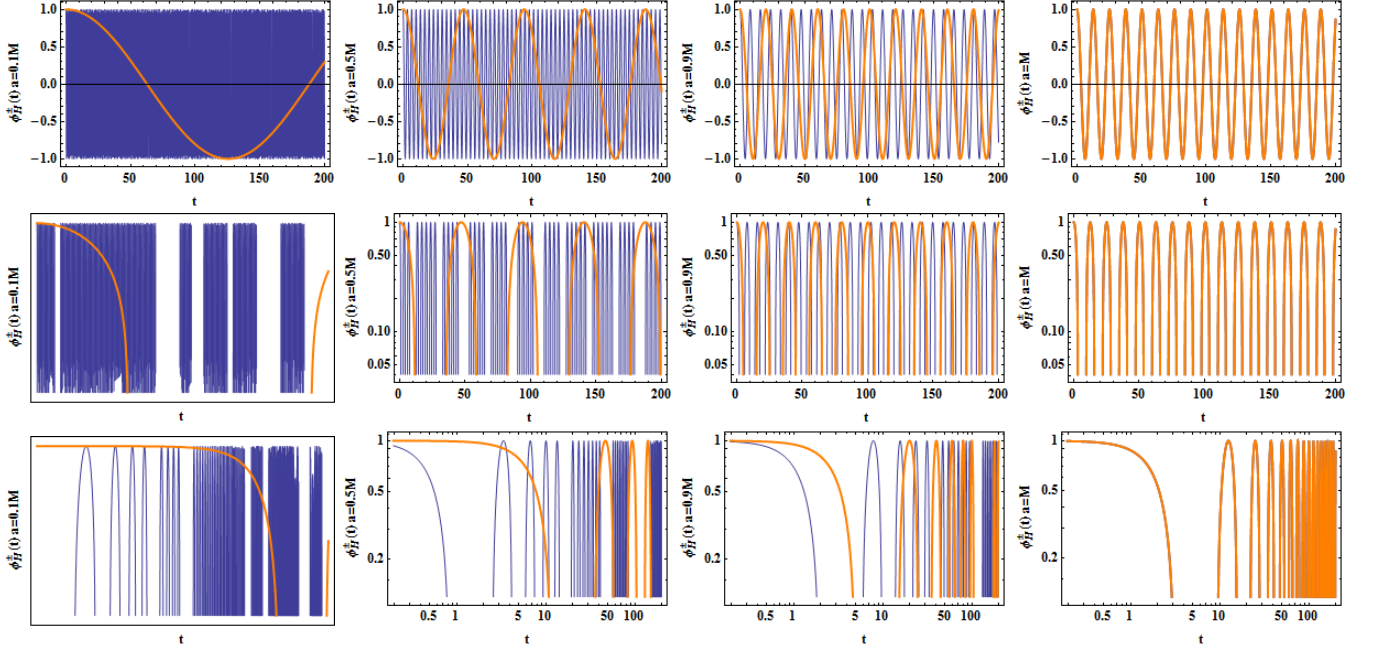


FIG. 26: Cosinusoidal signal $\phi_H^\pm(\omega_H^\pm)$ associated with metric bundles Γ_{a_g} with equal tangent spin. $\omega_H^+ < \omega_H^-$ are the frequencies of the outer and inner horizon, respectively, where $\omega_H^+ = \omega_H^-$ for $a = M$. Plots are for different tangent spins a_g and logarithmic (central panels) and di-logarithms scales (below panels). Based on the analysis of Sec. (B). See also Figs (25).

Appendix C: Solutions of the condition $\mathcal{L}_{\mathcal{N}} \equiv \mathcal{L} \cdot \mathcal{L} = 0$

1. Explicit expressions of metric bundles

Metric bundles a_ω for $\sigma \neq 1$ can be written as

$$\begin{aligned}
a_\omega^1 &\equiv \frac{\Upsilon_1 - 3\sqrt{\Upsilon - \Gamma - \Upsilon_3}}{6}, & a_\omega^2 &\equiv \frac{\Upsilon_1 + 3\sqrt{\Upsilon - \Gamma - \Upsilon_3}}{6}, & a_\omega^3 &\equiv \frac{-\Upsilon_1 - 3\sqrt{\Upsilon + \Gamma - \Upsilon_3}}{6}, & a_\omega^4 &\equiv \frac{-\Upsilon_1 + 3\sqrt{\Upsilon + \Gamma - \Upsilon_3}}{6}; \\
\Upsilon &\equiv \frac{4}{3} \left[\frac{r[2\sigma - r(\sigma - 2)]}{\sigma - 1} + \frac{1}{\sigma\omega^2} \right], & \Gamma &\equiv \frac{8\sqrt{3}r}{(\sigma - 1)\omega\sqrt{-2r^2 + \frac{2(r+2)r}{\sigma-1} + 4r + 3\Upsilon_3 + \frac{2}{\sigma\omega^2}}}; \\
\Upsilon_3 &\equiv \frac{4r(r^3\sigma\omega^2 - r + 2)}{\sqrt[3]{\Upsilon_4 + \Upsilon_2}} - \frac{[r\sigma\omega^2[2\sigma - r(\sigma - 2)] + \sigma - 1]^2}{3(\sigma - 1)\sigma\omega^2\sqrt[3]{\Upsilon_4 + \Upsilon_2}} + \Upsilon_5 \\
\Upsilon_5 &\equiv -\frac{\sqrt[3]{\Upsilon_4 + \Upsilon_2}}{3(\sigma - 1)\sigma\omega^2}, & \Upsilon_1 &\equiv \sqrt{\frac{-6r^2(\sigma - 2) + 12r\sigma + 9\Upsilon_3(\sigma - 1)}{\sigma - 1} + \frac{6}{\sigma\omega^2}}; \\
\Upsilon_4 &\equiv \frac{1}{2} \left([72r(\sigma - 1)\sigma\omega^2(r^3\sigma\omega^2 - r + 2)[r\sigma\omega^2[2\sigma - r(\sigma - 2)] + \sigma - 1] - 432r^2(\sigma - 1)\sigma^3\omega^4 + \right. \\
&\quad \left. 2[r\sigma\omega^2[2\sigma - r(\sigma - 2)] + \sigma - 1]^3 \right)^2 - 4 \left((r\sigma\omega^2(2\sigma - r(\sigma - 2)) + \sigma - 1)^2 - 12r(\sigma - 1)\sigma\omega^2(r^3\sigma\omega^2 - r + 2) \right)^3 \Big)^{1/2}, \\
\Upsilon_2 &\equiv 36r(\sigma - 1)\sigma\omega^2[r^3\sigma\omega^2 - r + 2](r\sigma\omega^2[2\sigma - r(\sigma - 2)] + \sigma - 1) - 216r^2(\sigma - 1)\sigma^3\omega^4 + \\
&\quad [r\sigma\omega^2[2\sigma - r(\sigma - 2)] + \sigma - 1]^3.
\end{aligned} \tag{C1}$$

2. Explicit expression for light surfaces

The expression (6) for the frequencies of a stationary observer can be considered as an equation for the radii $r_s^{(i)}$ ($i \in \{1, \dots, 4\}$) of the light surfaces, i.e., solutions of the condition $\mathcal{L} \cdot \mathcal{L} = 0$. Solutions are then given as functions of the frequency ω and the plane σ as

$$r_s^1 \equiv \frac{\ominus_{IV} - \sqrt{2\ominus - \ominus_{III} - \ominus_{II}}}{2}, \quad r_s^2 \equiv \frac{\ominus_{IV} + \sqrt{2\ominus - \ominus_{III} - \ominus_{II}}}{2}, \tag{C2}$$

$$r_s^3 \equiv \frac{-\sqrt{2\ominus + \ominus_{III} - \ominus_{II}} - \ominus_{IV}}{2}, \quad r_s^4 \equiv \frac{\sqrt{2\ominus + \ominus_{III} - \ominus_{II}} - \ominus_{IV}}{2}, \quad \text{where} \tag{C3}$$

$$\ominus_{IV} \equiv \sqrt{\ominus + \ominus_{II}}; \quad \ominus_{III} \equiv \frac{4(a\sigma\omega - 1)^2}{\sigma \ominus_{IV} \omega^2}; \quad \ominus \equiv +\frac{2}{3} \left(a^2(\sigma - 2) + \frac{1}{\sigma\omega^2} \right),$$

$$\ominus_{II} \equiv \frac{a^2\sigma\omega^2 [\sigma (a^2[(\sigma - 16)\sigma + 16]\omega^2 + 14) - 16] + 1}{9 \ominus_V \sigma^2\omega^4} + \ominus_V;$$

$$\ominus_V \equiv \frac{\sqrt[3]{-[a^2(\sigma - 2)\sigma\omega^2 + 1]^3 - 36a^2(\sigma - 1)\sigma\omega^2(a^2\sigma\omega^2 - 1)[a^2(\sigma - 2)\sigma\omega^2 + 1] + 54\sigma\omega^2(a\sigma\omega - 1)^4 + \frac{\ominus_I}{2}}}{3\sigma\omega^2}$$

$$\begin{aligned}
\ominus_I &\equiv \left(4 \left[(a^2(\sigma - 2)\sigma\omega^2 + 1)^3 + 36a^2(\sigma - 1)\sigma\omega^2(a^2\sigma\omega^2 - 1)[a^2(\sigma - 2)\sigma\omega^2 + 1] - 54\sigma\omega^2(a\sigma\omega - 1)^4 \right]^2 + \right. \\
&\quad \left. - 4(a^2\sigma\omega^2[\sigma(a^2[(\sigma - 16)\sigma + 16]\omega^2 + 14) - 16] + 1)^3 \right)^{1/2}.
\end{aligned} \tag{C4}$$

3. Planes σ in terms of (a, ω, r)

Finally, in this section we report some planes and limiting values for the spins and frequencies that are relevant for determining the existence of **MBs**:

$$\omega_{rad} = \sqrt{\frac{1}{r(r+2)}}, \quad \omega_{\sqrt{2}} \equiv \frac{1}{2\sqrt{2}}, \quad a_{\sqrt{2}} \equiv \sqrt{2}, \quad a_{\text{lim}}^{\sigma} \equiv \frac{1}{\sigma-1}, \quad a_{\lambda}^{\sigma} \equiv 4\sqrt{-\frac{\sigma-1}{(\sigma-2)^4}} \quad (\text{C5})$$

$$\sigma_{\omega}^{\pm} \equiv -\frac{4ar\omega - a^2 - r^4\omega^2 - a^4\omega^2 - 2a^2r^2\omega^2 \pm [a - \omega(a^2 + r^2)] \sqrt{\omega^2(a^2 + r^2)^2 + 2a\omega[a^2 + (r-4)r] + a^2}}{2a^2\omega^2\Delta},$$

where $\omega_{\pm}(a_{\epsilon}) = \frac{\sqrt{1 - \frac{(r-2)r}{\sigma-1}} \mp 1}{2\sqrt{\frac{(r-2)r}{\sigma-1}}}$. (C6)

In particular, σ_{ω}^{\pm} are solutions of $\mathcal{L} \cdot \mathcal{L} = 0$ – Fig. 4. Then, we obtain

$$\omega_{\pm}(a=0) = \mp \frac{(r-2)r}{\sqrt{(r-2)r^5\sigma}}, \quad \text{where} \quad \lim_{a \rightarrow \infty} \omega_{\pm} = 0, \quad \omega_{\pm}(r=0) = \mp \omega_0^{\pm} = \mp \frac{1}{a\sqrt{\sigma}}, \quad (\text{C7})$$

$$\omega_{\pm}(r=2M, \sigma=1) = (0, \frac{a}{a^2+2}), \quad \omega_{\pm}(r=M, \sigma=1) = \omega_{11}^{\pm} \equiv \frac{1}{2a \pm \sqrt{a^2-1}}, \quad \frac{r_{\omega}}{M} \equiv \sqrt{\frac{\omega^2+1}{\omega^2}} - 1 \quad (\text{C8})$$

As a function of σ , $\omega_{\pm}(a=0)$ has an extreme at $r=2M$, where it is $\omega_{\pm}(a=0)=0$, and as a function of r at $r=3M$, where $\omega_{\pm}(a=0) = 1/3\sqrt{3}\sqrt{\sigma}$. Moreover, the frequency ω_{11}^{\pm} has an extreme for $a = \mp 2/\sqrt{3}$, respectively, where $\omega_{11}^{\pm} = \mp 2/\sqrt{3}$. The frequency $\omega_{\pm}(r=2M, \sigma=1)$ has an extreme at $a = \pm\sqrt{2}$, where $\omega_{\pm}(r=2M, \sigma=1) = 1/2\sqrt{2}$. See Figs (1)–(4).

Appendix D: On the metric bundles of the extended plane

1. On negative frequencies

Solutions with frequencies $\omega > 0$ of the condition $\mathcal{L} \cdot \mathcal{L} = 0$ with $a < 0$ (counter-rotating, negative frequencies) exist for:

$$\mathcal{L}_{\mathcal{N}} = 0, \quad \text{with} \quad \omega = -\omega_H^+ > 0, \quad a < 0, \quad \sigma \in]0, 1], \quad r \geq 0 \quad \text{is } \sigma_{\mathcal{L}} \text{ for}$$

$$\bullet \quad r \in]0, 2M[\quad a \in [-1, -a_{\pm}[\quad \bullet \quad r > 2M \quad a \in]-1, a_{\mathcal{L}\mathcal{L}}].$$

$$\mathcal{L}_{\mathcal{N}} = 0, \quad \text{with} \quad \omega = -\omega_H^- > 0, \quad a < 0, \quad \sigma \in]0, 1], \quad r \geq 0 \quad \text{is } \sigma_{\mathcal{L}} \text{ for:}$$

$$\bullet \quad r \in]0, 2M[\quad a \in]-M, -a_{\pm}[\quad \bullet \quad r \geq 2M \quad a \in]-M, 0[$$

$$\text{where} \quad \sigma_{\mathcal{L}} \equiv \frac{a^2-1}{a^2}, \quad \text{or equivalently} \quad a_{\mathcal{L}}^{\pm} \equiv \pm \frac{1}{\sqrt{1-\sigma}}, \quad \text{where there is} \quad (\text{D1})$$

$$a_{\mathcal{L}\mathcal{L}} \equiv \frac{1}{3} \left(6\psi_{\mathfrak{N}} \cos \left(\frac{1}{3} \cos^{-1} [(r^{12} + 6r^{11} + 24r^{10} + 80r^9 - 216r^8 - 2256r^7 - 10304r^6 - 27264r^5 - 68736r^4 + \right. \right. \quad (\text{D2})$$

$$\left. \left. -127744r^3 - 147456r^2 + 24576r + 32768) (r+2)^{-6} \psi_{\mathfrak{N}}^{-3}] \right) - \frac{6[r(r+2)(r^2+4)+32]}{(r+2)^2} \right)^{1/2}$$

$$\text{where} \quad \psi_{\mathfrak{N}} \equiv \sqrt{\frac{r(r(r(r+4)+8)(r(r^3+4r+16)+256)+512)+1024}{(r+2)^4}}.$$

In particular, there are no solutions with inner horizon frequency for spins corresponding to **NSs**. The limiting cases $2M$ or M can be studied separately ($\sigma_{\mathcal{L}}$ is linked to the definition of ergosurface). Some relevant consequences of this analysis, evident also from Fig. (27), are listed here:

(1) Negative frequencies solutions are intrinsically related to the positive frequency solutions, as they are the extension in the extended plane of the **MBs** with positive characteristic frequencies.

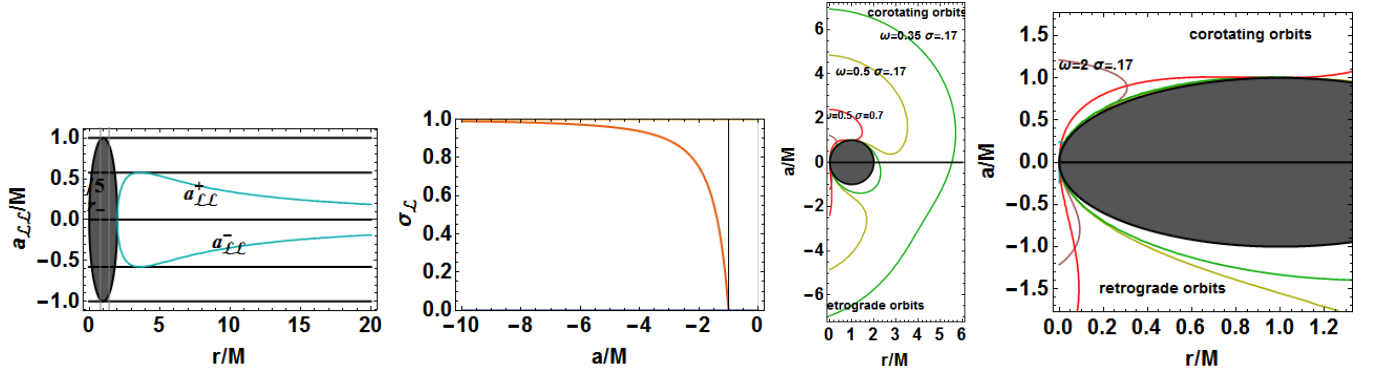


FIG. 27: Study of negative frequencies based on the analysis of Sec. (D1). Left panel: plots of spin $a_{\mathcal{L}\mathcal{L}}$ of Eq. (D2) as functions of r/M . The black region is the black hole on the extended plane (i.e. $a \in [-a_{\pm}, a_{\pm}]$). Second panel: limiting spin $\sigma_{\mathcal{L}}$ of Eq. (D1) as function of $a < 0$. Third panel: study of the metric bundles associated with retrograde photon motion represented by the solutions in the sector $a < 0$ of the extended plane, assuming $\omega > 0$. It is clear the absence of tangency points with the horizon on the extended plane and the coincidence with the bundles with equal magnitude origin $a_0^+ = -a_0 > 0$ with equal frequency on the extended plane sector $a_0 > 0$.

(2) Clearly, **MBs** with negative frequencies are not tangent to the horizon curve in the negative frequencies region of the extended plane—Fig. (2).

(3) These correspond to only one solution (with folding) for ω_- frequency.

(4) More precisely, we have confined all the negative frequencies solutions to the negative region of the extended plane (assuming $a < 0$ and $\omega > 0$).

(5) The existence of negative frequencies solutions are constrained by several specific conditions depending also on the ergosurfaces role.

(6) There are **MBs** with frequency equal in magnitude to the horizon frequencies (horizontal lines $a = -\bar{a} < 0$, such that there are bundle portions with frequency $\omega_H^{\pm}(\bar{a}) > 0$ at the same plane as shown in the figures). Therefore, there are orbits different from the horizons with frequencies equal in magnitude to the horizon's frequency—in the same geometry as confirmed by the analysis of Sec. (III). Then,

$$\mathcal{L} \cdot \mathcal{L} = 0 \quad r > 0 \quad \sigma \in]0, 1], \quad a < 0 \quad \omega > 0 \quad (D3)$$

$$a < -M \quad \omega = \omega_- \quad \bullet \quad r \in]0, 2M], \quad \sigma \in]0, \sigma_{\epsilon}^{\pm}[\quad \bullet \quad r > 2M \quad \sigma \in]0, M]$$

$$a \in [-M, 0[\quad \bullet \quad r \in]0, r_-[\quad \sigma \in]0, \sigma_{\epsilon}^{\pm}[\quad \bullet \quad r \in]r_+, 2M] \quad \sigma \in]0, \sigma_{\epsilon}^{\pm}[\quad \bullet \quad r > 2M \quad \sigma \in]0, 1]$$

$$\text{where } \sigma_{\epsilon}^{\pm} \equiv \frac{(r-2)r}{a^2} + 1, \quad \text{equivalently}$$

$$\text{for } a < -M \quad \text{Condition R holds, for } a \in [-M, 0[\quad \text{Condition S holds}$$

$$\text{Condition R : } \bullet \quad \sigma \in]0, \sigma_{\mathcal{L}}[\quad r > 0 \quad \bullet \quad \sigma \in]s, 1[\quad r \in]0, r_{\epsilon}^{-}[\quad \cup \quad r > r_{\epsilon}^{+}$$

$$\text{Condition S : } \bullet \quad \sigma \in]0, 1[\quad r \in]0, r_{\epsilon}^{-}[\quad \cup \quad r > r_{\epsilon}^{+}.$$

Conditions related to different boundary values and, particularly, for $\sigma = \sigma_{\mathcal{L}}$ should be evaluated separately. In this analysis, we will no further investigate values (other notable spins are $a = -\sqrt{6\sqrt{3}-9}M$ and $a = \sqrt{2}M/3$). The function σ_{ϵ}^{\pm} is linked to the existence of ergo-surfaces, specifically, it is the solution of $r_{\epsilon}^{\pm} = r$. The function $\sigma_{\mathcal{L}}$ is a solution of the following equation:

$$\begin{aligned} & 16 [a^3 + a(r-2)r]^2 + a^6 \sigma^4 \Delta^2 - 2a^4 \sigma^3 \Delta [a^4 + 2a^2(r^2-2) + r^4 + 8r + 8] + \\ & 8\sigma \Delta [a^6 + 2a^4(r^2-3) + a^2r(r^3-4r-8) - 2r^4] + a^2 \sigma^2 [a^8 + 4a^6(r^2-4) + a^4[6r^4 - 32r^2 + 48r + 48] + \\ & 4a^2 r^2 [r(r^3-4r+16) + 24] + r^2 [r[r(r^4+16r+32) - 64] + 64]] = 0 \end{aligned} \quad (D4)$$

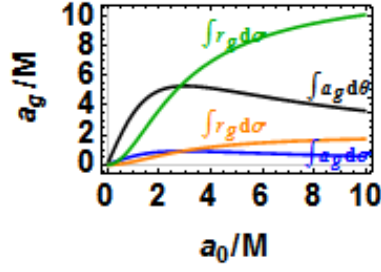


FIG. 28: Areas of regions bounded by special curves. Based on the analysis of Eq. (D5).

2. Consideration of areas

In this section, we focus on areas of extended plane regions bounded by remarkable curves; these areas characterize quantities invariants with respect to a spin shift, orbits translation or plane shift $\sigma \in]0, 1]$ (the integration region is on the extended plane). A part of this analysis has been done in Sec. (II), considering the linearized scheme of Fig. (2), where we showed the linearized conditions on the horizon. Therefore,

$$\begin{aligned} \text{Horizon curve} \quad \int_0^{2M} a_{\pm} dr = \pi/2; \quad \text{Origins} \quad \int_0^{2M} a_0(r) dr = 2\pi, \quad \int a_{\epsilon}^{\pm} d\sigma dr = \pi, \quad (D5) \\ \int a_g(a_0) d\theta = -\frac{16 \tan^{-1}\left(\frac{a_0}{\sqrt{-a_0^2-4}}\right)}{\sqrt{-a_0^2-4}}, \quad \int r_g(\omega) d\omega = \frac{1}{2} \int_{\omega_H^+} r_g(\omega) d\omega = \frac{\pi}{2}, \quad \int \omega_H^+ da = \frac{1 - \log(2)}{2}, \\ \int_{\omega_H^+} a_g(\omega_b) d\omega_b = \frac{\log(2)}{2}, \quad \int a_g(r_g) dr_g = \frac{2\pi}{\sqrt{\sigma}} \quad (D6) \end{aligned}$$

see Fig. (28).

3. Coincidence of radii: horizon replicas

The question we investigate here is whether the special orbits investigated in Sec. (III) and Sec. (B) on the **MBs** with characteristic frequencies $\omega_b(a) \in \{\omega_H^+(a_p), \omega_H^-(a_p)\}$, are located exactly in $r_{\pm}(a_p) > r_{\pm}(a)$, that is, on the horizon with frequency $\omega_b(a)$. Such orbits are, therefore, called horizon replicas. It is clear that these are given by the vertical lines $r = r_{\pm}(a_p)$ on the extended plane. Crossings with **MBs** of the Γ_{ω_b} class are clearly at $(a = a_g = a_p, r = r_g = r_{\pm}(a_p))$. The other radii are given by the intersections of the bundle branches with the vertical line. Note that eventually there can be also solutions with negative frequencies, that is, the crossing with the **MBs** branches in the extension to negative frequencies of the extended plane. The case of negative characteristic bundle frequencies is considered in Sec. (D 1).

Consider, in a fixed spacetime of a bundle, an orbit $r_{\pm}^*(a) > r_{\pm}(a)$ with frequency $\omega_H^{\pm}(a)$, respectively. Clearly, there are orbits $r_{\pm}^*(a) > r_{\pm}(a)$ with frequency $\omega_H^{\pm}(a_p)$ for a given spin $a_p \neq a$, as all the limiting frequencies $\omega_b = \omega_{\pm}$ are horizon frequencies on the extended plane. Eventually, we could ask for the conditions for the occurrence of $r_b^*(a) = r_b(a_p)$, where $\{b, \natural\} = \pm$. For a given spacetime with $a > 0$, there is an orbit, $r^*(a)$, with limiting frequency $\omega_H^*(a_p)$, that is, the frequency of the inner or outer horizon, respectively: $\omega_H^*(a_p) \in \{\omega_H^-(a_p), \omega_H^+(a_p)\}$. The following cases answer this problem:

(1) If $a > M$, then the radius can be $r^* > 0$ thus it could be in $r_-^*(a) = r_-(a_p) \in]0, M]$ or also $r_+^*(a) = r_+(a_p) \in [M, 2M[$.

(2) If, otherwise, $a \in [0, M]$, then the radius must satisfy the relation $r_+^*(a) = r_+(a_p) > r_+(a) \in [M, 2M[$ and, therefore, be only the outer horizon frequency (which is also another aspect of the horizons confinement). This

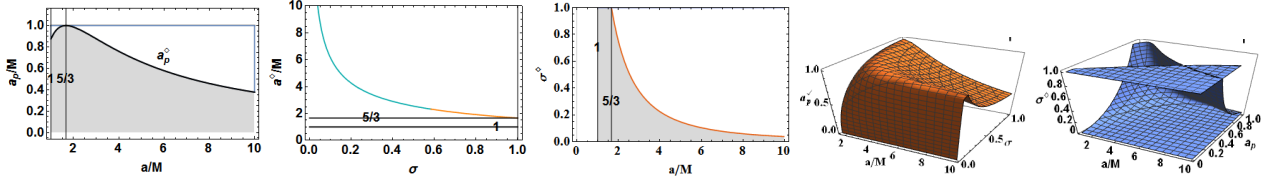


FIG. 29: Analysis of Eq. (D7). Orbits $r(a) = r_{\pm}(a_p)$ with characteristic frequency equal to that of the internal and external horizon $\omega_{\pm}^{\pm}(a_p)$. They correspond to solutions of $\mathcal{L} \cdot \mathcal{L} = 0$. Limiting spins ($a_p^{\diamond}, a^{\diamond}$), and plane σ_p^{\diamond} are plotted. The solutions (a^{\vee}, σ^{\vee}) are on 3D plots.

condition implies $a_p > a \in [0, M]$, with $\omega(r_+^*(a), a) = \omega_H^+(a_p)$. More precisely, the results are as follows:

$$\begin{aligned} \mathcal{L} \cdot \mathcal{L} = 0 \quad \text{for} \quad r = r_+(a_p), \quad \omega_b = \omega_H^+(a_p) \quad \text{for} \quad a_p = a^{\vee}, \quad a \geq 5M/3, \quad (a \geq a^{\diamond}) \quad a_p \in [a_p^{\diamond}, M], \quad \sigma \in [\sigma^{\diamond}, 1[\\ \sigma^{\diamond} \equiv \frac{a \left[7 - a(a+1) \left[\sqrt{\frac{(a-1)^3 [a(a+5)+11]-1}{a^4(a+1)^2}} - 1 \right] \right] - 1}{2a^2(a+1)}, \quad (D7) \\ a^{\diamond} \equiv \left\{ \frac{1}{3} \left[2\sqrt{\frac{12}{\sigma} + \frac{9}{\sigma-1} + 1} \cos \left(\frac{1}{3} \sec^{-1} \left[\frac{\sqrt{\frac{12}{\sigma} + \frac{9}{\sigma-1} + 1} [12 - \sigma(\sigma+20)]}{\sigma(\sigma+44) + 36}} \right] \right) - 1 \right], \right. \\ \left. \frac{1}{3} \left[-2\sqrt{\frac{12}{\sigma} + \frac{9}{\sigma-1} + 1} \sin \left(\frac{1}{3} \csc^{-1} \left[\frac{\sqrt{\frac{12}{\sigma} + \frac{9}{\sigma-1} + 1} [12 - \sigma(\sigma+20)]}{\sigma(\sigma+44) + 36}} \right] \right) - 1 \right] \right\} \\ a_p^{\diamond}: \quad (a^2 - 8) a_p^3 + (8a^2 + 32) a_p + 2aa_p^4 - 32a + a_p^5 = 0. \\ \text{There are no solutions for } a \in [0, M] \text{ and } a_p \in [0, M]. \end{aligned}$$

The spin a_p^{\vee} is a solution of the equation

$$\begin{aligned} -16a^4(\sigma-1)^2\sigma + 32a^3a_p(\sigma-1)\sigma + a_p^6\sigma [a^2\sigma(2\sigma-1) - 8] + 4aa_p^5(\sigma-1)\sigma (a^2\sigma+4) + \\ a_p^4 [\sigma (a^4\sigma(\sigma^2-1) + 8a^2\sigma(3-2\sigma) + 16) + 16] + 2aa_p^3 [\sigma (a^4(\sigma-1)^2\sigma - 8a^2(\sigma^2-1) - 16(\sigma+1)) + 16] + \\ a^2a_p^2(\sigma-1) [\sigma (a^4(\sigma-1)\sigma - 8a^2 + 16(\sigma+3)) - 16] + 2aa_p^7\sigma^2 + a_p^8\sigma^2 = 0. \quad (D8) \end{aligned}$$

See Fig. (29).

We now consider the problem for the inner horizon:

$$\begin{aligned} \mathcal{L} \cdot \mathcal{L} = 0 \quad \text{for} \quad r = r_-(a_p), \quad \omega = \omega_H^-(a_p) \quad \text{for} \quad \sigma = \sigma^{\vee} \quad \text{and} \\ \bullet \quad a \in]M, 5M/3], \quad a_p \in]0, a_p^{\diamond}], \quad \bullet \quad a > 5M/3, \quad a_p \in]0, M]. \quad (D9) \end{aligned}$$

The plane σ^{\vee} is a solution of the equation

$$\begin{aligned} \sigma^{\vee}: \quad a^4a_p^2\sigma^4(a+a_p)^2 - 2a^2\sigma^3(a+a_p) [a^3a_p^2 + (a^2+8)a_p^3 - aa_p^4 + 8a - a_p^5 - 8a_p] + 8\sigma [a^4(a_p^2-2) + \\ 2a^3a_p(a_p^2-2) - 8a^2a_p^2 - 2aa_p^3(a_p^2+2) - a_p^4(a_p^2-2)] + \sigma^2 [a^6a_p^2 + 2a^5a_p^3 - a^4(a_p^4 + 8a_p^2 - 32) - 4a^3(a_p^4 - 8)a_p + \\ a^2(-a_p^4 + 24a_p^2 + 32)a_p^2 + 2a(a_p^4 + 8a_p^2 - 16)a_p^3 + a_p^8] + 16a_p^2(a+a_p)^2 = 0, \quad (D10) \end{aligned}$$

–see Fig. (29). It is clear that for the causal structure (as determined by the condition $\mathcal{L}_{\mathcal{N}}$) the difference in frequencies is relevant for the orbits considered here as horizon replicas. This analysis has been also addressed in Eq. (29), where a fixed geometric with spin a , orbit r and plane σ was considered. Here, we are interested in this aspect again considering the differences for $\omega_b(a, r \pm (a_p)) - \omega_H^{\pm}(a_p)$ and for $b = \pm 1$ –see Fig. (30).

[1] R. Beig and P. T. Chrusciel, “Stationary black holes,” gr-qc/0502041

[2] Bini D., Damour T., Geralico A., Kavanagh C. and van de Meent M., 2018, Phys. Rev. D **98**, 10, 104062

[3] Bini D. and Geralico A., 2019a arXiv:1907.11082 [gr-qc].

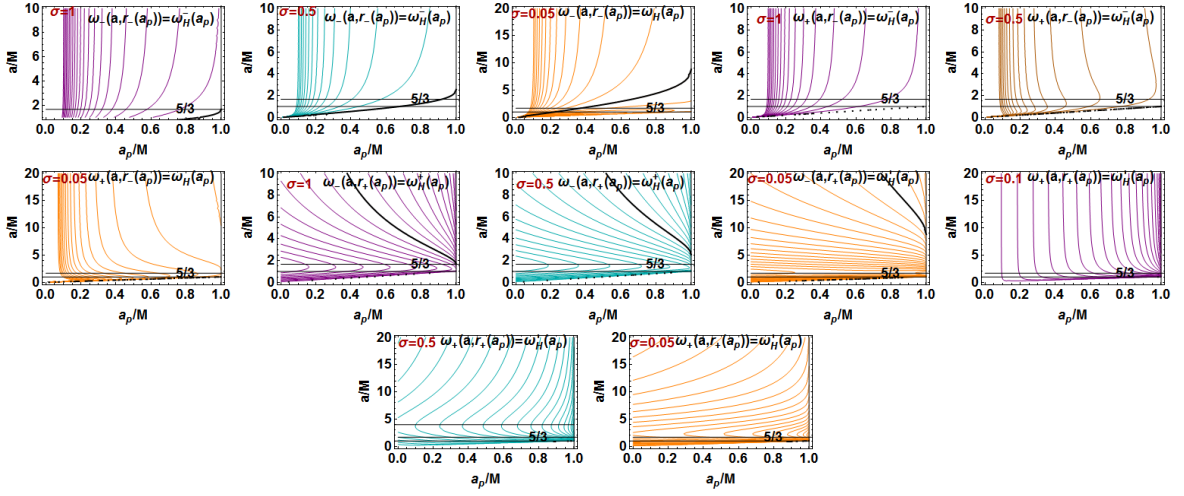


FIG. 30: Differences for the second frequencies $\omega_b(a, r \pm (a_p)) - \omega_H^\pm(a_p)$ for $b = \pm 1$, where $\sigma \in \{0.05, 0.5, 1\}$ on the plane (a_p, a) . The limiting spins $a/M = 5/3$ and $a = M$ are also shown. Solutions of $\omega_b(a, r \pm (a_p)) = \omega_H^\pm(a_p)$ –see Eqs (D10).

- [4] Bini D. and Geralico A., 2019b, arXiv:1907.11080 [gr-qc].
- [5] Chakraborty C., Patil M., Kocherlakota P., Bhattacharyya S., Joshi P. S. and Królak A., 2017, Phys. Rev. D **95**, no.8, 084024
- [6] Chrusciel P. T., Lopes Costa J. and Heusler M., 2012, Living Rev. Rel. **15**, 7
- [7] Clarke, C.J.S. ; De Felice, F., 1984, Gen. Rel. Grav., 16, 2, 139-148
- [8] de Felice F., 1991, Mont. Notice R. astr. Soc 252 197-202
- [9] de Felice F., 1994, Class. Quantum Grav. 11, 1283-1292
- [10] de Felice F. and Sigalotti L. Di G., 1992, Ap.J. 389, 386-391
- [11] de Felice F. and Usseglio-Tomasset S., 1991, Class. Quantum Grav. 8., 1871-1880
- [12] de Felice F. and Usseglio-Tomasset S., 1992, Gen. Rel. Grav. 24, n. 10
- [13] de Felice F. and Usseglio-Tomasset S., 1996, Gen. Rel. Grav. 28, n. 2
- [14] de Felice F. and Yunqiang Y., 1993, Class. Quantum Grav. 10, 353-364
- [15] Dotti G., Gleiser R. J., Ranea-Sandoval I. F. and Vucetich H., 2008, Class. Quant. Grav. **25**, 245012
- [16] Malament D. B., 1977, J. Math. Phys., 18, 1399
- [17] Mukherjee S. and Nayak R. K., 2018, Astrophys. Space Sci. **363** no.8, 163
- [18] Pugliese D. and Montani G., 2015, Phys. Rev. D **91**, 8, 083011
- [19] Pugliese D. and Quevedo H., 2015, Eur. Phys. J. C **75** no.5, 234
- [20] Pugliese D. and Quevedo H., 2018, Eur. Phys. J. C **78**, 1, 69
- [21] Pugliese D. and Quevedo H. 2019a, Eur. Phys. J. C **79**, no.3, 209
- [22] Pugliese D., Quevedo H., 2020, to be submitted
- [23] D. Pugliese and H. Quevedo, “Killing horizons, throats and bottlenecks in the ergoregion of the Kerr spacetime,” arXiv:1910.02808 [gr-qc]
- [24] D. Pugliese and H. Quevedo, “On the metric bundles of axially symmetric spacetimes,” arXiv:1910.04996 [gr-qc].
- [25] D. Pugliese and G. Montani, *to be submitted*
- [26] Pugliese D., Quevedo H. and Ruffini R. 2011, Phys. Rev. D , 84, 044030
- [27] Pugliese D., Quevedo H. and Ruffini R., 2011, Phys. Rev. D **83**, 024021
- [28] Pugliese D., Quevedo H. and Ruffini R., 2011, Phys. Rev. D **83**, 104052
- [29] Pugliese D., Quevedo H. and Ruffini R., 2012, *in* Proceedings, 12th Marcel Grossmann Meeting on General Relativity, Paris, France, July 12-18, 2009. Vol. 1-3,” p.1017-1021, edited: T. Damour, R. T. Jantzen and R. Ruffini, Singapore, Singapore: World Scientific
- [30] Pugliese D., Quevedo H. and Ruffini R., 2013, Phys. Rev. D **88**, 024042
- [31] Pugliese D., Quevedo H. and Ruffini R., 2017, Eur. Phys. J. C **77**, 4, 206
- [32] Tanatarov I. V. and Zaslavskii O. B., 2017, Gen. Rel. Grav. **49**, no.9, 119
- [33] Wald R. M., 1999 Class. Quant. Grav. **16**, A177
- [34] Wald R. M., 2001, Living Rev. Relativ. 4(1), 6
- [35] Zaslavskii O. B., 2018, Phys. Rev. D **98**, 10, 104030
- [36] Zaslavskii O. B., 2019, Phys. Rev. D **100**, no.2, 024050